USGS
science for a changing world

Prepared in cooperation with the
UPPER SAN PEDRO PARTNERSHIP and BUREAU OF LAND MANAGEMENT

Ground-Water Flow Model of the Sierra Vista Subwatershed and Sonoran Portions of the Upper San Pedro Basin, Southeastern Arizona, United States, and Northern Sonora, Mexico

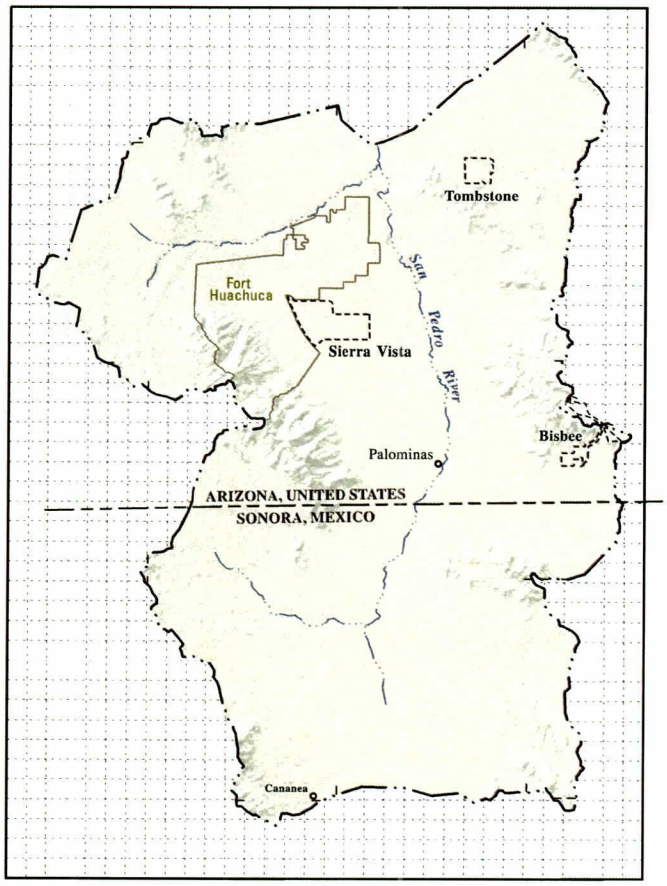

Scientific Investigations Report 2006–5228

U.S. Department of the Interior
U.S. Geological Survey

FMC000561

Inside Front Cover
BLANK

Ground-Water Flow Model of the Sierra Vista Subwatershed and Sonoran Portions of the Upper San Pedro Basin, Southeastern Arizona, United States, and Northern Sonora, Mexico

By D.R. Pool and Jesse E. Dickinson

Prepared in cooperation with the

UPPER SAN PEDRO PARTNERSHIP and the
U.S. BUREAU OF LAND MANAGEMENT

Scientific Investigations Report 2006–5228

U.S. Department of the Interior
U.S. Geological Survey

FMC000563

U.S. Department of the Interior
DIRK KEMPTHORNE, Secretary

U.S. Geological Survey
Mark D. Myers, Director

U.S. Geological Survey, Reston, Virginia: 2007

For product and ordering information:
World Wide Web: http://www.usgs.gov/pubprod
Telephone: 1-888-ASK-USGS

For more information on the USGS--the Federal source for science about the Earth, its natural and living resources, natural hazards, and the environment:
World Wide Web: http://www.usgs.gov
Telephone: 1-888-ASK-USGS

Any use of trade, product, or firm names is for descriptive purposes only and does not imply endorsement by the U.S. Government.

Although this report is in the public domain, permission must be secured from the individual copyright owners to reproduce any copyrighted materials contained within this report.

Suggested citation:
Pool, D.R., and Dickinson, J.E., 2007, Ground-water flow model of the Sierra Vista Subwatershed and Sonoran portions of the Upper San Pedro Basin, southeastern Arizona, United States, and northern Sonora, Mexico: U.S. Geological Survey Scientific Investigations Report 2006–5228, 48 p.

Contents

Abstract 1
Introduction 1
Purpose and Scope 1
Approach 1
Description of Study Area 2
Climate 2
Land and Water Use 2
Acknowledgments 4
Conceptual Model of the Ground-Water Flow System 4
Hydrogeologic Framework 4
Aquifers 4
Pre-Tertiary Rocks 7
Tertiary Pre-Basin Fill Sediments 7
Basin Fill 8
Stream Alluvium 8
Ground-Water Flow System 9
Ground-Water Budget 9
Predevelopment 13
Postdevelopment 14
Artificial Recharge 14
Evapotranspiration 14
Ground-Water Withdrawals 15
Simulation of Ground-Water Flow 18
Previous Models 18
Model Framework 18
Model Boundaries 18
Spatial and Temporal Discretization 19
Aquifer Hydraulic Properties 19
Layer Distribution 19
Transmissive Properties 20
Storage Properties 20
Simulated Inflows and Outflows 26
Recharge 26
Natural Recharge 26
Artificial and Incidental Recharge 26
Evapotranspiration of Ground Water 29
Streamflow Routing 30
Ground-Water Withdrawals 30
Initial Conditions 31
Model Calibration 32
Steady State 32
Average-Annual Steady-State Conditions 32
Oscillatory Steady-State Conditions 35

Contents—Continued

Transient-State Conditions 35
Model Limitations and Possible Improvements 42
Summary and Conclusions 44
References Cited 45

Figures

1. Model area within the Upper San Pedro Basin, Arizona, United States and Sonora, Mexico 3
2. Geology and saturated thickness of the regional aquifer, Upper San Pedro Basin, United States and Mexico 6
3. Generalized hydrogeologic section and extent of numerical model layers, Upper San Pedro Basin, United States and Mexico 7
4. Extent and altitude of thick silt and clay interval in the basin fill, Upper San Pedro Basin, United States and Mexico. 4A, Top of thick silt and clay interval; 4B, Base of thick silt and clay interval 10
5. Ground-water flow system, boundary conditions for the model, streamflow routing network, evapotranspiration areas, and predevelopment water-level comparison sites, Upper San Pedro Basin, United States and Mexico 12
6. Annual ground-water withdrawal rates for selected uses, 1902 to 2002, Upper San Pedro Basin, United States and Mexico. 6A, Mine uses; 6B, Non-mine uses; 6C, Total uses 16
7. Extent and lithology of hydrogeologic units and altitude of the base of numerical model layers, Upper San Pedro Basin, United States and Mexico. 7A, Model layer 5; 7B, Model layer 4; 7C, Model layer 3; 7D, Model layer 2; 7E, Model layer 1 21
8. Simulated total transmissivity of the numerical model layers, Upper San Pedro Basin, United States and Mexico 27
9. Pre-1961 water-level hydrographs for the Sierra Vista subwatershed of the Upper San Pedro Basin, United States 33
10. Observed and simulated predevelopment water-level altitude error for selected monitoring wells, Upper San Pedro Basin, United States and Mexico. 10A, Observed and simulated predevelopment water-level altitudes; 10B, Residual of observed and simulated predevelopment water-level altitudes 34
11. Distributions of simulated withdrawal wells and selected hydrograph comparison sites, Upper San Pedro Basin, United States and Mexico 38
12. Hydrographs showing observed and simulated water-level altitudes at selected wells, 1940–2003, Upper San Pedro Basin, United States and Mexico 39
13. Estimated and simulated seasonal baseflow at streamflow-gaging stations on the San Pedro River, Arizona, 1929–2003. 13A, Charleston; 13B, Palominas 41
14. Observed and simulated water-level altitudes, winter 2002, Upper San Pedro Basin, United States and Mexico 43

Tables

1. Correlation of hydrogeologic units and model layers 5
2. Estimated predevelopment ground-water budget 13
3. Simulated hydraulic properties of hydrogeologic units for the ground-water flow model of the Upper San Pedro basin, United States and Mexico 28
4. Simulated predevelopment ground-water budget 36
5. Simulated ground-water budget for March 2002 to March 2003 44

Conversion Factors and Datum

Multiply	By	To obtain
centimeter (cm)	0.3937	inch
meter (m)	3.281	foot
kilometer (km)	0.6214	mile
square meter (m^2)	0.0002471	acre
square kilometer (km^2)	0.3861	square mile
cubic hectometer (hm^3)	810.7	acre-foot
cubic hectometer per year (hm^3/yr)	811.03	acre-foot per year
cubic meter per day (m^3/yr)	3.378	acre-foot per year
cubic meter per second (m^3/s)	35.31	cubic foot per second
square hectometer (hm^2)	2.471	acre

Vertical coordinate information is referenced to the North American Vertical Datum of 1988 (NAVD 88).

List of Abbreviations

DEM	Digital elevation model
ENSO	El Niño Southern Oscillation
ft bls	feet below land surface
GIS	Geographic Information System
Landsat	Landsat satellites
LIDAR	Light Detection And Ranging
MF2K	MODFLOW 2000
ohm-m	ohm-meters
PDO	Pacific Decadal Oscillation
SPRNCA	San Pedro Riparian Conservation Area
STR1	Streamflow Routing package for MODFLOW
USDA	U.S. Department of Agriculture
USGS	U.S. Geological Survey
BLM	Bureau of Land Management

Arizona Well-Numbering System

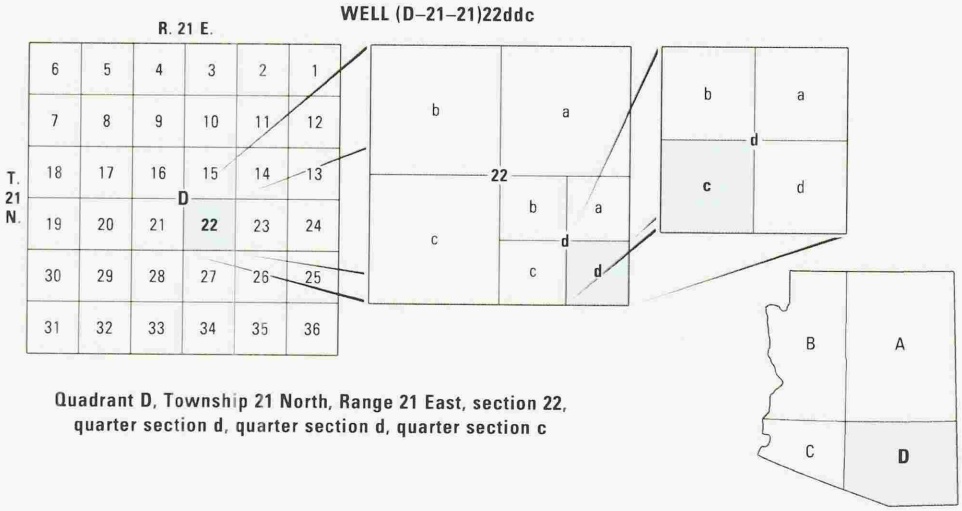

The well numbers used by the U.S. Geological Survey in Arizona are in accordance with the Bureau of Land Management's system of land subdivision. The land survey in Arizona is based on the Gila and Salt River meridian and base line, which divide the State into four quadrants and are designated by capital letters A, B, C, and D in a counterclockwise direction beginning in the northeast quarter. The first digit of a well number indicates the township, the second the range, and the third the section in which the well is situated. The lowercase letters a, b, c, and d after the section number indicate the well location within the section. The first letter denotes a particular 160-acre tract, the second the 40-acre tract, and the third the 10-acre tract. These letters are also assigned in a counterclockwise direction beginning in the northeast quarter. If the location is known within the 10-acre tract, three lowercase letters are shown in the well number. When more than one well is within a 10-acre tract, consecutive numbers beginning with 1 are added as suffixes. In the example shown, well number (D–21–21)22ddc designates the well as being in the SE1/4, SE1/4, SW1/4, section 22, Township 21 North, and Range 21 East.

Ground-Water Flow Model of the Sierra Vista and Sonoran Portions of the Upper San Pedro Basin, Southeastern Arizona, United States, and Northern Sonora, Mexico

By D.R. Pool and Jesse E. Dickinson

Abstract

A numerical ground-water model was developed to simulate seasonal and long-term variations in ground-water flow in the Sierra Vista subwatershed, Arizona, United States, and Sonora, Mexico, portions of the Upper San Pedro Basin. This model includes the simulation of details of the ground-water flow system that were not simulated by previous models, such as ground-water flow in the sedimentary rocks that surround and underlie the alluvial basin deposits, withdrawals for dewatering purposes at the Tombstone mine, discharge to springs in the Huachuca Mountains, thick low-permeability intervals of silt and clay that separate the ground-water flow system into deep-confined and shallow-unconfined systems, ephemeral-channel recharge, and seasonal variations in ground-water discharge by wells and evapotranspiration.

Steady-state and transient conditions during 1902–2003 were simulated by using a five-layer numerical ground-water flow model representing multiple hydrogeologic units. Hydraulic properties of model layers, streamflow, and evapotranspiration rates were estimated as part of the calibration process by using observed water levels, vertical hydraulic gradients, streamflow, and estimated evapotranspiration rates as constraints. Simulations approximate observed water-level trends throughout most of the model area and streamflow trends at the Charleston streamflow-gaging station on the San Pedro River. Differences in observed and simulated water levels, streamflow, and evapotranspiration could be reduced through simulation of climate-related variations in recharge rates and recharge from flood-flow infiltration.

Introduction

Increased water use has increased demand on the water supply in the Sierra Vista subwatershed of the Upper San Pedro Basin. Ground water is the primary source of water in the basin for many uses, including riparian, agricultural, private, public, and industrial; and supply for the military installation at Fort Huachuca. Baseflows in perennial-stream reaches of the San Pedro River are sustained by ground-water flow from upgradient recharge areas. Increasing demand on the ground-water supply likely will result in decreasing amounts of ground-water available to baseflow and riparian vegetation. Basic water-budget analysis shows that ground-water withdrawals for upgradient uses will eventually result in a reduction in discharge from the basin owing to reduced baseflow and evapotranspiration by plants. The amount of the reduced discharge will be equivalent to the amount withdrawn from the system assuming that inflow to the ground-water system does not change. The rate and location of reduced discharge, however, is not well known because of a lack of information about the hydrogeologic system in the basin. Improved knowledge of interactions between the stream and ground-water systems is needed to make informed decisions about the management of the water resources in the basin.

Purpose and Scope

A new numerical ground-water flow model of the study area was constructed to simulate new conceptualizations of the ground-water flow system in the Upper San Pedro Basin. Hydrologic investigations and monitoring during the mid-1990s–2004 have improved understanding of the ground-water flow system beyond that simulated the by previous models. The new model can be used to aid management of the resources and to assess the impacts of ground-water withdrawals and artificial recharge on streamflow and riparian vegetation in the basin. This report documents the development and calibration of the new numerical ground-water flow model.

Approach

Information from extensive hydrologic investigations and monitoring by multiple agencies and investigators during the mid-1990s–2004 was used to refine the conceptual model of the ground-water flow system in the study area. Investigations provided new information to better define the spatial and temporal distribution of recharge, vertical

hydraulic-head gradients, interactions between the stream and the aquifer, and the subsurface distribution of silt and clay layers in the primary aquifer. Definition of the spatial and temporal distribution of recharge was improved by new data from several streamflow-gaging stations, unsaturated-zone monitoring beneath several ephemeral streams and in interdrainage areas, monitoring ground-water levels and ground-water storage, and geochemical analysis of runoff and ground water in recharge areas. Definition of vertical hydraulic-head gradients near the San Pedro River and stream–aquifer interactions was improved by using water levels measured bimonthly or more frequently at multiple piezometers. Geophysical investigations were used to augment drill-log information defining the distribution of silt and clay layers in the primary aquifer. Rates of evapotranspiration for several important vegetation types were better defined for the period 2002-03. Much of the new information was acquired in the Arizona portion of the watershed. New information in Mexico also was provided by recent geologic and hydrogeologic investigations and ground-water flow models. New and existing information was integrated to develop a multilayered, numerical model of steady-state and transient ground-water flow conditions. Hydraulic and flow properties of the numerical model were constrained by using observations of hydraulic head and streamflow.

Description of Study Area

The study area includes the upper drainage area of the San Pedro River in northern Sonora, Mexico, and the Sierra Vista subwatershed in southeastern Ariz., United States (fig. 1), and includes about 4,500 km^2 extending from the southern boundary near Cananea, Mexico, to about Fairbank, Ariz. The watershed is bounded by mountains and intervening broad alluvial passes. Mountains that bound the study area on the west include the Mustang Mountains and Huachuca Mountains, but most of both mountain ranges are completely within the San Pedro River drainage and study area. Mountains to the east include the Mule Mountains, Tombstone Hills, and Sierra San Jose. Mountains to the south include the Sierra Mariquita and Sierra Los Ajos. Altitude of the watershed ranges from about 1,052 m at the streamflow-gaging station near Tombstone, Ariz., to more than 2,700 m in the Huachuca Mountains.

The major streams are intermittent within the study area and include the San Pedro River, Babocomari River, and Rio Los Fresnos. The San Pedro River flows perennially near Hereford, Ariz., and from south of Arizona Highway 90 into the Boquillas area (fig. 1), but perennial reaches prior to development extended south of Palominas. Major perennial reaches along the Babocomari River occur between the Mustang Mountains and Huachuca Mountains and near the confluence with the San Pedro River. Perennial reaches occur along Rio Los Fresnos. Other tributary streams are ephemeral. Major ephemeral streams include Walnut Gulch near Tombstone and Greenbush Draw between the Mule Mountains and Sierra San Jose.

Streamflow and shallow ground water support a narrow corridor of riparian vegetation along the floodplain of the intermittent streams. Riparian vegetation includes phreatophytes, such as cottonwood, willow, and mesquite. The riparian area is a valued resource that supports several endangered species and is an important migratory bird habitat. Much of the riparian area in the United States has been protected by designation as the San Pedro Riparian National Conservation Area (SPRNCA) and is managed by the U.S. Bureau of Land Management.

Climate

Climate of the study area is arid to semiarid. Precipitation data are available during 1905–2002 from a gage at Tombstone, at an altitude of 1,384 m, and during 1956–2002 from a gage at the southern end of the Huachuca Mountains (Coronado National Memorial), at an altitude of 1,692 m (fig. 1). Historically, the wettest season is July through September, averaging 21 cm of precipitation at the Tombstone gage and 27 cm of precipitation at the Huachuca Mountains gage. Precipitation during October through March averages 12 and 23 cm at the Tombstone and Huachuca Mountain gages, respectively. Precipitation during April through June averages less than 3 cm at both gages. Long-term monitoring indicates that annual precipitation rates were above average before about 1940 and during the early to mid-1980s, below average from about 1940 to 1980, and about average after the mid-1980s (Pool and Coes, 1999). Trends in seasonal precipitation, however, are different from trends in annual precipitation. "Winter" (November–February) precipitation and streamflow varies with identifiable multi-year and decadal-scale fluctuations in temperature and precipitation (Webb and Betancourt, 1992; Dickinson and others, 2004; Pool, 2005). High rates of winter precipitation tend to occur during El Niño periods (Pool, 2005). Decadal-scale variations include above-average winter precipitation rates before 1940 and during 1956–97. "Summer" (July–September) precipitation rates and streamflow runoff generally decreased during the later half of the 1900s (Pool and Coes, 1999; Thomas and Pool, 2006).

Land and Water Use

Water use in the study area changed from use primarily for livestock grazing and mining before 1940 to primarily agricultural use during the mid-1900s and mining, industrial, and domestic use during the late 1900s. Some of the water that was derived from dewatering of the mine workings beginning in 1902 at Tombstone (Hollyday, 1963) and in 1906 at Bisbee, Ariz., was used for domestic, industrial, and irrigation purposes. The remainder of the water derived from the mines was allowed to evaporate or recharge the aquifer. Dewatering at the Tombstone mine ceased in 1911, but continued at the Bisbee mine until 1986. Extensive water use began at the Cananea mine during the mid-1980s (Consultores en Agua Subterranea S.A. por Mexicana de Cananea, S.A. de C.V., 2000). The earliest agriculture likely began with the irrigation south of Bisbee by using water derived from mine dewatering. Agricultural water use near the San Pedro River began before 1935 near Hereford by using supplies that were derived from streamflow and wells near the river.

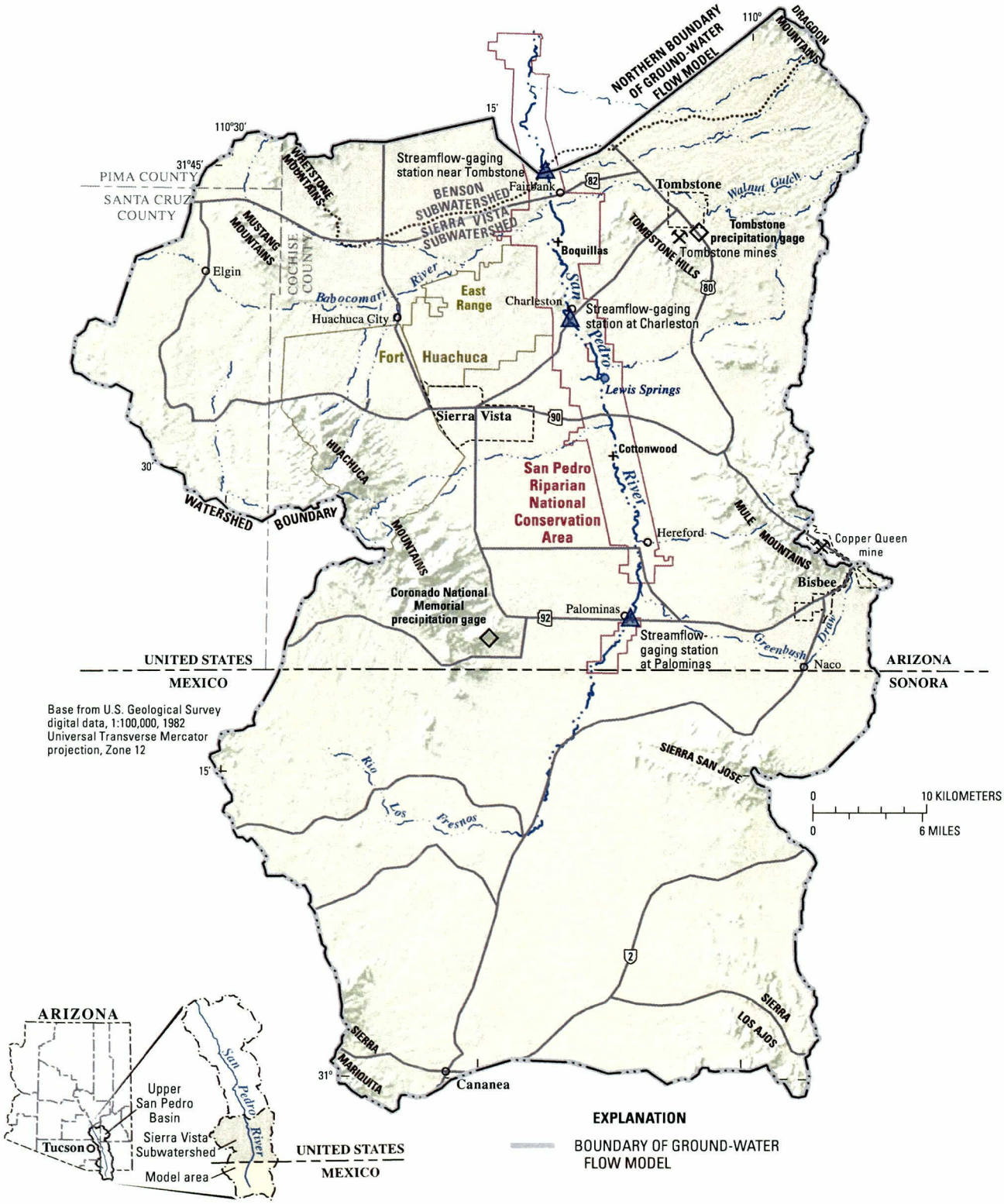

Figure 1. Model area within the Upper San Pedro Basin, Arizona, United States and Sonora, Mexico.

Agricultural water use near the San Pedro River in the Sierra Vista subwatershed increased throughout the 1970s in areas south of Highway 90. Agriculture was eliminated in the area north of Hereford during the mid-1980s and further decreased after 1998 to only a few irrigated fields in the Palominas area. Agriculture in the Mexico portion of the study area is not well documented; however, satellite remote-sensing information (Kepner and Edmonds, 2002) indicates that several agricultural areas existed near the Rio Los Fresnos and San Pedro River in 1973. Industrial and domestic water use began to be significant as the population increased in the Fort Huachuca and the Sierra Vista areas after the mid-1960s and near Cananea beginning in the 1980s.

Acknowledgments

Member agencies and individuals of the Upper San Pedro Partnership were helpful in collecting and disseminating information used to construct the ground-water flow model. Individual knowledge of historical water use was often useful in developing model input when documentation was insufficient. The Morris K. Udall Center was instrumental in arranging for the dissemination of hydrogeologic information that was collected in support of mining operations in Mexico. Recent studies and data made available by the U.S. Department of Interior, U.S. Bureau of Land Management; University of Arizona Department of Hydrology; and U.S. Department of Agriculture, Agricultural Research Service were used in the model construction. The Phelps Dodge Corporation made available hydrogeologic and ground-water withdrawal information for areas near the Copper Queen mine near Bisbee.

Conceptual Model of the Ground-Water Flow System

A conceptual model of the ground-water flow system is a general understanding of where and at what rate recharge occurs, how water flows through the aquifer, and where water discharges. Though conceptual models are constrained by observations of water levels in wells, discharge rates and distributions, and estimates of recharge rates and distributions, observed ground-water conditions may be explained by many different conceptual models. Conceptual models evolve with improved knowledge about ground-water flow systems and provide a basis for construction of numerical models.

Previous concepts of ground-water flow in the Upper San Pedro Basin were simple because of limited data availability. A more complex conceptual model was developed as more details of the system became known. Important new advances include improved quantification of evapotranspiration rates and distributions and a better understanding of the spatial distribution of recharge, vertical ground-water flow, stream-aquifer interactions, spatial distribution of silt and clay in the alluvial aquifer, the influence of natural variations in recharge and discharge, and response of the ground-water flow system to variations in recharge and discharge. A general description of the conceptual ground-water flow system includes descriptions of the aquifers and quantification of recharge rates and distributions, ground-water flow to the discharge areas, and discharge rates and distributions.

Hydrogeologic Framework

The hydrogeologic framework includes descriptions of the thickness, distribution, and hydraulic properties of water-bearing rocks within a ground-water flow system. The hydrogeologic framework of the Upper San Pedro Basin has been described in several reports (Brown and others, 1966; Pool and Coes, 1999; Fleming and Pool, 2002; Condor Consulting Inc., 2003; and Coes and Pool, 2005). The primary aquifer is as much as 520 m of basin fill, alluvial deposits that overlie relatively impermeable crystalline and sedimentary rocks (table 1, fig. 2 and fig. 3). Secondary aquifers of local importance include sedimentary rocks that crop out in the mountains and underlie the basin fill and stream alluvium along the major streams. Ground water generally flows from recharge areas near the mountains, through sand and gravel layers in the basin fill, and toward the San Pedro or Babocomari Rivers. Ground water discharges near the San Pedro and Babocomari Rivers as baseflow, near the San Pedro River as small springs, as ground-water outflow, and as evapotranspiration in riparian areas. A portion of the ground-water flow is intercepted upgradient of the streams by pumping wells and phreatophytes where depths to water are shallow along ephemeral streams.

Aquifers

The primary regional aquifer includes upper and lower basin fill, described by Brown and others (1966), that accumulated in the structural depression between mountain ranges during the late Tertiary and early Pleistocene (table 1, fig. 2 and fig. 3). The saturated thickness of the regional aquifer is 200–400 m within two structural depressions. The largest depression occurs throughout much of the extent of the basin fill in the United States. A smaller structural depression is in Mexico between Sierra San Jose and Sierra Mariquita (fig. 1). The saturated thickness of the regional aquifer is less than 100 m in small structural basins that coincide with the upper parts of Walnut Gulch, Babocomari River, and Greenbush Draw drainage basins (fig. 1).

Secondary aquifers include Quaternary terrace and alluvial deposits that are less than about 10 m thick and generally coincide with the floodplains of the San Pedro and Babocomari Rivers and tributary streams (Pool and Coes, 1999). Tertiary prebasin fill sediment and Mesozoic and Paleozoic limestone that crop out in the mountains also are secondary aquifers in places. Other rocks that crop out in the mountains and hills surrounding the basin are insignificant aquifers and include Tertiary and older granitic and volcanic rocks and Mesozoic sedimentary rocks consisting of mudstone, quartzite, and conglomerate.

Table 1. Correlation of hydrogeologic units and model layers.

Hydrogeologic unit	Lithologic description	Thickness, in meters[1]		Model layer
		Range in thickness of individual unit	Range in thickness of combined model layers	
Post-entrenchment stream alluvium	sand and gravel	0–10	0–520	1
Pre-entrenchment stream alluvium	clay, silt, and fine sand	0–10		
Upper basin fill	sand and gravel facies	0–100		
	sand and gravel facies, and silt and clay facies	0–300		2
Lower basin fill	sand and gravel facies, and siltstone and mudstone facies	0–170		3
	sand and gravel facies	0–400		4
	sand and gravel facies on the perimeter of the alluvial basin	1,500+	1,500	5
Pantano formation	siltstone and conglomerate	1,500+		
Consolidated rocks	limestone, sandstone, mudstone, quartzite, conglomerate, granite, and volcanic rocks	1,500+		

[1]Thickness includes the unsaturated material between the land surface and top of the upper-most layer.

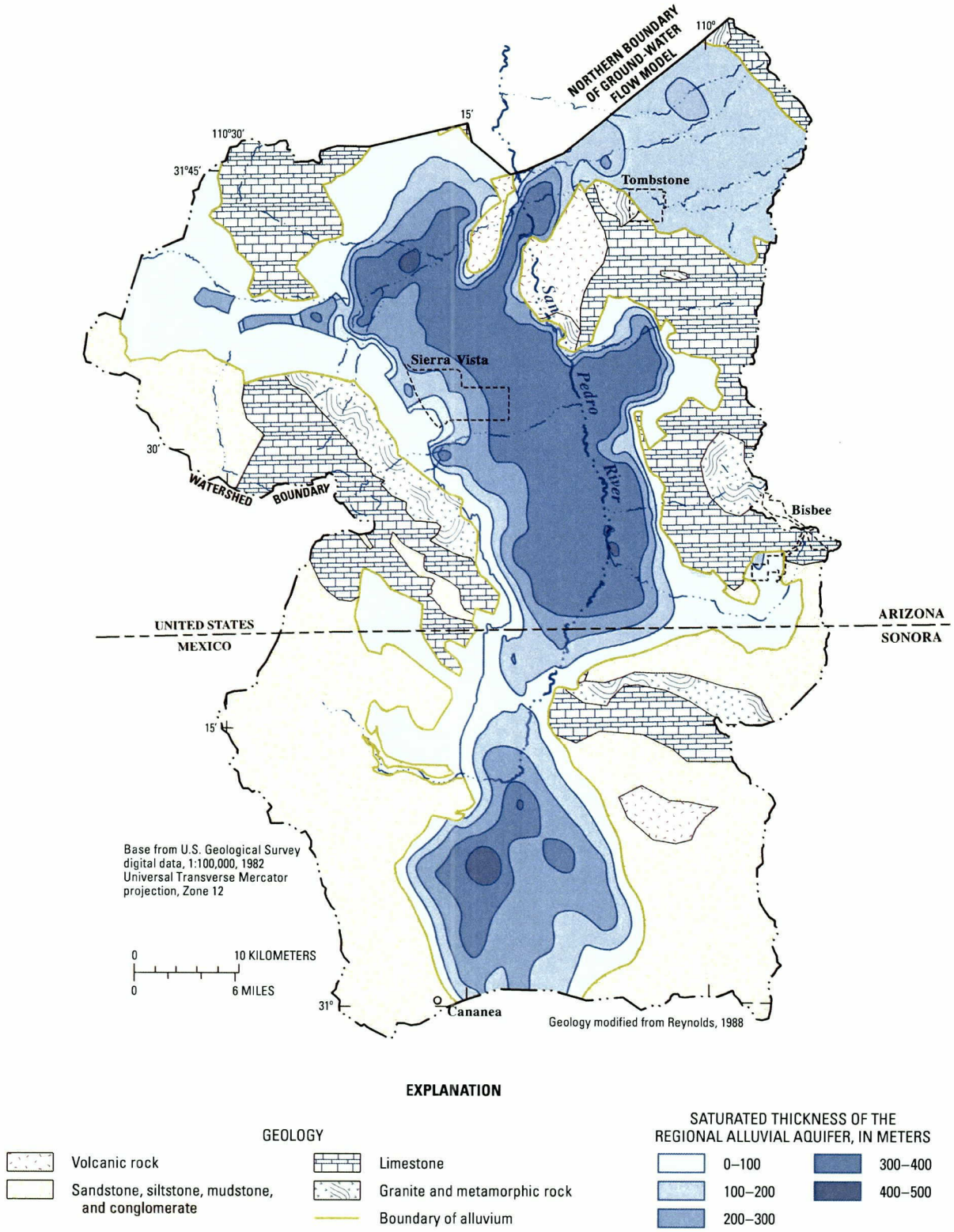

Figure 2. Geology and saturated thickness of the regional aquifer, Upper San Pedro Basin, United States and Mexico.

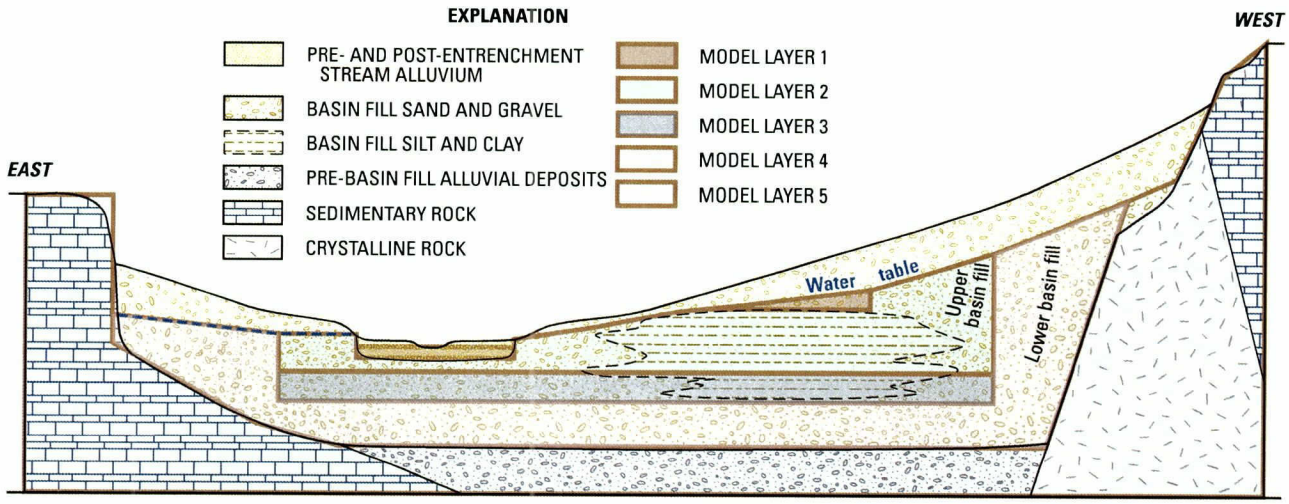

Figure 3. Generalized hydrogeologic section and extent of numerical model layers, Upper San Pedro Basin, United States and Mexico.

Ground water is transmitted primarily through layers of permeable sand and gravel within the basin fill and Quaternary terrace and alluvial deposits. Poorly permeable silt and clay layers are interbedded with the sand and gravel layers and significantly influence ground-water flow. The silt and clay layers result in confined ground-water flow within the underlying permeable sand and gravel layers; and limit the ability of recharge water to infiltrate downward to the aquifer where the silt and clay layers lie above the water table.

Pre-Tertiary Rocks

Outcrops of pre-Tertiary rocks in the study area are predominantly limestone and clastic rocks (fig. 2) with local areas of crystalline rocks. Ground-water flow through these rocks may be an important part of the overall ground-water flow system, but permeability of the rocks is not well known. Much of the limestone is likely permeable because springs are common near the contact with low-permeability rock. Clastic sediments include sandstone, siltstone, and mudstone. Sandstone likely has variable permeability, and the siltstone and mudstone have low permeability. Outcrops of low-permeability crystalline rocks are barriers to ground-water flow in pre-Tertiary sedimentary rocks.

Limestone occurs in the Huachuca Mountains, Whetstone Mountains, Mustang Mountains, Dragoon Mountains, Mule Mountains, and Sierra Los Ajos. Limestone likely underlies the alluvial-basin deposits in much of the region south of the Tombstone Hills and between the Huachuca Mountains and Mule Mountains.

Clastic sedimentary rocks are common in the Mustang Mountains, along the western and southern flanks of the Huachuca Mountains, in the southern Mule Mountains, and throughout much of the portion of the basin in Mexico. Clastic sedimentary rocks underlie much of the alluvial-basin deposits in the area between the Tombstone Hills and the Mustang Mountains and in Mexico.

Granite and metamorphic crystalline rocks occur on the eastern flank of the Huachuca Mountains, Mule Mountains, Sierra Los Ajos, and the Tombstone Hills. Two types of crystalline rocks occur in the Tombstone Hills—granidiorite exists in a small region on the northern edge of the Tombstone Hills, and volcanic rocks exists, in the western part of the Tombstone Hills. The crystalline rock has low permeability. Little is known about the permeability of the volcanic rocks; however, some volcanic rocks may have moderate permeability. In some areas, such as the southwestern flank of the Huachuca Mountains, volcanic rocks are interbedded with clastic sediments, and ground water occurs in caves and issues from springs.

Tertiary Pre-Basin Fill Sediments

The Pantano Formation is a conglomerate that was deposited in an alluvial basin during low-angle tectonic extension of the region and before the Basin and Range structural disturbance. The unit was tilted and faulted by later tectonism, resulting in a southwestern dip of 15–45 degrees (Brown and others, 1966). The unit is generally of low permeability because of cementation (Brown and others, 1966), but can yield water to wells through fractures and may be an important local water-bearing unit. Gravity studies (Gettings and Houser, 1995; Halverson, 1984) indicate the Pantano Formation is likely several hundred meters thick in two structural depressions in the west-central part of the Sierra Vista subwatershed. The two depressions are separated by an east-west trending ridge in the subsurface near Sierra Vista (Gettings and Houser, 1995).

Basin Fill

The basin fill in the San Pedro River Basin is similar in lithology and structure to basin fill throughout southern Arizona (Anderson and others, 1992). The unit was deposited during and after Basin and Range structural deformation that created the current distribution of basins. Coarse-grained and fine-grained facies of the alluvial sediments generally occur at the basin margins and basin centers, respectively. Vertically, the sediments generally grade from coarse-grained sediments of sand and gravel in the lowest part to fine-grained sediments of silt and clay in the middle part and interbedded coarse-grained and fine-grained sediments in the upper part. The sediments that accumulated in the basins are generally divided into upper and lower hydrostratigraphic units. The lower basin fill tends to be more massively bedded and indurated and includes coarse-grained parts commonly described as conglomerate and fine-grained parts commonly described as siltstone and mudstone. The upper basin fill is more heterogeneous and poorly indurated. The basin fill in the study area differs only in detail from basin fill in nearby basins. The upper and lower basin fill units are well defined only in the northern part of the Sierra Vista subwatershed for which good subsurface information from lithologic and electric logs is available (Pool and Coes, 1999). The top and bottom of the basin fill units and the contact between the units in the southern part of the subwatershed were defined for the ground-water flow model on the basis of a few lithologic and electric logs and electrical geophysical surveys. The basin fill in Mexico is undifferentiated because lithologic information is insufficient to distinguish between the two basin fill units.

The lower basin fill is an important water-bearing unit throughout most of the basin. The unit unconformably overlies the Pantano Formation and older rocks, consists of interbedded sand and gravel of variable cementation on the basin margins, and includes thick facies of siltstone and mudstone (Brown and others, 1966; table 1). Information from several test wells indicates that the thickness of the lower basin fill ranges from about 45 m to 100 m near Fort Huachuca. The unit is much more thick, however, in the two major structural depressions.

The upper basin fill lies above a depth of 120 m in all wells where it has been recognized. Saturated thickness is generally greatest near the basin center and thinnest near areas of bedrock outcrop and ranges from 0 to 57 m at test wells on Fort Huachuca where it has been identified. Other lithologic and geophysical data indicate that the thickness of the unit generally is less than 100 m, but is as much as 300 m thick near Hereford and Palominas (fig. 1). The unit is conformable with the lower basin fill and consists of weakly cemented and compacted soft reddish brown clay, gravel, sand, and silt (Brown and others, 1966; table 1). The upper basin fill includes a relatively permeable fan gravel facies near the mountains that grades laterally to a poorly permeable silt and clay facies with interspersed sand and caliche beds near the basin center. The unit is primarily a confining bed of silt and clay where it is saturated between Sierra Vista and the San Pedro River and between Hereford and Highway 90 along the San Pedro River (fig. 1). The upper basin fill is an important aquifer where the fan gravel facies is saturated. Sand beds within the silt and clay facies also may transmit substantial amounts of water provided individual beds are sufficiently interconnected; however, the extent of individual beds is not well known because of a lack of detailed subsurface information. The upper basin fill is equivalent to the St. David Formation described by Gray (1965), which crops out extensively north of the study area near St. David, Ariz..

Distribution of silt and clay in the basin fill is defined by subsurface data from lithologic logs, vertical electrical soundings (Pool and Coes, 1999; Consultores en Agua Subterranea S.A. Por Mexicana de Cananea, S.A. de C.V., 2000; Fleming and Pool, 2002), and other surface and aerial geophysical surveys (University of Arizona Geophysics Field Camp 2001, 2002, 2004; Condor Consulting, 2003; fig. 4).

The vertical and lateral extent of significant silt and clay intervals was estimated as the extent of the basin fill where the aerial electromagnetic survey mapped an electrical resistivity of 12 ohm-m or less (fig. 4). The data were discretized at 10 m intervals; therefore, intervals of silt and clay of less than about 10 m thickness were excluded from the results. The base of the silt and clay is uncertain in areas where the basin fill is underlain by electrically conductive sedimentary rocks, such as siltstone and mudstone, in much of the southern half of the study area and near the Babocomari River. The extent of the silt and clay defines the extent of confined parts of the aquifer. The silt and clay intervals are generally 10–300 m thick. Local unconfined aquifers occur where as much as 100 m of sand and gravel facies overlie silt and clay in the south-central part of the Sierra Vista subwatershed.

Stream Alluvium

Stream alluvium along the San Pedro and Babocomari Rivers is a locally important water-bearing unit that forms a local unconfined aquifer. The unit unconformably overlies lower basin fill and volcanic rocks in the Charleston, Ariz., area and overlies upper basin fill above and below Charleston and along the Babocomari River. The oldest deposits of stream alluvium are clay, silt, and fine sand, with interbedded coarse sand and pebble to cobble gravel that were deposited before the river was entrenched in about 1890 (Hereford, 1993). The pre-entrenchment deposits are as much as 6 m thick and 1.5 km wide. Sand and gravel in the post-entrenchment alluvium were deposited after stream entrenchment of 1–10 m in a narrow channel within the floodplain and pre-entrenchment alluvium. The younger deposits are a few meters thick. The post-entrenchment alluvium is permeable. Pre-entrenchment alluvium transmits water, but generally is less permeable than overlying and adjacent post-entrenchment alluvium and underlying deposits of basin fill.

Ground-Water Flow System

Water recharges the ground-water flow system of the Upper San Pedro Basin in the higher elevations of the basin and discharges as spring flow and stream flow, and through riparian vegetation, in regions at lower elevations and as underflow to the downgradient basin. No ground water is assumed to enter the basin from adjacent basins. The distribution of ground-water flow and locations of discharge areas (fig. 5) are influenced by locations and rates of recharge, basin topography, and the distribution of hydraulic properties in the subsurface. The flow system has been modified by changes in discharge, including changes in ground-water withdrawals by wells and vegetation, and changes in recharge rates due to changes in climate and land use.

Recharge occurs through deep percolation of precipitation that is in excess of evaporation, transpiration by vegetation, and runoff. Recharge is concentrated in two areas: (1) at high elevations and (2) in ephemeral stream channels, where permeable near-surface materials, soil or rock, facilitate infiltration. At high elevations, precipitation rates are greatest, and evaporation and transpiration demands are low, allowing high potential rates of infiltration through permeable rocks, such as limestone or sandstone. Surface runoff of precipitation in excess of infiltration is concentrated in ephemeral channels that commonly have highly permeable deposits that readily transmit excess infiltrated water below depths accessible by vegetation. The resulting recharge distribution is concentrated in areas of permeable rocks in the mountains and along stream channels underlain by sand and gravel and the alluvial aquifer. The greatest rates of infiltration are along ephemeral stream channels near the mountains and are commonly referred to as mountain-front recharge.

Ground water flows through the permeable rocks and sediments toward the low-elevation discharge areas along the major streams (fig. 5). Ground water discharges naturally to streams, springs, and riparian vegetation. Springs in incised canyons where erosion has exposed an underlying rock of low permeability are common discharge areas for water that flows in the limestone and sandstone aquifers in the mountains. These types of springs are common at the lower elevations of the Huachuca Mountains, Mule Mountains, and Sierra San Jose. Not all of the water flowing through the sedimentary-rock aquifers discharges at high-elevation springs. Some of the water flows downgradient into the alluvial aquifer at the southern end of the Huachuca Mountains, below much of the Mule Mountains, and throughout much of the alluvial basin in Mexico. Common areas of discharge from the alluvial aquifer occur where stream channels incise the top of the saturated zone (water table). Several tributary channels have incised the water table where it closely overlies thick intervals of silt and clay, creating springs and perennial stream reaches. Discharge also occurs through evapotranspiration near the springs and along perennial-stream reaches.

Ground water in the Sierra Vista subwatershed also discharges to the adjacent ground-water flow system in the Benson subwatershed as underflow through aquifers that are common to both basins (fig. 5). Most of the ground water flowing to the Benson subwatershed flows through stream alluvium near the streamflow-gaging station near Tombstone and through basin fill west of the Dragoon Mountains and east of outcrops of crystalline rock adjacent to the streamflow-gaging station (fig. 5). Much of the recharge within the Walnut Gulch watershed likely discharges to the Benson subwatershed ground-water system through basin fill in this area. Ground water flowing to the Benson subwatershed also may flow through basin fill between the Tombstone streamflow-gaging station and outcrops of crystalline rock about 5 km northwest of the streamflow-gaging station. Little ground water probably flows northward across the boundary between the two basins beneath the broad alluvial plain east of the Whetstone Mountains. Water-level elevations indicate that flow is parallel to the boundary in this area (fig. 5).

The rate of ground-water flow between the Sierra Vista and Benson subwatersheds likely varies with changes in recharge rates and ground-water withdrawals in both basins. Hydrographs of wells in the basin fill near the boundary, however, indicate that water levels changed little in the area (Barnes and Putman, 2004), and that variations in ground-water discharge through the basin fill to the Benson subwatershed are small.

Ground-Water Budget

Ground-water budgets were constructed for both steady-state and transient conditions. Estimates of the steady-state budget determine the average rate of natural flow through the aquifer system and include the naturally occurring components of recharge and discharge through ground-water flow to adjacent aquifers, streams, drains, and evapotranspiration. The transient budget includes variations in ground-water withdrawals, evapotranspiration, and artificial and incidental recharge. The steady-state ground-water budget can be estimated by using water-balance methods because most recharge to the aquifer system discharges as stream baseflow. Baseflow from about 70 percent of the watershed has been measured continuously since the early 1930s at the streamflow-gaging station at Charleston, Ariz. Steady-state discharge through evapotranspiration is uncertain, but was estimated for the riparian area along the San Pedro River within the United States for 2002 and 2003 (Leenhouts and others, 2005). The transient budget is estimated from available data on ground-water withdrawals, irrigated area, riparian vegetation, and artificial recharge.

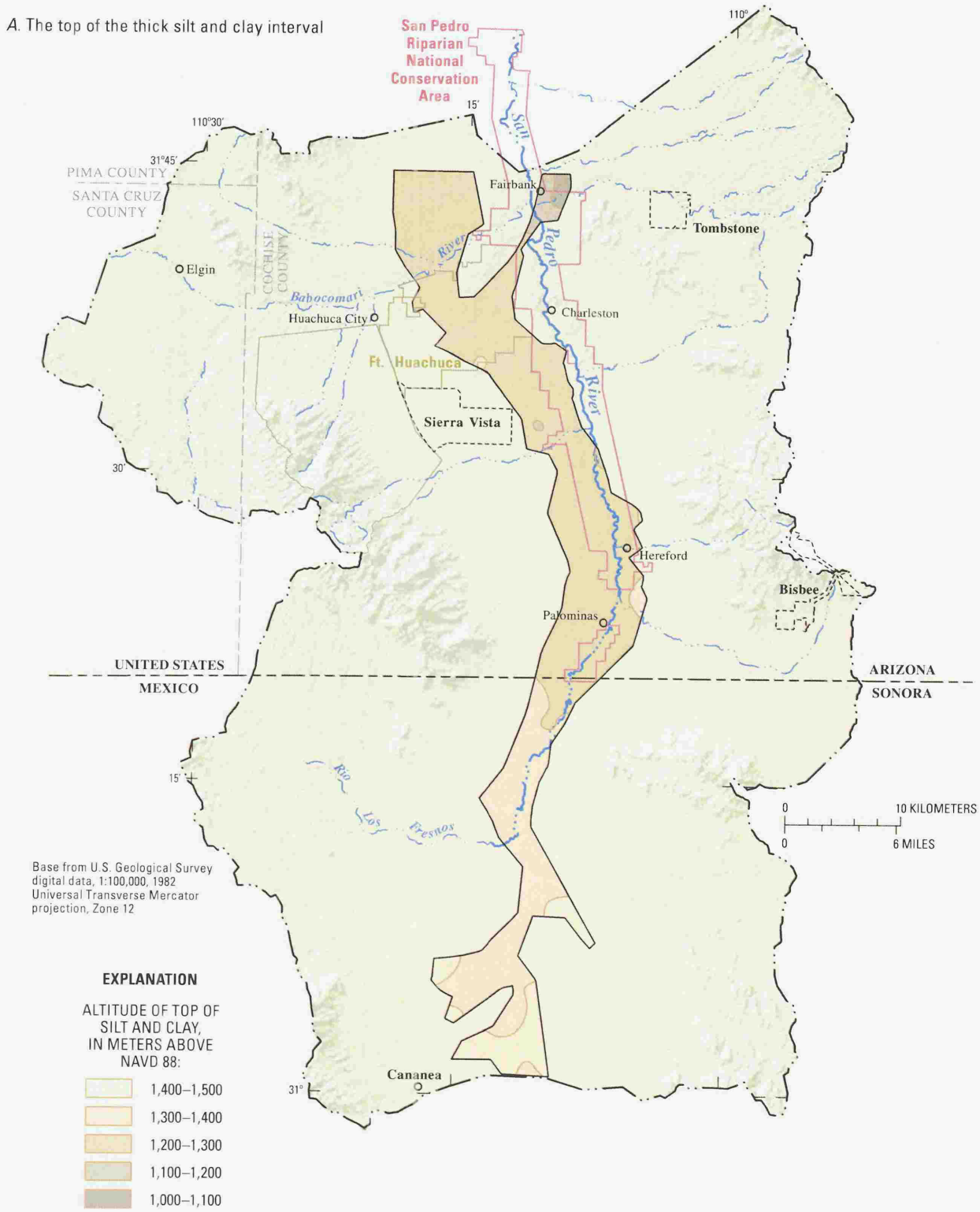

Figure 4. Extent and altitude of thick silt and clay interval in the basin fill, Upper San Pedro Basin, United States and Mexico. 4*A*, Top of thick silt and clay interval; 4*B*, Base of thick silt and clay interval.

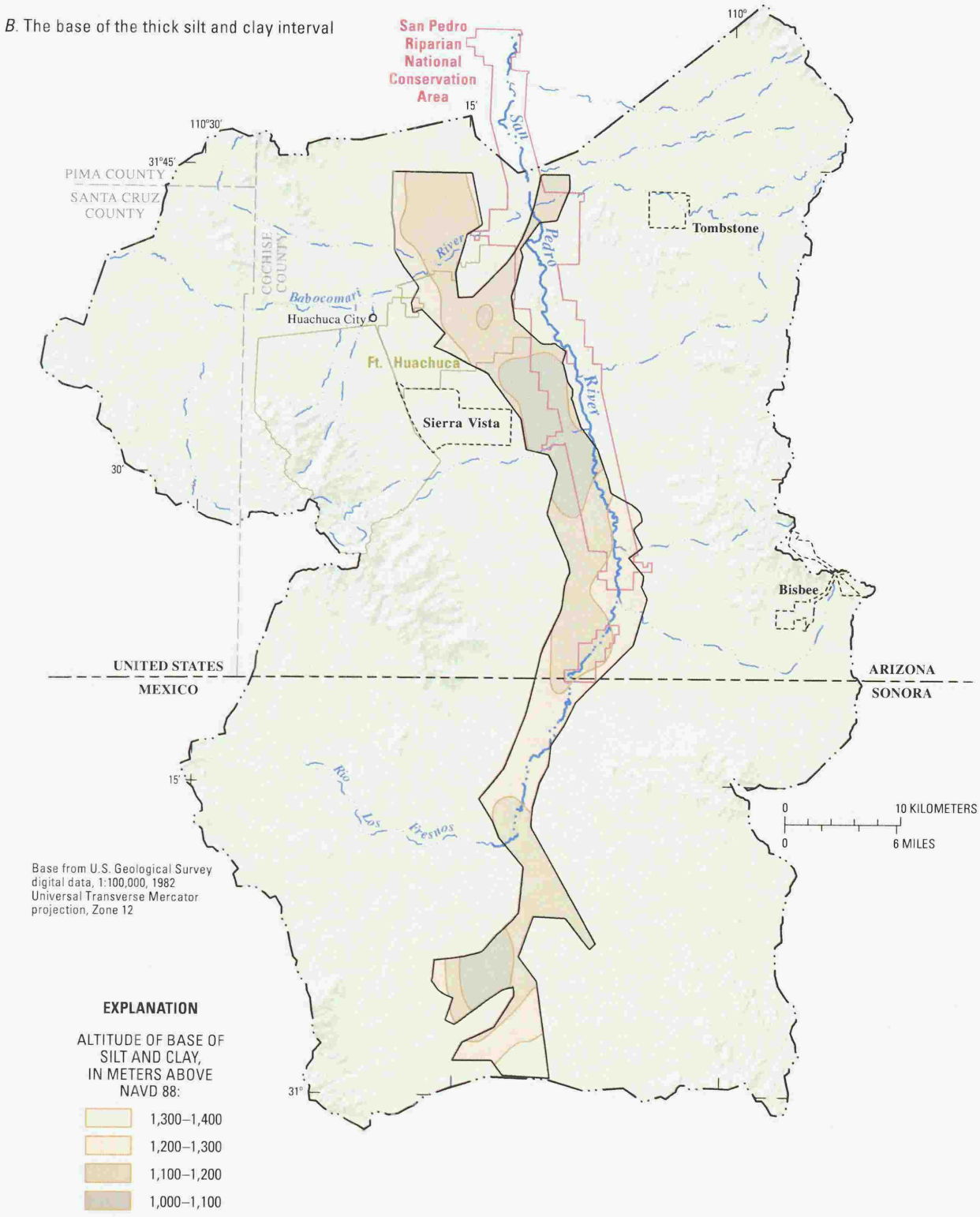

Figure 4. Continued.

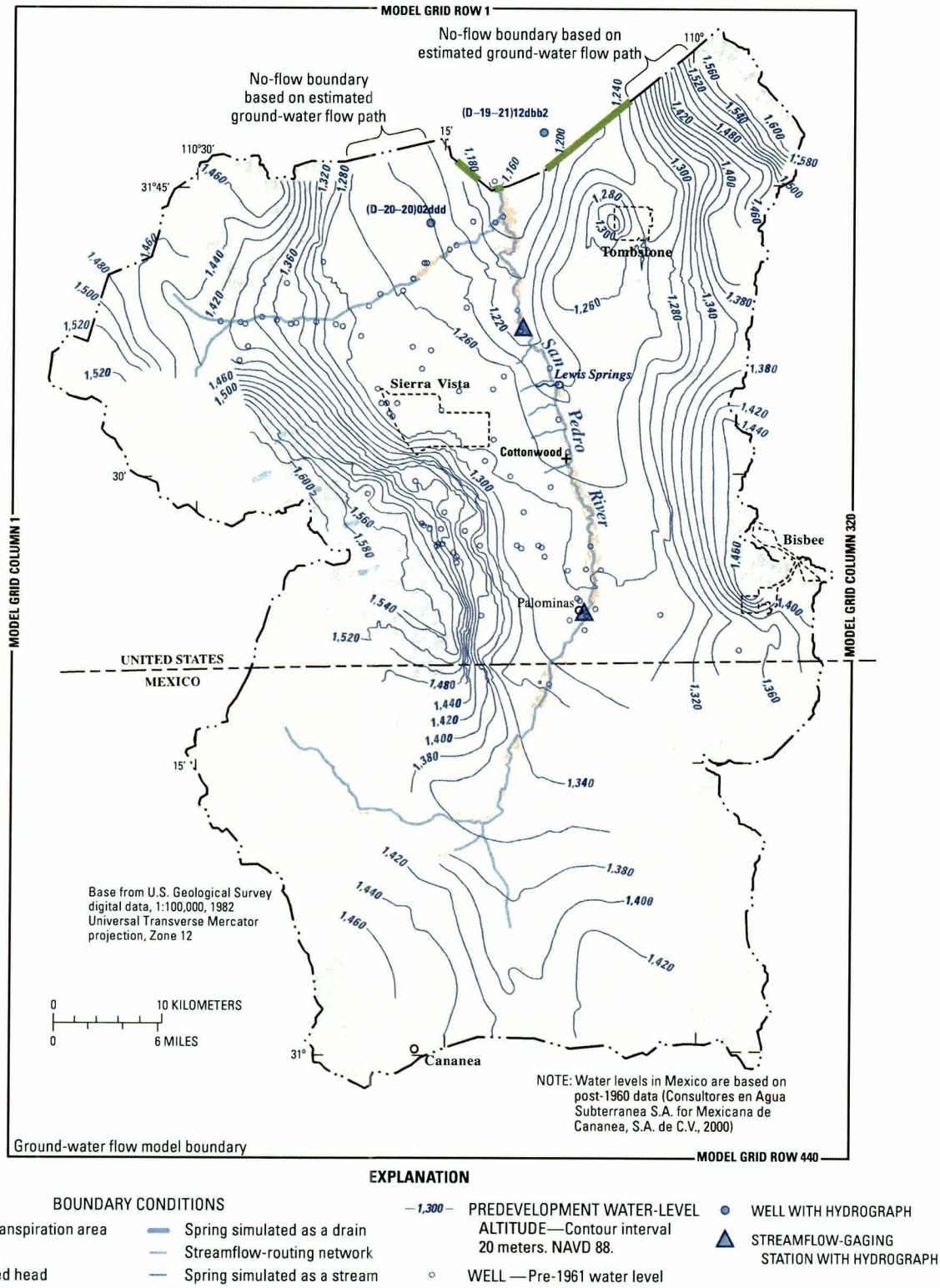

Figure 5. Ground-water flow system, boundary conditions for the model, streamflow-routing network, evapotranspiration areas, and predevelopment water-level comparison sites, Upper San Pedro Basin, United States and Mexico.

Predevelopment

A predevelopment steady-state period is difficult to define in the Upper San Pedro Basin because of documented stream-channel incision, observed variations in stream baseflow, estimated variations in evapotranspiration rates, and the uncertain transient effects of early withdrawals at mines for dewatering purposes. Stream-channel incision prior to 1900 and subsequent widening of the stream channel through the mid-1950s (Hereford, 1993) likely induced ground-water level decline and increased rates of baseflow discharge from the ground-water system for an undetermined period. Previous studies of the aquifer system have assumed that steady-state conditions existed during 1940, prior to extensive development of the ground-water supply (Freethey, 1982; Corell and others, 1996; Goode and Maddock, 2000). Variations in baseflow at Charleston since the mid-1930s, however, indicate that rates of discharge from the aquifer system changed throughout the period in response to changing rates of recharge and discharge (Pool and Coes, 1999). One likely cause of variations in discharge rates is climate-induced variations in recharge that occur on decadal (PDO) and more frequent (ENSO/El Niño) scales (Hanson and others, 2004; Dickinson and others, 2004; Pool, 2005). The steady-state period assumed by previous investigations to occur in 1940 was a wet year at the end of a decadal wet period. Mine dewatering at Tombstone and near Bisbee prior to 1940 also caused changes to the ground-water flow system; however, the effects were largely unmonitored and uncertain. As a result of mine dewatering before 1940, hydrologic information for 1940 may not represent steady-state conditions. The predevelopment ground-water budget developed for the ground-water flow model described in this report includes the earliest data available as well as data from the streamflow-gaging station at Charleston during 1935–39 and estimates of evapotranspiration rates during 1935. Estimates of predevelopment discharge rates are assumed to be balanced by an equivalent recharge rate.

Discharge as ground-water underflow was estimated for three locations along the northern extent of the model area; the combined rate was about 4,000 m^3/d (table 2). Ground-water discharge through basin fill east of the San Pedro River was estimated to be equivalent to recharge in the Walnut Gulch Watershed, about 2,700 m^3/d. Ground-water discharge from the Sierra Vista subwatershed through stream alluvium at the streamflow-gaging station near Tombstone is 1,000 m^3/d on the basis of previous estimates (Corell and others, 1996). Spring discharge measurements of 300 m^3/d (John Sottilare, Hydrologic Technician, U.S. Bureau of Land Management, written commun., 2005) at the northern extent of the modeled area were used to estimate minimum rates of ground-water discharge through basin fill west of the San Pedro River. Additional unaccounted ground water may flow through basin fill south of the springs.

Natural discharge of ground water occurs as baseflow to the San Pedro and Babocomari Rivers, at several springs near the San Pedro River, and at several springs in the Huachuca Mountains (fig. 5). San Pedro River baseflow at the Charleston and Palominas streamflow-gaging stations (fig. 5) varied seasonally with evapotranspiration demands and near-stream agricultural withdrawals. Stream baseflow at the Charleston streamflow-gaging station varied seasonally during 1936–40 from about 35,750 m^3/d during the winter to about 8,661 m^3/d during June and averaged about 19,900 m^3/d annually. Stream baseflow to the Babocomari River is not well documented but is estimated to be about 8,300 m^3/d on the basis of an analysis by Schwartzman (1990). Discharge to springs that issue from the basin fill near Lewis Springs and springs in the Huachuca Mountains (fig. 5) was much less than that in the other discharge areas and averaged about 1,500 m^3/d (table 2).

The predevelopment rate of ground-water discharge is poorly defined. Previous investigations of the Upper San Pedro basin in the United States and Mexico have estimated about 26,400 m^3/d of ground-water discharge through riparian evapotranspiration (Freethey, 1982; Esparza, 2002; table 2). Previous investigations of changes in the riparian area in the San Pedro Valley (Reichardt and others, 1978) and recent comparisons of repeat aerial photographs in the Sierra Vista subwatershed (Russ Scott, Research Hydrologist, Agriculture Research Service, written commun., 2005) indicate that predevelopment evapotranspiration rates may be as little as 40 percent of post-1970 rates.

Total annual discharge from the predevelopment system was about 60,600 m^3/d, which included estimated discharge components of 4,000 m^3/d for ground-water discharge, 28,700 m^3/d for baseflow discharge to streams and springs, and 26,400 m^3/d for evapotranspiration through riparian vegetation (table 2). The annual rate of recharge to the ground-water flow system was equivalent to the annual rate of ground-water discharge, 60,600 m^3/d, provided that steady-state conditions existed during predevelopment.

Table 2. Estimated predevelopment ground-water budget.

[cubic-meters per day]

Water-budget component	Average annual	
	Inflow	Outflow
Recharge[1]	60,600	0
Stream baseflow[2]	0	28,700
Evapotranspiration	0	26,400
Ground-water underflow	0	4,000
Drains[3]	0	1,500
Storage[4]	0	0
TOTAL	60,600	60,600

[1]Recharge is estimated as equivalent to the estimated outflow components.

[2]Stream baseflow represents net baseflow because predevelopment gaining and losing reaches are poorly defined.

[3]Drains include discharge at several springs in the Huachuca Mountains.

[4]Storage inflow represents removal from storage and input to the ground-water flow system. Storage outflow represents removal from the ground-water flow system and input to storage. No storage change is assumed to occur during predevelopment.

Postdevelopment

The postdevelopment ground-water budget includes variations in natural and artificial recharge rates, evapotranspiration, and ground-water withdrawals. Variations in natural recharge (Hanson and others, 2004; Dickinson and others, 2004; Pool, 2005) were not considered in this analysis, but may contribute significantly to water-level and stream-baseflow trends. Variations in artificial recharge were considered and result from changes in the amounts of infiltration of excess irrigation water, sewage effluent near municipalities, waste water at individual domestic septic systems, and water discharged from mines for dewatering purposes. Variations in evapotranspiration rates are not well known for most of the postdevelopment period, but variations were estimated on the basis of vegetative mapping that was done at different times. Variations in ground-water withdrawals were estimated on the basis of both monitored and estimated withdrawals. Except for documented withdrawals at mines and at Fort Huachuca, ground-water withdrawals prior to about 1970 were estimated by using data from previous publications. After about 1970, withdrawals were documented for the mines and for Fort Huachuca, and deliveries of ground-water withdrawals were documented for municipal water systems and private water companies. Withdrawals for other uses, including irrigation and private use, were estimated on the basis of previous investigations. Variations in all water-budget components, except natural recharge, were estimated for 1902–2002.

Artificial Recharge

Artificial recharge in the study area occurs as the result of infiltration of excess irrigation water; sewage effluent near Sierra Vista, Fort Huachuca, Tombstone, Bisbee, and Naco; waste water at individual domestic septic systems; and water discharged for dewatering purposes from mines near Bisbee and Tombstone. Incidental recharge also occurs in the distribution of potable water from supply wells to individual users. Water providers report deliveries to individual users rather than well withdrawals, therefore, incidental recharge from the distribution systems is implicitly included by reported deliveries.

Recharge of excess irrigation water occurred primarily in the agricultural areas near the San Pedro River near Palominas and in Sonora, Mexico (fig. 1). Recharge occurred also at Warren Ranch near Bisbee beneath agricultural fields that were irrigated with water pumped from mine workings during 1905–87. Recharge of irrigation water occurred also beneath golf courses. Rates of recharge from excess irrigation depend on irrigation practices and efficiencies. Previous ground-water flow models of the area assumed that irrigation efficiencies were about 70 percent, which resulted in 30 percent of the irrigation withdrawals returning to the aquifer through deep percolation (Freethey, 1982; Corell and others, 1996; Goode and Maddock, 2000). Deep percolation beneath golf courses near Naco, Sierra Vista, and Fort Huachuca was estimated as 1.4×10^{-3} m/d to the turf area (Phelps Dodge Corporation, 1998).

Recharge from deep percolation of sewage effluent occurred at individual septic systems and below sewage treatment facilities at Sierra Vista, Naco, Bisbee, Fort Huachuca, Huachuca City, and Tombstone (fig. 1). Effluent treated prior to 1970 was typically discharged into ephemeral channels. Improved facilities often used treated effluent to irrigate turf and crops, or discharged it to evaporation or infiltration ponds. Since early treatment records were unavailable, the average of recent estimates of multiple municipal effluent-recharge rates in the Sierra Vista subwatershed (Arizona Department of Water Resources, 2005), which was 14 percent of total delivered withdrawals, was used to estimate recharge rates. The City of Sierra Vista began treating sewage effluent in 1967, increased the capacity with an additional facility in 1978, and converted the treatment facility to a recharge facility in 2001. During 1967–79, effluent was discharged into a nearby ephemeral channel. Beginning in 1980, effluent was disposed of through irrigation of 3.4×10^6 m^2 near the facility. Beginning in July 2002, effluent was discharged to recharge basins and recharged at a rate of 2,960 m^3/d (Arizona Department of Water Resources, 2005). Effluent was discharged to ponds near Naco and Bisbee beginning in about 1930 (Phelps Dodge Corporation, 1998); however, the Bisbee effluent ponds were outside of the watershed. Effluent was recharged at Fort Huachuca during 1978–95 at two turf sites, a golf course and parade grounds, and below the treatment facility at rates of about 1,360 m^3/d (United States Department of Defense, 2002). During 2001, about 1,825 m^3/d, or approximately 33 percent of withdrawals, was estimated to have been recharged. Treatment facilities at Huachuca City discharge to evaporation ponds where little recharge occurs (Arizona Department of Water Resources, 2005). Treatment facilities at Tombstone began discharging effluent into Walnut Gulch in 1972. Recharge at individual septic systems was estimated to be 14 percent of withdrawals on the basis of estimates made for a decision support system developed for the Upper San Pedro Partnership (Kevin Lansey, professor, University of Arizona Department of Civil Engineering and Engineering Mechanics, written commun., 2005).

Evapotranspiration

Evapotranspiration from riparian vegetation near the San Pedro and Babocomari Rivers was defined by investigations that mapped historical extents of riparian vegetation and recent extents and evapotranspiration rates for several riparian-vegetation types. Unpublished maps of riparian-vegetation extent in 1935 were available from the Arizona Department of Water Resources. Several studies of riparian vegetation were used to estimate change, including those by Reichardt and others (1978), U.S. Army Corps of Engineers (2001), Kepner and Edmonds (2002), and Leenhouts and others (2005).

The extent of riparian vegetation changed during the 20th century. Reichardt and others (1978) evaluated total-acreage changes for dense riparian vegetation and other land uses by using aerial photographs taken in 1935, 1966, and 1977. Total dense riparian land along the San Pedro River in the United States increased by 79 percent from 1935 to 1966 and increased by more than 100 percent from 1935 to 1978. Comparable results were derived from comparing 2001 maps (U.S. Army Corps of Engineers, 2001) with 1935 aerial photographs, which indicated the extent of riparian vegetation had increased by 150 percent within the Sierra Vista subwatershed (Russ Scott, research hydrologist, Agriculture Research Service, written commun., 2005). Results of vegetation-type mapping across the Upper San Pedro Basin from Landsat satellite photos taken in 1973, 1986, 1992, and 1997 (Kepner and Edmonds, 2002) indicate mesquite landcover increased significantly and riparian landcover decreased about 20 percent during 1973–86 but recovered to 106 percent of the 1973 coverage during 1992–97.

Changes in extent of riparian vegetation imply variations in rates of evapotranspiration. Estimates of changes in rates of riparian evapotranspiration, however, require information on changes in the extent and density of several vegetation types that use ground water from different depths and at different rates. Major vegetation types within the riparian area that use ground water at different rates include mesquite, cottonwood and willow, and sacaton grass. Detailed maps of each vegetation type are not available for the 1935 period; therefore, estimates of change in riparian evapotranspiration can only be derived from available information that documents change in the extent of riparian vegetation. The most recent and accurate estimates of evapotranspiration rates are available from Leenhouts and others (2005). Estimated rates of evapotranspiration within the Sierra Vista subwatershed range from 32,400 to 40,700 m^3/d during 2003, but rates vary annually by as much as 30 percent on the basis of 3 years of data. An estimate of the rate of evapotranspiration in the part of the basin in Mexico is 4,500 to 5,700 m^3/d, assuming rates of riparian evapotranspiration per unit area in the Mexico part of the basin are the same as rates in the Sierra Vista subwatershed. Total estimated evapotranspiration in the model area during 2003 ranges from 37,000 to 46,000 m^3/d, which is 50–90 percent greater than the predevelopment estimate of 26,400 m^3/d. The percent difference between estimated predevelopment and 2003 rates of evapotranspiration is similar to the estimated percent change in extent of riparian vegetation; both values suggest that recent evapotranspiration rates within the model area may be about twice the evapotranspiration rates during 1935.

Ground-Water Withdrawals

Demand for ground water in the study area is divided into five main categories: (1) mine withdrawals from mines near Tombstone, Bisbee, and Cananea, which also includes withdrawals for municipal and domestic use; (2) agricultural withdrawals for irrigated areas primarily near the San Pedro River; (3) municipal and industrial withdrawals by water purveyors for deliveries within incorporated cities and some adjacent unincorporated areas; (4) Fort Huachuca withdrawals for military use; and (5) withdrawals in the Sierra Vista subwatershed from domestic wells in unincorporated areas and stock wells (figs. 1 and 6). Withdrawals prior to about 1940 were dominated by mine dewatering near Tombstone and Bisbee. Large volumes of ground water withdrawn for other purposes became possible with the widespread use of high-powered pumps around 1940. Subsequent increases in agriculture, municipal, military, and industrial water demands have been met by drilling new wells and installing well pumps with larger capacities. Total ground-water withdrawals in the study area varied from about 38 to 55 hm^3/yr (30,800 to 46,000 acre-ft/yr) during 1979–2002 and peaked in 1988 (fig. 6).

Ground-water withdrawals were estimated by using historical data from previous studies. Withdrawals in the Sierra Vista subwatershed generally were estimated by using indirect estimates for agricultural use and reported population to indicate pumping volumes for domestic withdrawals in unincorporated areas. Reported- and metered-delivery records from water suppliers were used when available. Records of withdrawals at the Tombstone and Copper Queen mines were available from Hollyday (1963) and Southwest Ground-water Consultants (2004), respectively. Annual withdrawals for all uses were estimated in previous studies for the period 1940–97. Withdrawals for different periods were apportioned for this study by using information from several previous studies, including those for 1940–77 by Freethey (1982), 1978–88 by the Arizona Department of Water Resources (1990), 1989–90 by Corell and others (1996), 1991–97 by Goode and Maddock (2000), and 1998–2002 by Arizona Department of Water Resources (2005). Withdrawals for use at the Cananea mine and domestic and agricultural uses in Mexico were reported by Esparza (2002). Withdrawals for the Cananea mine were used, in part, for the City of Cananea. Reported and metered withdrawals in the Sierra Vista subwatershed for 1998–2002 were estimated by deliveries of public-water purveyors reported to the Arizona Corporation Commission. Fort Huachuca withdrawals have been documented since 1940 (Mike Shaughnessey, Directorate of Public Works Real Property Office, U.S Army Garrison, Fort Huachuca, Arizona, written commun., 2003). Data for domestic use in unincorporated areas of the Sierra Vista subwatershed was provided by the Arizona Department of Water Resources for 1990 and 2002 (Arizona Department of Water Resources, 2005).

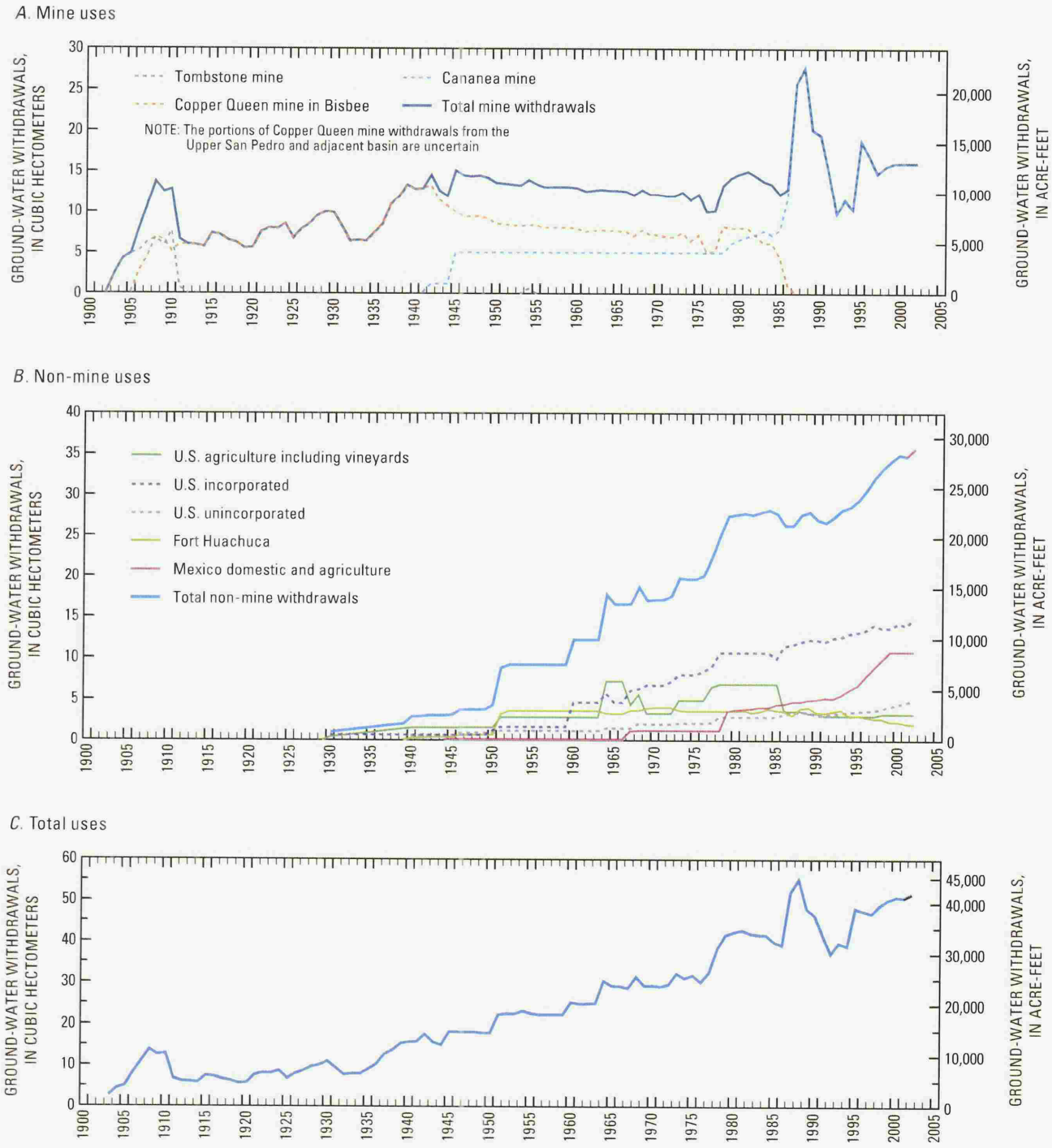

Figure 6. Annual ground-water withdrawal rates for selected uses, 1902 to 2002, Upper San Pedro Basin, United States and Mexico. 6*A*, Mine uses; 6*B*, Non-mine uses; 6*C*, Total uses.

Withdrawals for dewatering of mines and other mining uses exceeded all other withdrawals in the study area during 1902–60 (fig. 6). The earliest mining withdrawals began with pumping 44 hm^3 (35,700 acre-ft) of water from the underground mine workings at Tombstone during 1902–11. Additional small amounts of withdrawals occurred from the mines at Tombstone during later periods. Water was withdrawn from the Copper Queen mine at Bisbee to dewater the mine workings and for leaching operations during 1906–87 at rates that ranged from 1 hm^3/yr to more than 62 hm^3/yr (800–16,400 acre-ft/yr). The withdrawals, however, were likely derived from both the Upper San Pedro and adjacent ground-water flow systems because the withdrawals straddle the surface-water divide between the basins. The part of the withdrawals that were derived from each ground-water basin is uncertain. Furthermore, low-permeability faults may isolate the water in rocks of the mine from the regional aquifer (Southwest Ground-water Consultants, 2004), therefore, withdrawal of water from storage at the mine should have little influence on the regional aquifer in the Upper San Pedro Basin.

Ground-water withdrawals from the Cananea mine and City of Cananea began in 1940 and increased to 7.8 hm^3/yr (6,300 acre-ft/yr) in 1985 (fig. 6). Withdrawal rates increased significantly during 1986–2002 and ranged from 12 to 27 hm^3/yr (9,700-21,800 acre-ft/yr, Esparza, 2002). Ground water was withdrawn near Cananea from many wells that tap the basin fill throughout a large area between Sierra San Jose and Sierra Mariquita (fig. 1).

Agricultural withdrawals were determined by using previous estimates, crop consumptive-use rate, irrigated area determined from aerial photographs, remote sensing, and agricultural surveys in the United States portion of the study area. The most accurate data are available from field surveys conducted in the United States in the late 1980s and in 2002 by the Arizona Department of Water Resources (Arizona Department of Water Resources, 1990 and 2005). Other useful data included aerial photographs in the United States from 1935 and Landsat scenes of the entire study area for 1973, 1986, 1992, and 1997 (Kepner and Edmonds, 2002). Total rates of irrigation withdrawals during 1930–86 were derived from previous estimates in the United States (Freethey, 1982; Corell and others, 1996; Goode and Maddock, 2000). Total rates of agricultural withdrawal were estimated on the basis of 70-percent irrigation efficiency for nondeficit irrigation and 100-percent efficiency for deficit irrigation. The residual 30 percent of withdrawals was assumed to infiltrate and return to the aquifer. Consumptive-use rates in the United States were assumed to be 1.00 m/yr for all agriculture, except for some fields in the Palominas and Hereford area that were determined to be deficit irrigated in 2002 (Arizona Department of Water Resources, 2005). Deficit irrigation implies that all applied irrigation water is transpired by the crops, and no water recharges the aquifer. Consumptive-use rates for fields under deficit irrigation in 2002 were assumed to be 0.79 m/yr during 1986–2002 (Arizona Department of Water Resources, 2005) and 1.00 m/yr prior to 1986.

The earliest agriculture in the Sierra Vista subwatershed was likely in the Warren Ranch area south of Bisbee, which was irrigated with water pumped from the Copper Queen mine at Bisbee beginning in 1905 (Southwest Ground-water Consultants, 2004). Aerial photos indicate that several hundred hectares (a few hundred acres) of agricultural land near Hereford may have been actively irrigated in 1935 (Arizona Department of Water Resources, unpublished aerial photographs, 2005) and, therefore, that withdrawals from the regional aquifer in this area began before 1935. The initiation of irrigation in the Hereford area is uncertain, and for this analysis agricultural withdrawals were assumed to have begun in 1930. Irrigation of other areas in the United States and Mexico was assumed to have begun in 1940. Rates of total ground-water withdrawals for agriculture in the United States portion of the study area was about 2 hm^3/yr (1,600 acre-ft/yr) or less before 1950, about 3–4 hm^3/yr (2,400 to 3,200 acre-ft/yr) during 1950–63, about 3–7 hm^3/yr (2,400– 5,700 acre-ft/yr) during 1964–85, and about 3 hm^3/yr (2,400 acre-ft/yr) during 1986–2002 (fig. 6).

Agricultural withdrawal rates in the Mexico portion of the study area were derived from Esparza (2002) for the post-1980 period and were distributed across agricultural areas near Rio Los Fresnos and the San Pedro River defined by Kepner and Edmonds (2002). Mexico agriculture during 1940–80 was assumed to be in the same locations documented by Kepner and Edmonds (2002) and to increase at the same rate as agriculture in the United States. Rates of total ground-water withdrawals for domestic and agricultural uses in Mexico increased about 3.5 hm^3/yr (2,800 acre-ft/yr) in 1980 to more than 10 hm^3/yr (8,100 acre-ft/yr) during 1999–2002 (fig. 6).

Deliveries of withdrawals for domestic and industrial uses in incorporated areas of the United States increased from less than 2 hm^3/yr (1,600 acre-ft/yr) before 1960, to about 5 hm^3 (4,100 acre-ft) in 1960, to 12 hm^3 (9,700 acre-ft) in 1989, and to 14.9 hm^3 (12,100 acre-ft) in 2002 (fig. 6). Incorporated areas in the United States include Sierra Vista, Huachuca City, Tombstone, and Bisbee (fig. 1).

Fort Huachuca withdrawals have been documented since 1940. Most of the wells are near Highway 90 and a few are across the eastern range of the facility (fig. 1). Early withdrawals included wells east of Highway 90. Later withdrawals were at wells near Highway 90. Annual rates of withdrawals increased from less than 1 hm^3/yr (800 acre-ft/yr) before 1951, to 3.6 hm^3 (2,900 acre-ft) in 1951, to a maximum of 4 hm^3 (3,200 acre-ft) in 1989, and decreased thereafter to less than 2 hm^3 (1,600 acre-ft) in 2002 (fig. 6).

Domestic withdrawals in unincorporated areas in most of the United States portion were estimated for later years by using Arizona Department of Water Resources reports (1990–2005) and estimated for earlier years by calculating the difference between estimated withdrawals for other uses and

total withdrawals. Unincorporated withdrawals in the United States increased from less than 1 hm^3/yr (800 acre-ft/yr) before 1950 to about 2 hm^3/yr (1,600 acre-ft/yr) during 1968–77 and 4.9 hm^3/yr (4,000 acre-ft/yr) in 2002 (fig. 6).

Simulation of Ground-Water Flow

Ground-water flow was simulated by using MODFLOW 2000 (MF2K; Harbaugh and others, 2000 a,b). MF2K uses finite-difference numerical methods to solve the ground-water flow equation throughout a discretized three-dimensional grid that represents the aquifer system. MF2K is a modular modeling system that has many processes and packages available to simulate many possible conditions that might affect ground-water flow. Simulation of the ground-water flow system in the study area required several packages for the processes of recharge, drains, general-head boundaries, streams (Prudic, 1989), and evapotranspiration.

Previous Models

Several published numerical models simulate ground-water flow in the Upper San Pedro Basin. The earliest was a two-dimensional model of ground-water flow within the alluvial aquifer of the Sierra Vista subwatershed during 1940–78 (Freethey, 1982). This model was a generalized model that was one of many constructed to compare ground-water flow systems in alluvial basins in southern Arizona as part of the U.S. Geological Survey Southwest Alluvial Basins Regional Aquifer-System Assessment (Anderson and others, 1992). All later numerical models use the same or similar assumptions and conceptual model of the ground-water flow system as the initial model by Freethey (1982). Later models extended the simulation period beyond 1978, however, and included a more detailed horizontal and vertical discretization of the system. Later numerical ground-water models of the Sierra Vista subwatershed included those developed by Vionnet and Maddock (1992) and Corell and others (1996). Goode and Maddock (2000) simulated ground-water flow in the alluvial aquifer of the entire Upper San Pedro Basin, including Mexico. Esparza (2002) simulated ground-water flow in the Mexico portion of the alluvial aquifer.

Lack of information required that previous models incorporate a simplified conceptualization of the ground-water flow system. All recharge was assumed to occur near the mountains and to be constant through time. The influence of silt and clay layers on ground-water flow and the distribution of gaining and losing reaches of the rivers was not recognized. Little information was available to describe the vertical distribution of hydraulic head and ground-water flow. As a result, the simulation of the vertical distribution of ground-water flow was not important in previous models. The vertical component of ground-water flow was simulated, however, by using as many as four layers. Ground-water flow through the permeable rocks in the mountains and flow through basin fill that underlies the silt and clay was not simulated in previous models. Springs that discharge from the regional aquifer and carbonate rocks were not simulated. Stress conditions, including ground-water withdrawals and stream baseflow, were simulated as average-annual or average conditions during multiple years.

Model Framework

Model Boundaries

The area of the simulated ground-water flow system includes the portion of the Upper San Pedro Basin in Mexico, the Sierra Vista subwatershed in the United States, and a small portion of the Benson Subwatershed that lies north of the Babocomari River and between the Mustang Mountains and the San Pedro River. Simulated boundary conditions include no-flow at the lower model boundary and along most of the lateral model boundaries and specified head at the subwatershed outflow (fig. 5). The upper boundary is simulated as a water-table aquifer with evapotranspiration, streams, and drains. The upper boundary of the model is the land surface interpolated from 60-m DEMs for Mexico, and 1-m, 10-m, and 30-m DEMs for the United States. One-meter DEMs were only available for areas near the San Pedro River in the United States. Ten-meter DEMs were used for most of the area near the Babocomari River and along some major tributaries to the San Pedro and Babocomari Rivers.

No-flow conditions were assumed to occur at more than 1,500 m below land surface, at the surface-water divide of the upper San Pedro Basin, and at outcrops of impermeable rock near the San Pedro River. No-flow conditions also were assumed to occur along two ground-water flow paths at the northern boundary of the model. The region between the outcrops of impermeable rock near the San Pedro River and the drainage divide in the Whetstone Mountains was simulated as a no-flow boundary because water-level data indicated that the boundary approximates a ground-water flow path (fig. 5), and gravity data indicated a bedrock high exists in the region (Gettings and Houser, 1995). A portion of the northern subwatershed boundary that extends from near the Dragoon Mountains to the streamflow-gaging station near Tombstone was simulated as a no-flow boundary by using water-level data that indicated it approximates a ground-water flow path (fig. 5).

A portion of the boundary at the northern extent of the model was simulated as a specified-head flow boundary. Interpolated water-level data were used to estimate the specified head. Head values were assumed to be constant throughout the simulation period because water levels varied less than 2 m at wells (D-19-21)12dbb2 and (D-20-20)02ddd (fig. 5) during 1960–2001 with no apparent trend (Barnes and Putman, 2004).

Spatial and Temporal Discretization

The model domain was discretized into grids in the horizontal and vertical dimensions. Horizontal discretization was 250 m throughout the model extent resulting in grids that included 440 rows and 320 columns (fig. 5). The model domain was discretized vertically among five layers where ground-water flow is primarily horizontal through laterally extensive hydrogeologic units (fig. 3). The spatial extent of model layers was determined by the saturated extent of the hydrogeologic units. Extents generally were limited to regions of each hydrogeologic unit where the saturated thickness was a minimum of 10 m. Saturated thickness was based on winter 2002 water-level data for the United States and on water levels in Mexico reported in a hydrogeology report of the area (Consultores en Agua Subterranea S.A. for Mexicana de Cananea, S.A. de C.V., 2000). Layer 5 encompassed the entire simulated area. Each successively shallower layer included a shallower hydrogeologic unit and a less extensive area. The extent of each layer was nested within the extent of the next deeper layer to allow ground-water flow between vertically adjacent layers.

The simulation of transient ground-water conditions included the earliest known withdrawals from the aquifer that began in December 1902 (Hollyday, 1963) and continued through February 2003. Transient stresses included artificial recharge and seasonal ground-water withdrawals by evapotranspiration and wells. Each of the transient stresses varied in magnitude, which was represented by temporal discretization throughout the transient simulation. Temporal discretization in MF2K included stress periods and time steps. Stress periods for this model included two seasons per year. Spring/summer conditions were from March 12 to October 15 of each year. The remaining period represented fall/winter conditions. The greatest annual rate of ground-water withdrawal for evapotranspiration and wells was during the spring/summer period. The fall/winter period had low rates of evapotranspiration, no agricultural ground-water withdrawals, and reduced rates of withdrawal for domestic and municipal supply. The ground-water flow equation was solved by MF2K for each of 10 time steps in each seasonal stress period. Multiple time steps allowed more accurate simulation of the transient system response to variations in stresses and reduced computational errors in solving the ground-water flow equation.

Aquifer Hydraulic Properties

Key properties of the aquifer that control ground-water flow and response of the ground-water flow system to stresses were saturated thickness, horizontal hydraulic conductivity (K_h), vertical hydraulic conductivity (K_v), specific storage, and specific yield. Each property, except K_v, was spatially distributed throughout the model based on lithology represented by polygons in each model layer. K_v was calculated in the model by assuming a vertical anisotropy (K_h/K_v) for each lithology. Properties of each rock type vary within a range of values developed on the basis of published values. Additional detail beyond the lithologic polygons in the distribution of hydraulic properties was added by subdividing some polygons when hydrologic information, such as spatial variation in hydraulic gradients, indicated a need for additional variation in hydraulic properties.

Layer Distribution

The five model layers represent the primary hydrogeologic units and several lithologies within each layer (figs. 3 and 7). Layer 5 represents pre-Tertiary granite and metamorphic rock, limestone, sandstone, siltstone, mudstone, conglomerate, volcanic rock, and Tertiary Pantano formation and basin fill in areas along the margin of the alluvial basin where subsurface data are insufficient to define the base of the alluvium. Layer 4 represents sand and gravel of lower basin fill that lie adjacent to and underlie the thick interval of silt and clay within basin fill. Layer 4 includes stream alluvium and the silt and clay facies, sand, and gravel of basin fill in Mexico. Layers 2 and 3 represent the silt and clay facies of upper and lower basin fill, respectively, and include adjacent sand and gravel facies and interbedded facies within the Sierra Vista subwatershed. Layers 1, 2, and 3 are not defined in Mexico because of a lack of subsurface information. Layer 1 includes the stream alluvium and shallow unconfined ground water in the sand and gravel overlying the silt and clay of the upper basin fill within the Sierra Vista subwatershed. Each layer, except layer 1, was convertible between confined and unconfined ground-water flow conditions where no overlying layer exists, or where overlying layers were desaturated during the transient simulation. Layer 1 was simulated as a water-table aquifer throughout the extent of the layer.

The thickness of each layer was a function of the base and top surfaces of each layer and the water table. The land surface forms the top surface of each layer where no overlying layer exists; otherwise, the base of the overlying layer forms the top of each layer. The simulated base of layer 5 was uniformly 1,500 m below land surface. The base of layer 4 includes a large trough in the Sierra Vista subwatershed and a small trough in Mexico (fig. 7*B*). The large trough was asymmetric and had its lowest areas near the San Pedro River and west of the river where the river traverses the Tombstone Hills. The deepest areas of the large trough in layer 4 are as much as 500 m below the margins of the trough. The smaller trough in Mexico lies between the Sierra Mariquita and Sierra San Jose and has deep areas that are 350 m below the margins. The base of layer 3 includes three troughs (fig. 7*C*). The largest trough in layer 3 falls near and west of the San Pedro River in two areas: the Palominas-Hereford area and the area near Highway 90 (fig. 1), where the base of the trough was as much as 200 m lower than along the margins. Other troughs in layer 3 are north of the Babocomari River and near Fairbank where the lowest parts of the troughs were as much as 130 m lower than along the margins. The base of layer 2 includes

three troughs that are similar to those in layer 3 (fig. 7*D*). The largest trough in layer 2, near and west of the San Pedro River, includes the lowest areas that are as much as 200 m lower in the base than along the trough margins. The two other troughs, north of the Babocomari River and near Fairbank, include low areas where the base is as much as 130 m lower than the base along the trough margins (fig. 7*D*). The base of layer 1 (fig. 7*E*) slopes gradually upward from north to south along the San Pedro River at about the gradient of the stream. The base of layer 1 outside of the San Pedro River generally was flat where the layer represents sand and gravel of the basin fill near Palominas. Near Highway 90 and west of the San Pedro River, the base of layer 1 was as much as 60 m lower than it was near Palominas.

Saturated thicknesses of the layers are less than or equal to the maximum simulated thicknesses of 1,500 m in layer 5, 400 m in layer 4, 170 m in layer 3, less than 300 m in layer 2, and generally less than 100 m in layer 1. Where layer 5 was overlain by layer 4, the simulated thickness was between 1,100 and 1,490 m. Where layer 4 was overlain by layer 3, the simulated thickness was between 100 and 300 m. Elsewhere, layer 4 ranges from 10 to 400 m in thickness. The simulated thickness of layer 3 was limited by the base of layer 2 throughout the layer extent and varies between 10 and 130 m. Layer 2 was generally less than 180 m in thickness except in a region near Palominas and Hereford where the layer was as much as 310 m thick. The extent of layer 1 was generally less than 50 m in thickness, except where the layer represents sand and gravel overlying the silt and clay facies in the area near Highway 90 and west of the San Pedro River where the layer was more than 100 m thick. Layer 1 was 3–10 m thick along the San Pedro River where the layer represents the stream alluvium.

Transmissive Properties

Calibrated hydraulic conductivity values range from 0.0001 to 12.5 m/d (table 3). Granite and metamorphic rocks were assigned values ranging from 0.0001–0.050 m/d. Hydraulic conductivity estimates for the pre-Tertiary sedimentary rocks resulted from investigations in the Bisbee (Phelps Dodge Corporation, 1998) and Tombstone (Hollyday, 1963) areas. In the Bisbee area, hydraulic conductivity of the sandstone was simulated as 6.0 m/d, and the simulated hydraulic conductivity of the mudstone, siltstone, and conglomerate ranged from 0.18–0.9 m/d throughout an effective thickness of about 1,500 m (Phelps Dodge Corporation, 1998). In the Tombstone area, the simulated transmissivity of the sedimentary rocks ranged from about 900–11,000 m^2/d. An equivalent hydraulic conductivity, assuming an effective saturated thickness of about 1,500 m, was about 0.6–0.7 m/d. Calibrated hydraulic conductivity of pre-Tertiary sedimentary and volcanic rocks for this model included a range of values from 0.0001 to 0.625 m/d. Hydraulic conductivity of sedimentary rocks was 0.0006–0.625 m/d for limestone and 0.0001–0.15 m/d for other sedimentary rocks that include low-permeability mudstone and permeable conglomerate. Pre-Tertiary volcanic rock hydraulic-conductivity values ranged from 0.0001 to 0.063 m/d. Basin fill included a range of values from 0.0002 to 10.0 m/d for the sand and gravel facies. Silt and clay facies of the lower basin fill were assigned values of 0.001–0.01 m/d. Intervals in the upper basin fill dominated by silt and clay were assigned values of 0.05–1.0 m/d. Regions of interbedded basin fill were assigned hydraulic-conductivity values of 0.01–4.0 m/d in the lower basin fill and 0.02–4.0 m/d in the upper basin fill. Sand and gravel within the lower basin fill (conglomerate) were assigned values of 0.0001–6.25 m/d. Sand and gravel in the upper basin fill were assigned values ranging from 0.05 to 7.0 m/d. Stream alluvium was assigned values of 7.5 m/d for both the pre-entrenchment and post-entrenchment alluvium.

No horizontal anisotropy was simulated throughout the model, and vertical anisotropy values varied with lithology. Vertical anisotropy values (K_v/ K_h) ranged from 3.5 in some parts of the aquifer system dominated by sand and gravel to 122.5 in silt and clay facies of basin fill (table 3). Sedimentary, granitic, and metamorphic rocks were assigned vertical anisotropy values ranging from 5–17.5. Basin fill vertical anisotropy values ranged from 3.5 to 75 for sand and gravel facies, 8.8 to 122.5 for interbedded facies, and 3.5 and 122.5 for silt and clay facies, respectively. Stream alluvium was assigned anisotropy values ranging from 3.5 to 22.5.

The overall ability of the aquifer system to transmit ground water was determined by the spatial distribution of transmissivity (fig. 8), which was the product of saturated layer thickness and hydraulic conductivity. The overall transmissive properties of the regional aquifer estimated for this model are similar to those of previous models. Values of total transmissivity range from about 1 to 2,000 m^2/d. Low values, less than 50 m^2/d, generally coincide with regions of sedimentary and crystalline rock and parts of the basin fill that have large thicknesses of silt and clay. Regions having transmissivity values that range from 50 to 1,000 m^2/d are associated with regions of basin fill surrounding the regions of silt and clay and thick sequences of sandstone and conglomerate. The highest values of transmissivity, 1,000–3,000 m^2/d, are associated with the thick regions of sand and gravel that surround the regions of silt and clay.

Storage Properties

Two types of storage properties were assigned to model cells to simulate the movement of water into and out of storage in pore spaces with variation in hydraulic head. Specific-yield values were assigned to represent the ratio of drainable pore spaces to total cell volume when the water table intersects the cell. Specific-storage values also were assigned to each cell to represent the change in storage of water that results from expansion and contraction of the aquifer skeleton and water within the aquifer.

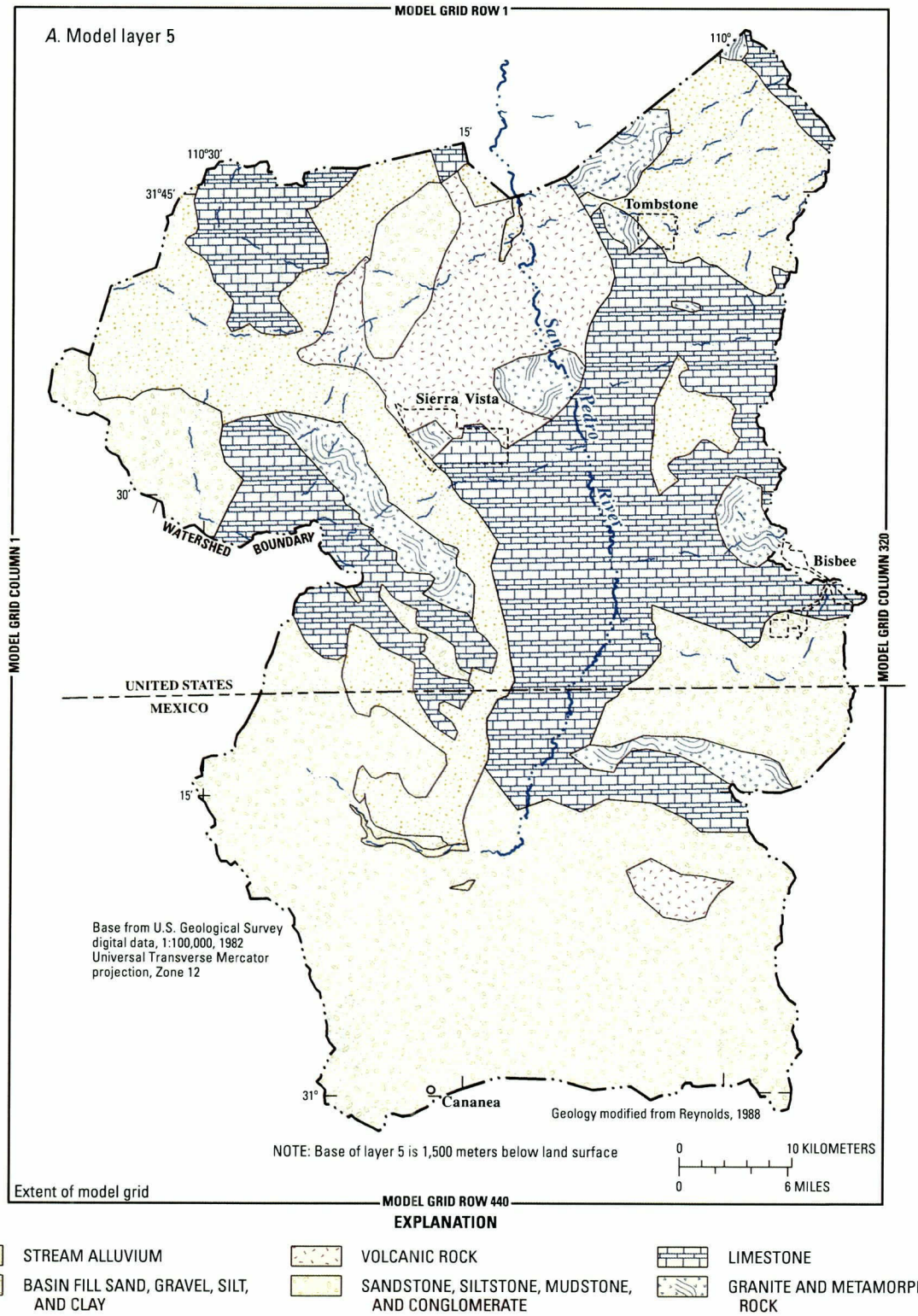

Figure 7. Extent and lithology of hydrogeologic units and altitude of the base of numerical model layers, Upper San Pedro Basin, United States and Mexico. 7A, Model layer 5; 7B, Model layer 4; 7C, Model layer 3; 7D, Model layer 2; 7E, Model layer 1.

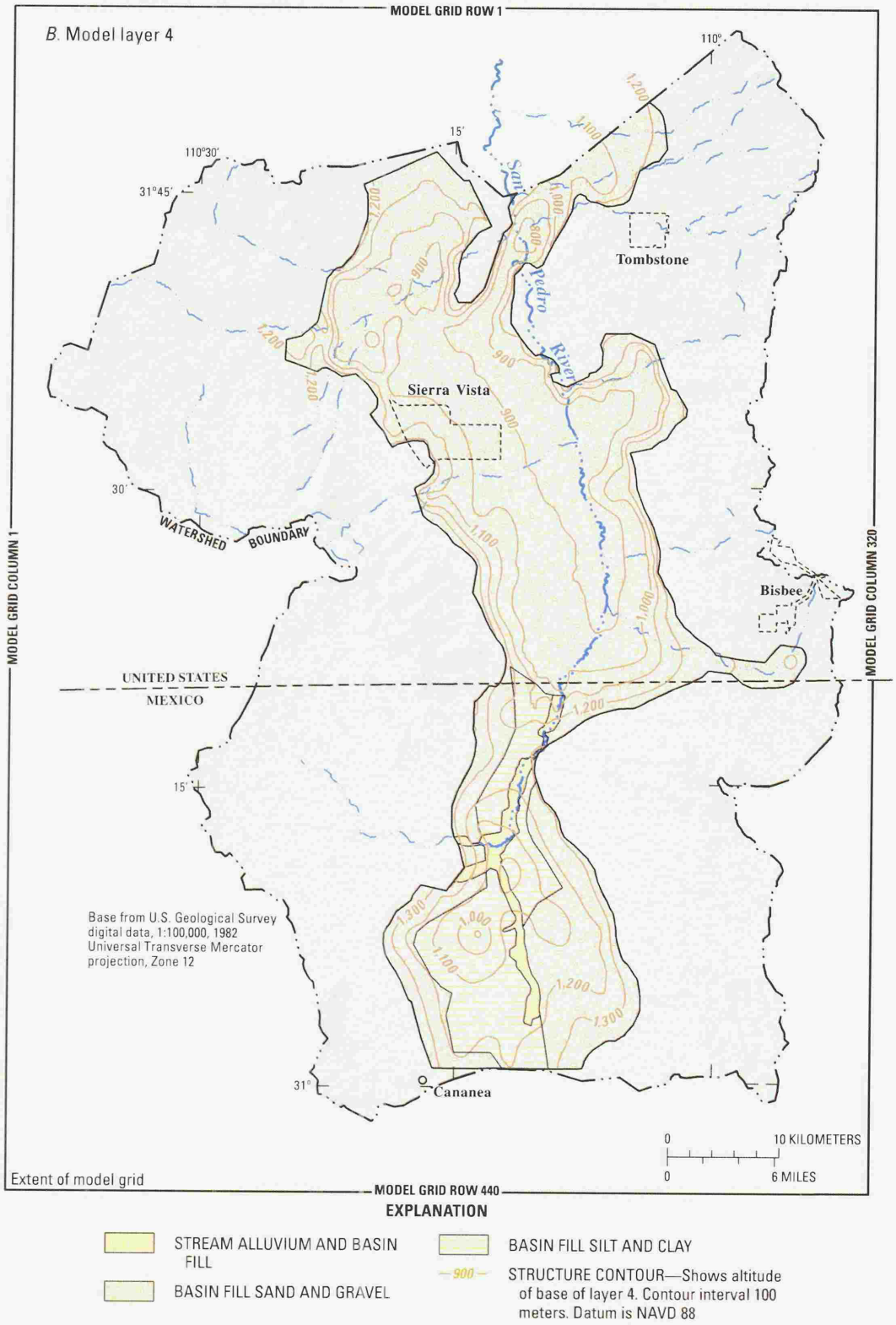

Figure 7. Continued.

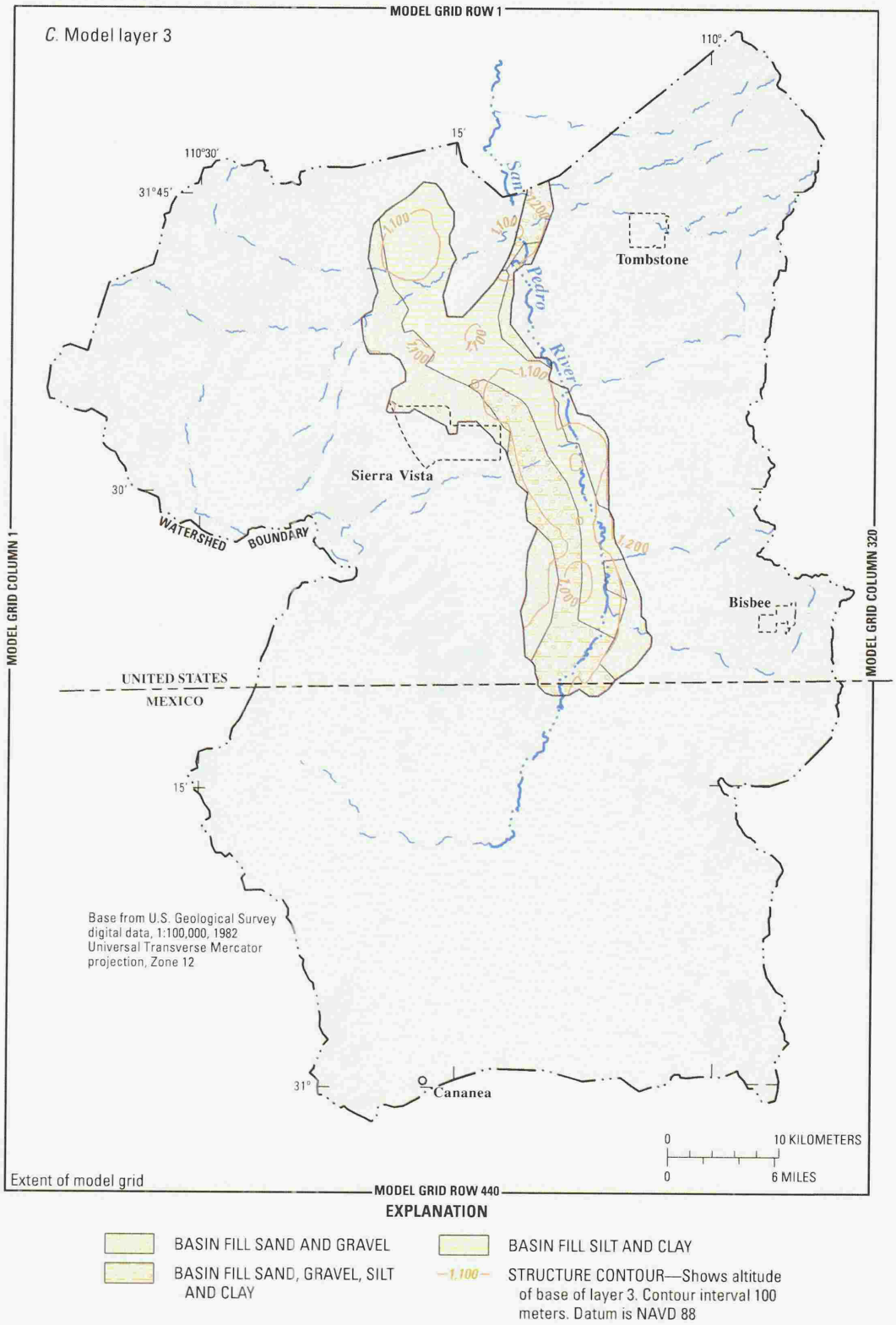

Figure 7. Continued.

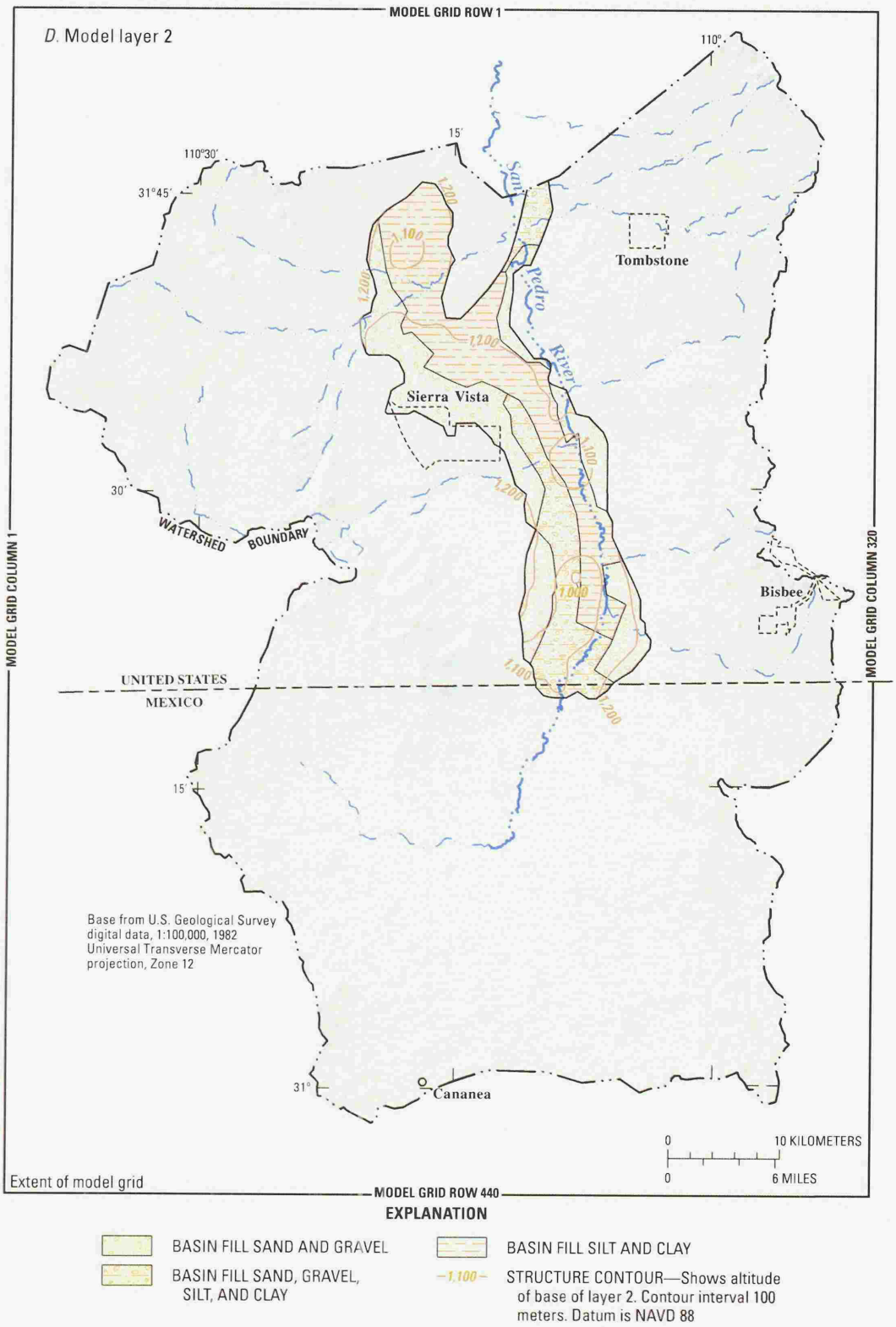

Figure 7. Continued.

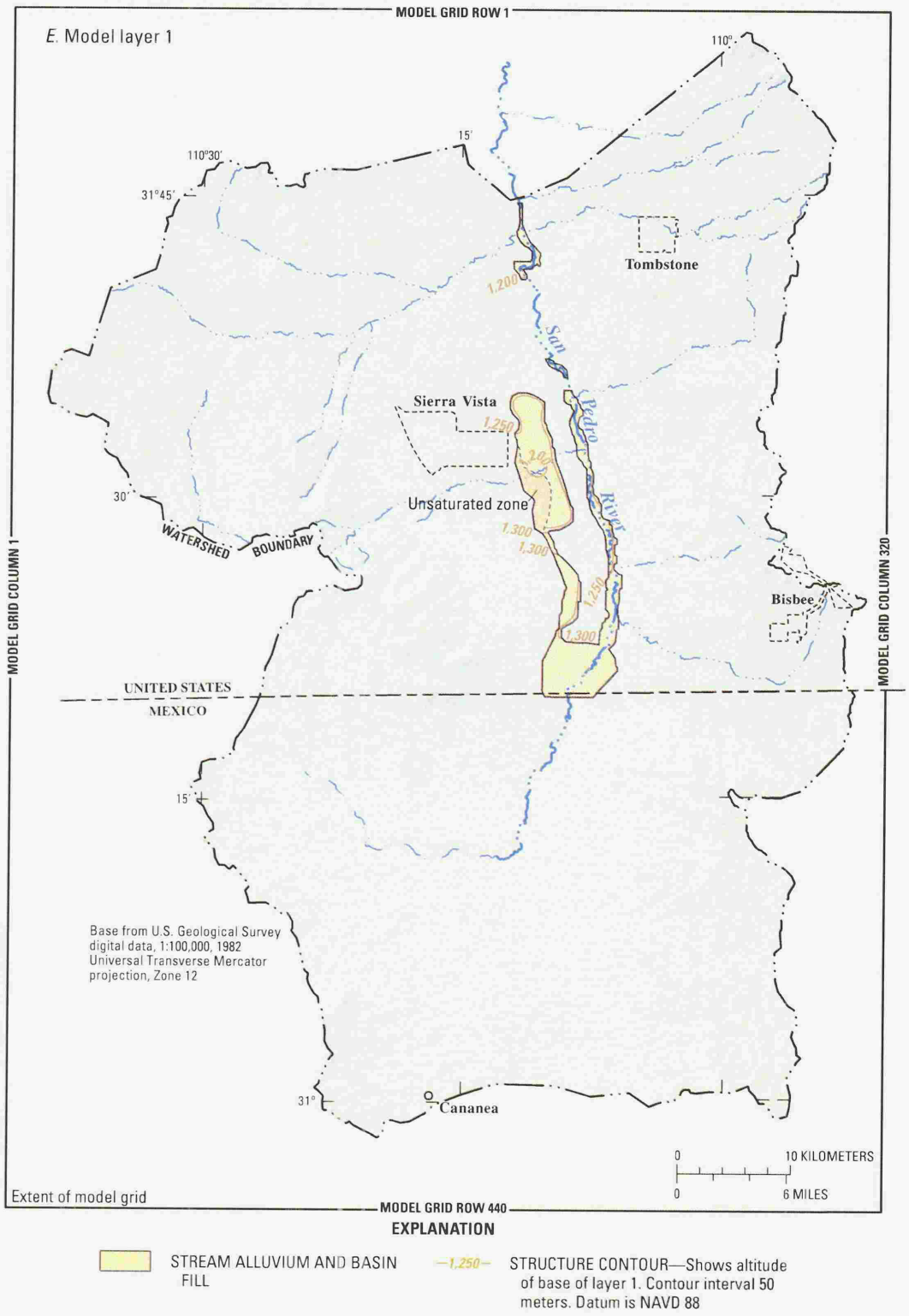

EXPLANATION

STREAM ALLUVIUM AND BASIN FILL

—1,250— STRUCTURE CONTOUR—Shows altitude of base of layer 1. Contour interval 50 meters. Datum is NAVD 88

Figure 7. Continued.

Calibrated storage properties (table 3) ranged from a specific storage coefficient of 1.0×10^{-6} m^{-1} for confined portions of the model layers to specific-yield values of 0.30 in unconfined portions of the model layers. A specific-storage coefficient value of 1×10^{-6} m^{-1} was assigned to the sedimentary and crystalline rocks in layer 5. Lower basin fill, simulated by layers 3 and 4, was assigned values of 1×10^{-6} m^{-1}–1×10^{-5} m^{-1}. Upper basin fill, simulated by layer 2, was assigned values of 1×10^{-6} m^{-1}–2×10^{-5} m^{-1}. Stream alluvium, simulated by layer 1, was assigned values of 1×10^{-6} m^{-1}–5×10^{-6} m^{-1}. Specific yield for crystalline rocks and low-permeability sedimentary rocks in layer 5 was assigned values of 0.001–0.01. Limestone was assigned a specific-yield value of 0.01 throughout the extent of the layer except in the area near the Tombstone mine, which was assigned a value of 0.02. Sandstone was assigned specific-yield values of 0.01–0.20. Specific–yield values for lower basin fill in layer 4 ranged from 0.05 in areas of consolidated basin fill to 0.20 in areas of unconsolidated coarse-grained basin fill. Specific-yield values for basin fill in layers 2 and 3 ranged from 0.05 in areas of silt and clay to 0.30 in areas of coarse-grained basin fill. The specific yield of layer 1 was 0.25 in areas where the layer represents basin fill that lies to the west of the San Pedro River, 0.20–0.30 in the pre-entrenchment stream alluvium, and 0.30 in the post-entrenchment stream alluvium.

Simulated Inflows and Outflows

Recharge

Recharge to the aquifer system includes natural sources and artificial sources that result from human water use. Natural recharge occurs in areas where rates of infiltration of precipitation and runon are greater than rates of evaporation, transpiration, and runoff. Rates of infiltration are influenced by slope, near-surface materials, and rates of precipitation. Rates of evaporation are influenced by vegetation type and elevation. Artificial recharge occurs as excess applied irrigation water and as incidental infiltration of water in the distribution and sewage systems and as intended infiltration of sewage effluent and discharge from mine dewatering. Rates of recharge varied throughout the investigation because of variations in climate, vegetation, land use, and mining practices. Variations in natural recharge were not included in the simulation of ground-water flow, but variations in artificial recharge were included.

Natural Recharge

Natural recharge has been assumed by previous investigations to occur primarily near the mountain fronts through infiltration of runoff in ephemeral channels. Mountain-front recharge often has been assumed to occur within 1.6 km of the bedrock of the mountains. Recent investigations, however, indicate that significant infiltration also occurs in the limestone in the mountains, along ephemeral channels that cross the alluvial slope below the mountain-front recharge areas (Coes and Pool, 2005; Goodrich and others, 2004) and along ephemeral reaches of the San Pedro River (Pool and Leenhouts, 2002). Predevelopment natural recharge rates were distributed across the watershed for the ground-water flow model by using water-budget methods. The overall amount of water flowing through the ground-water system was determined by the sum of estimated predevelopment discharge to stream baseflow, evapotranspiration, and ground-water flow to the Benson subwatershed. The total recharge rate along ephemeral stream channels was estimated as 15 percent of the total rate of flow through the ground-water system (Coes and Pool, 2005). Recharge along ephemeral channels was approximated by uniformly distributing 15 percent of the total recharge throughout the alluvial deposits that lie below mountain-front recharge areas. A spatial average rate of annual recharge to sedimentary rocks was estimated as the average annual baseflow discharge per unit area from four watersheds in the Huachuca Mountains: Garden Canyon, Huachuca Canyon, Ramsey Canyon, and the Upper Babocomari River. Mountain-front recharge was distributed within 1.6 km of the mountains as the residual of the total recharge and the sum of total estimated recharge along ephemeral channels below the mountain-front recharge area and recharge to sedimentary rock. Simulated rates of predevelopment natural recharge were set to 0 m/d in areas of crystalline rock and ranged from 1.0×10^{-6} to 2×10^{-5} m/d in areas of sedimentary rocks, 2.0×10^{-5} to 1.35×10^{-4} m/d within 1.6 km of the mountain fronts. The remainder of the alluvial surface was assigned a rate of 1.0×10^{-6} m/d.

Artificial and Incidental Recharge

Artificial recharge in the study area results from of infiltration of sewage effluent near Sierra Vista, Naco, Bisbee, Fort Huachuca, and Tombstone; waste water from individual domestic septic systems; and water discharged from the mines near Bisbee and Tombstone for dewatering purposes. Incidental recharge occurs as excess irrigation water and during the distribution of potable water withdrawn by wells. Each source of artificial and incidental recharge was simulated either explicitly as a transient recharge rate or implicitly as reduced withdrawal rates. Incidental recharge from distribution systems was implicitly simulated through the use of reported deliveries to customers by water providers rather than actual total well withdrawals.

Recharge though deep percolation of sewage effluent was simulated for sewage treatment facilities and individual septic systems. Sewage treatment facilities exist for Sierra Vista, Naco, Bisbee, Fort Huachuca, Huachuca City, and Tombstone. Recharge was distributed near each treatment facility on the basis of the method of discharge. Early treated effluent typically was discharged into ephemeral channels. Improved facilities often used treated effluent to irrigate turf and crops, or discharged it to evaporation or infiltration ponds.

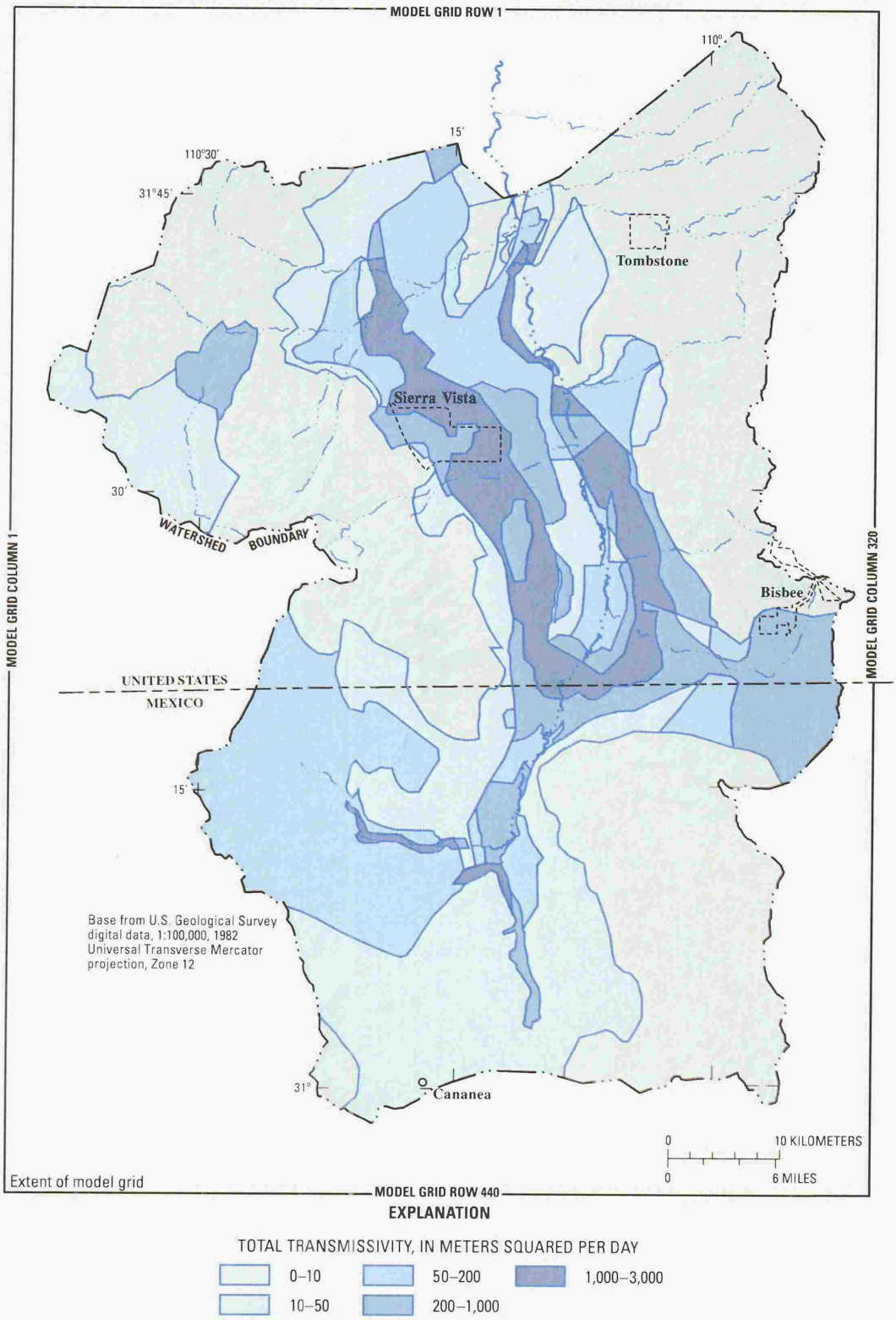

Figure 8. Simulated total transmissivity of the numerical model layers, Upper San Pedro Basin, United States and Mexico.

Table 3. Simulated hydraulic properties of hydrogeologic units for the ground-water flow model of the Upper San Pedro basin, United States and Mexico.

[m, meter; m/d, meter per day; K_h, horizontal hydraulic conductivity; K_v, vertical hydraulic conductivity; max, maximum; min, minimum; average values represent the average of values assigned to several polygons; average values are not area weighted]

	Hydraulic conductivity			Vertical anisotropy			Specific storage			Specific yield		
	m/d			K_h/K_v			m^{-1}					
Hydrogeologic unit	Average	max	min	Average	max	min	Average	max	min	Average	max	min
Limestone	0.072	0.625	0.0006	7.9	17.5	5.0	$1.0x10^{-6}$	$1.0x10^{-6}$	$1.0x10^{-6}$	0.011	0.020	0.010
Sedimentary rocks	.039	.300	.0001	7.3	17.5	5.0	$1.0x10^{-6}$	$1.0x10^{-6}$	$1.0x10^{-6}$	.088	.200	.010
Granitic and metamorphic rocks	.006	.050	.0001	8.8	17.5	5.0	$1.0x10^{-6}$	$1.0x10^{-6}$	$1.0x10^{-6}$	.006	.010	.001
Volcanic rocks	.018	.063	.0001	7.1	17.5	5.0	$1.0x10^{-6}$	$1.0x10^{-6}$	$1.0x10^{-6}$	.002	.010	.001
Undifferentiated basin fill												
Undifferentiated sand and gravel[1]	.795	10.000	.0003	9.4	17.5	3.5	$2.4x10^{-6}$	$5.0x10^{-6}$	$1.0x10^{-6}$	.120	.200	.010
Undifferentiated silt and clay[1]	.285	1.250	.0013	3.5	3.5	3.5	$5.0x10^{-6}$	$5.0x10^{-6}$	$5.0x10^{-6}$	.250	.250	.250
Upper basin fill												
Sand and gravel	3.459	7.000	.0500	26.8	75.0	8.8	$1.5x10^{-5}$	$2.0x10^{-5}$	$1.0x10^{-6}$	.177	.300	.100
Interbedded	.887	4.000	.0200	27.3	87.5	8.8	$2.0x10^{-5}$	$2.0x10^{-5}$	$2.0x10^{-5}$	.150	.250	.050
Silt and clay	.229	1.000	.0500	65.0	87.5	8.8	$2.0x10^{-5}$	$2.0x10^{-5}$	$2.0x10^{-5}$	.057	.100	.050
Lower basin fill												
Sand and gravel	.979	6.250	.0002	10.8	36.1	3.5	$3.5x10^{-6}$	$5.0x10^{-6}$	$1.0x10^{-6}$	.119	.200	.010
Interbedded	.785	4.000	.0100	38.2	122.5	12.3	$6.7x10^{-6}$	$1.0x10^{-5}$	$5.0x10^{-6}$	.092	.100	.050
Silt and clay	.005	.010	.0010	122.5	122.5	122.5	$6.3x10^{-6}$	$1.0x10^{-5}$	$5.0x10^{-6}$	.050	.050	.050
Stream alluvium												
Undifferentiated[1]	4.929	12.500	2.5000	8.9	22.5	3.5	$3.9x10^{-6}$	$5.0x10^{-6}$	$1.0x10^{-6}$	.264	.300	.250
Pre-entrenchment	7.500	7.500	7.5000	22.5	22.5	22.5	$1.0x10^{-6}$	$1.0x10^{-6}$	$1.0x10^{-6}$	.291	.300	.200
Post-entrenchment[2]	7.500	7.500	7.5000	7.5	7.5	7.5	$1.0x10^{-6}$	$1.0x10^{-6}$	$1.0x10^{-6}$	.300	.300	.300

[1]Hydrogeologic units designated as undifferentiated represent units in layers 4 and 5.

[2]Values represent a single polygon.

In the absence of early treatment records, recharge rates were estimated as 14 percent of total delivered withdrawals on the basis of the average of recent effluent recharge estimates in the Sierra Vista subwatershed (Arizona Department of Water Resources, 2005). The City of Sierra Vista began treating sewage effluent in 1967, increased the capacity with an additional facility in 1978, and converted to a recharge facility in 2001. During 1967–79, effluent was discharged into a nearby ephemeral channel. Beginning in 1980, effluent was disposed of through irrigation of 3.4 x 10^6 m^2 near the facility. Beginning in July 2002, effluent was discharged to recharge basins and recharged at a rate of 2,960 m^3/d (Arizona Department of Water Resources, 2005). Effluent was discharged to ponds near Naco and Bisbee beginning about 1930 (Phelps Dodge Corporation, 1998); however, the Bisbee effluent ponds were outside of the watershed. Effluent at Fort Huachuca during 1978–95 was recharged at two turf sites—a golf course and parade grounds—and below the treatment facility at about 1,360 m^3/d (U.S. Department of Defense, 2002). During 2001 about 1,825 m^3/d, about 33 percent of withdrawals, was estimated to have recharged. Treatment facilities at Huachuca City discharge to evaporation ponds where little recharge occurs. Treatment facilities at Tombstone began discharging effluent into Walnut Gulch in 1972 at a rate of about 300 m^3/d. Recharge at individual septic systems was simulated assuming recharge wells return 14 percent of withdrawals to the uppermost model layer near each well site. The 14 percent value was based on estimates made for a decision support system developed for the Upper San Pedro Partnership (Kevin Lansey, Professor, University of Arizona Department of Civil Engineering and Engineering Mechanics, written commun., 2005). Recharge in municipal areas before

construction of treatment facilities also was assumed to occur as deep percolation at individual septic systems and was simulated by assuming that a recharge well was near each withdrawal well.

Recharge of excess irrigation water has primarily occurred in the agricultural areas near the San Pedro River near Palominas and in Sonora, Mexico. Recharge of irrigation water also occurs beneath golf courses. Rates of recharge depend on irrigation practices and efficiencies. Previous ground-water flow models of the area have assumed that agricultural irrigation efficiencies are about 70 percent, which results in 30 percent of the irrigation withdrawals returning to the aquifer through deep percolation (Freethey, 1982; Corell and others, 1996; Goode and Maddock, 2000). Deep percolation of excess applied irrigation water was simulated in the numerical model as recharge to the upper most layer at each well by using an additional recharge well. Deep percolation beneath golf courses near Naco, Sierra Vista, and Fort Huachuca was simulated by applying a recharge rate of 1.4×10^{-3} m/d to the turf area (Phelps Dodge Corporation, 1998).

Evapotranspiration of Ground Water

Evapotranspiration from riparian vegetation was simulated near the San Pedro and Babocomari Rivers on the basis of recent studies that improve definition of extents of riparian vegetation and evapotranspiration rates of several riparian vegetation types (Leenhouts and others, 2005). Vegetation type across the model area has been mapped to 50 m grids from Landsat satellite photographs taken in 1973, 1986, 1992, and 1997 (Kepner and Edmonds, 2002) and GIS coverages of vegetation type near the San Pedro River in the United States developed by using aerial photos in 2001 (U.S. Army Corps of Engineers, 2001).

Simulation of evapotranspiration by using MODFLOW requires three types of input data: evapotranspiration surface elevation, maximum evapotranspiration rate, and extinction depth. Evapotranspiration surface elevation was commonly taken to be the land surface derived from DEMs. Maximum evapotranspiration rates and extinction depths for various phreatophyte types are available from published reports. Extinction depth was the maximum depth to water below the evapotranspiration surface where the phreatophytes can withdraw water from the aquifer. Evapotranspiration rate was calculated in MODFLOW by using the model-calculated water-level altitude and depth to water below the evapotranspiration surface. Where the water-level altitude was at or above the evapotranspiration surface, the simulated evapotranspiration rate equaled the maximum rate. No evapotranspiration occurred where the depth of the calculated water level below the evapotranspiration surface was greater than the extinction depth. The evapotranspiration rate was calculated from a linear relation between the two extremes where the depth of the calculated water level below the evapotranspiration surface was between zero and the extinction depth.

The spatial distribution of evapotranspiration (fig. 5) was derived from mapped distributions of the dominant phreatophyte vegetation types of mesquite and riparian woodland, which was predominantly cottonwood, willow, and sycamore. An additional phreatophyte type, sacaton grass, was not explicitly simulated because maps of the distribution were not available for areas in Mexico or along the Babocomari River. In addition, the evapotranspiration extinction depth for sacaton grass was 3 m below land surface, which was greater than the depth to water across most of the area. The phreatophyte types were mapped as polygonal areas. Each polygon was assigned maximum evapotranspiration rates and extinction depths that were mapped to the model grid. The evapotranspiration surface was assigned to the model grid as 1.5 m below average land-surface altitude within each 250 x 250-m model grid cell. The evapotranspiration surface was below the average land surface within a grid cell for two reasons: (1) the evapotranspiration rate was greatest where the water table was more than a meter below the land surface for most phreatophyte vegetation types, and (2) most phreatophytes were at the lower elevations within grid cells. High resolution LIDAR data (1 m^2) within the area of evapotranspiration indicate that minimum land surface within each model cell was 1–4 m below the average land surface in each model cell. Each evapotranspiration cell also required an assigned model layer from which evapotranspiration rates were calculated. Evapotranspiration rates were assigned to the upper-most active model layer at each evapotranspiration cell, which was predominantly layer 1 along the San Pedro River in the Sierra Vista subwatershed; layers 2, 4, and 5 along the Babocomari River; and layers 4 and 5 in Mexico.

Maximum evapotranspiration rates and extinction depths were assigned on the basis of data from recent investigations within the SPRNCA (Leenhouts and others, 2005). Available evapotranspiration rates represent rates for 100 percent coverage for each vegetation type. Maximum rates, therefore, need to be scaled for the percentage of area covered by phreatophytes within each model grid cell. Cover percentage was not known, however, throughout most of the simulation period. Estimation of cover percentage would require detailed analysis of aerial photographs taken at several times during the simulation period and was not done for this analysis. A multiplying factor was, therefore, uniformly applied to the maximum rate of evapotranspiration to match the estimated total evapotranspiration rates. Maximum rates of evapotranspiration for each phreatophyte type for transient conditions were 1.3×10^{-3} and 5.2×10^{-5} m/d for mesquite and riparian woodland, respectively. Multiplying factors and maximum evapotranspiration rates were scaled upward by a factor of 3 through the simulated periods to match increasing rates of estimated evapotranspiration. Extinction depths were 6 m and 14 m for riparian woodland and mesquite, respectively.

Streamflow Routing

Ground-water discharge to streams was simulated by using the MODFLOW streamflow-routing package STR1 (Prudic, 1989). Input to the package requires stage, elevation of the bottom of the streambed, elevation of the top of the streambed, conductance, width, slope, sinuosity, and Manning's roughness coefficient. STR1 routes the streamflow through a network of channels and uses Manning's equation to calculate stream stage at a hypothetical rectangular channel cross section. The application of STR1 does not allow for simulation of surface runoff from individual or seasonal runoff events; therefore, no stream inflow from upland channels was simulated. Improved simulation of streamflow routing requires the additional capability of simulating more complex stream-channel geometry, including overbank flow and temporal routing of flow.

Streams in the model area were simulated by using a network of channels along the San Pedro and Babocomari Rivers and several tributaries that include springs that could contribute to surface flow in the San Pedro River. The stream network extends from the model outflow near the streamflow-gaging station near Tombstone on the San Pedro River to north of Cananea on the San Pedro River. The simulated portion of the Babocomari River extends from the confluence with the San Pedro River to near Elgin. Major simulated tributaries include the lower reaches of Lyle Creek, a Babocomari River tributary, and Rio Los Fresnos in Mexico. Springs that issue from the regional aquifer along several ephemeral channels, including Coyote Wash (Moson Spring), Murray Wash (Murray Spring), Bakarich-McCool Wash (Horse-Thief Spring), and Government Draw (Lewis Springs), were simulated along channels that are tributary to the San Pedro River. Streams also were simulated along the lower reaches of Garden Canyon Wash and Miller Creek where riparian vegetation indicates shallow ground water and possible past springflow.

Simulated streams were divided into ninety-nine segments and reaches within segments. Each segment was assigned top and bottom elevations of the streambed at the upper and lower extent of the segment, streambed conductance, stream width, sinuosity, and Manning's roughness coefficient. Slope was calculated by STR1 for each reach within segments. Elevations of the top of the streambed were estimated using DEMs. The most accurate DEMs are available from LIDAR surveys completed during 2003 along the San Pedro River (David Goodrich, Research Hydrologist, Agriculture Research Service, written commun., 2003). The streambed elevation was estimated on the basis of the minimum elevation within any 250-m reach of the stream. The bottom of the streambed was set at 0.5 m below the streambed elevation. Stage initially was set to 1 m above the streambed and allowed to vary with head in the adjacent model cell. Streambed conductance varied from 0.10–10 m/d. Low values were assigned in areas where the stream overlies layer 5. Higher values were assigned where the stream overlies layer 1. Stream width varied from narrow widths of 1 m in the upper stream reaches, to 3 m along the middle reaches of the San Pedro River, to 5 m below Highway 90. The number of stream vertices specified in STR1 did not adequately define the stream sinuosity. Sinuosity was, therefore, estimated for each segment by using the ratio of the length of the simulated stream segment to the actual stream length and applied to the stream length in each cell. Manning's roughness coefficient was 0.22 for all segments.

Ground-Water Withdrawals

Different methods were used to spatially distribute simulated withdrawals of ground water for various uses. Withdrawals could be assigned to particular well locations where withdrawals were reported by well, such as withdrawals at Fort Huachuca wells, the Tombstone mines and Copper Queen mine, and after 1970 at wells of many large water purveyors. Other withdrawals were distributed on the basis of available information, such as locations of irrigated areas for agricultural uses and existing domestic wells for most unincorporated uses. Withdrawals in Mexico for mine uses were assigned equally to the approximate locations of withdrawal wells. More information is available for the distribution of ground water withdrawn before 1940, when withdrawals were predominantly for mine use, and for recent decades when most withdrawals were reported by large water purveyors.

Rates and distributions of agricultural withdrawals were generalized on the basis of irrigated areas prior to the mid-1980s and are uncertain for any particular year. Agricultural withdrawal rates in Mexico were distributed across agricultural areas near Rio Los Fresnos and the San Pedro River on the basis of agricultural areas defined by Kepner and Edmonds (2002). Irrigation withdrawals in the United States before 1987 were assigned to known irrigation wells near the irrigated areas. Irrigation withdrawals during 1987–98 were assigned to individual wells near agricultural areas that were documented by the Arizona Department of Water Resources (Arizona Department of Water Resources, 1990). Agricultural withdrawals during 1999 through 2002 were assigned to wells on the basis of irrigation practices documented in 2002 (Arizona Department of Water Resources, 2005).

The rates and distributions of withdrawals in unincorporated areas are poorly defined throughout the simulation period. Withdrawal estimates must be made from indirect sources, including population and well-construction records. Unincorporated withdrawals in the area between Bisbee and Naco were derived from a ground-water flow model of the area (Phelps Dodge Corporation, 1998).

Rates of ground-water withdrawals were distributed among the two simulated seasons, spring/summer and fall/winter. The withdrawal seasons were determined on the basis of variations in evapotranspiration rates, recent agricultural irrigation practices, and monthly variations in deliveries during 1998–2002 for some of the largest water suppliers: Bella Vista

Water Company, Arizona Water Company, Pueblo del Sol Water Company, and Fort Huachuca. Public withdrawal rates varied seasonally from 84 percent of the average-annual rate during the fall/winter season to 115 percent of the annual rate during the spring/summer season. Agricultural withdrawals were simulated for the spring/summer season. Withdrawals for mine use did not vary seasonally.

Knowledge of the vertical distribution of withdrawals is important for proper simulation of the transient response of the aquifer system to pumping stress, especially in regions of confined aquifers. Withdrawals were assigned to model layer 5 in areas where layers 1, 2, 3, and 4 do not exist or the saturated thickness was thin. Withdrawals from model layer 5 include withdrawals at the Tombstone mines and Copper Queen mine, some withdrawals for domestic use near the base of the Huachuca Mountains and in the Bisbee area, and some mine withdrawals in Mexico. In parts of the aquifer system that are dominated by unconfined ground-water flow and where a good hydraulic connection exists among the upper and lower basin fill units, withdrawals were assumed to derive from the coarse-grained facies of lower basin fill, model layer 4. These unconfined areas lie outside of the region of silt and clay (fig. 4) and include most withdrawals in the Sierra Vista and Fort Huachuca area, withdrawals in the Bisbee and Tombstone areas, and most of the domestic withdrawals in the region between the base of the Huachuca Mountains and the western extent of the silt and clay. The vertical distribution of withdrawals was less certain in regions of confined ground water where silt and clay exist. Withdrawals in areas of confined aquifers were distributed among model layers 1, 2, 3, and 4 according to the hydraulic conductivity and saturated thickness of the layers with a few exceptions. Withdrawals for domestic purposes were assigned to layer 2 outside of the regions dominated by silt and clay (fig. 4). Agricultural withdrawals between Highway 90 and Hereford can reasonably be assumed to originate from confined portions of the ground-water system on the basis of significant variations in hydraulic head in abandoned irrigation wells that are 100–300 m deep. Agricultural withdrawals between Highway 90 and Hereford were, therefore, assigned to model layer 4. Pre-1940 agricultural withdrawals near Hereford were assigned to model layer 2. Construction information for some agricultural wells near Palominas indicated that the withdrawals were derived exclusively from beneath the silt and clay layers and, therefore, were assigned to model layer 4.

Initial Conditions

Initial conditions for simulating transient ground-water flow approximate steady-state conditions, which were defined by a period of negligible changes in inflow, outflow, or storage. Hydrologic records indicate that the ground-water system in the Upper San Pedro Basin has undergone storage change in response to several types of changes in recharge or discharge since about 1900. Observed variations in baseflow at the Charleston and Palominas streamflow-gaging stations during the period of record indicate that the ground-water system has changed (Pool and Coes, 1999) and that true steady-state conditions have not existed. A period of minimal change must, therefore, be chosen as the initial conditions to calibrate the steady-state aquifer hydraulic properties and flow terms and to simulate the transient variations in the ground-water system. Ideally, initial conditions also would represent a period before the system changed significantly. The temporal and spatial distribution of hydrologic data, however, prevented definition of the pre-ground-water withdrawal period and required approximation of steady-state conditions by using later data. Initial hydrologic conditions that existed prior to mine withdrawals beginning in 1902 were used for this ground-water flow model. The hydrologic system in 1902 was assumed to be approximated by later data, including streamflow conditions in 1940 and water-level distributions during 1940–60. Initial conditions in 1902 allow the simulation of all known ground-water withdrawals.

Previous models also assumed that hydrologic conditions existing in about 1940 were adequate for the initial conditions of the steady-state ground-water flow model. Several changes in the ground-water flow system, however, are known to have occurred, including lowering of stream elevation through stream-channel incision along the major streams (Hereford, 1993) and associated changes in riparian vegetation and evapotranspiration; mine dewatering beginning in 1902 (Phelps Dodge Corporation, 1998; Hollyday, 1963); ground-water withdrawals for agricultural, stock, domestic, and municipal use; and climate-induced recharge variations (Dickinson and others, 2004; Pool, 2005). The uncertain transient effects of these changes decreases the confidence of the adequacy of 1940 as the initial conditions for the steady-state model.

The steady-state hydrologic conditions were defined by baseflow and hydraulic gradients, indicated by water levels in wells, throughout the ground-water flow system. Streamflow monitoring at the Charleston and Palominas streamflow-gaging stations documented conditions since 1904 and 1930, respectively. The spatial distribution of water-level data, however, was not sufficient to define hydraulic gradients before about 1961 throughout most of the United States portion of the study area and later in Mexico. Hydrographs of water levels for eight wells during 1945–60 (fig. 9) indicate, however, that water-level declines were minimal during that period and, therefore, water levels measured before 1961 can be used to approximate 1940 conditions. Water-level data for the wells generally varied within a range of about 3 m and showed a slight decline, less than 2 m per decade. The water level in well (D-23-21)06ccc2 (fig. 9) increased a few meters. Only the earliest water levels at any well that had multiple measurements before 1961 were used to approximate 1940 conditions. Water levels in wells in Mexico prior to the mid-1980s were not available. Mexico data used to estimate steady-state hydraulic gradients were derived from published data (Consultores en Agua Subterranea S.A. por Mexicana

de Cananea, S.A. de C.V., 2000). Steady-state water levels in wells were insufficient to define vertical ground-water gradients throughout the model area. Recent data collected in nested piezometers near the river, however, limit the magnitude of vertical hydraulic gradients during steady-state conditions in those areas.

Model Calibration

Model calibration included adjustment of hydraulic properties and some flux terms to match hydrologic observations. Hydraulic properties that were adjusted include horizontal and vertical hydraulic conductivity, stream-bed hydraulic conductivity, and storage properties—specific storage and specific yield. Riparian evapotranspiration rates were adjusted to match overall estimated rates of riparian evapotranspiration throughout the model area. The steady-state simulation was used to calibrate hydraulic properties—hydraulic conductivity and vertical anisotropy—by matching simulated with observed steady-state hydraulic gradients, and the average-annual steady-state water-budget components of recharge rates, stream baseflow, estimated ground-water underflow, and ground-water discharge with riparian vegetation. Transient calibration included adjusting storage properties to match hydrographs of selected wells and the overall magnitude of evapotranspiration rates to match estimated changes in evapotranspiration. Calibration of aquifer-storage properties was achieved by matching slopes of long-term water-level trends and magnitude of seasonal water-level variations. In addition, vertical anisotropy was adjusted to match the seasonal timing and magnitude of the water-level and streamflow variations.

Steady State

Methods and data used for steady-state calibration of this model are similar to those used for previous models. The model was calibrated to average-annual steady-state conditions. Ground-water response to seasonal variations in evapotranspiration also was simulated. Seasonal variations can be in a dynamic oscillatory steady state when storage and other flux components vary seasonally, but storage does not change during a period of 1 or more years.

Average-Annual Steady-State Conditions

The estimated (table 2) and simulated (table 4) average-annual steady-state ground-water budgets are in agreement. Effects of transient ground-water withdrawals and artificial recharge near the Bisbee and Tombstone mines were assumed to have had no impact on basin discharge in 1935. Simulated recharge was 58,100 m^3/d (17,200 acre-ft/yr). Simulated net ground-water discharge included 58,700 m^3/d (17,400 acre-ft/yr) to streams, 1,500 m^3/d (400 acre-ft/yr) to drains, 2,700 m^3/d (800 acre-ft/yr) as ground-water underflow, and 22,000 m^3/d (6,500 acre-ft/yr) as evapotranspiration. Simulated stream baseflow at Charleston was 19,600 m^3/d (5,800 acre-ft/yr or 8.0 ft^3/s) in comparison with the estimated annual baseflow of about 19,900 m^3/d (5,900 acre-ft/yr or 8.1 ft^3/s).

The distribution of predevelopment hydraulic gradients and stream baseflow was approximated in the calibration process by adjusting the hydraulic properties of streams and the hydraulic conductivity of polygonal regions representing different hydrogeologic conditions in each layer. The resulting distribution of hydraulic properties produced the simulated water-level altitudes at predevelopment observation wells (fig. 9). Simulated predevelopment hydraulic head was generally within 10 m of seventy-seven pre-1961 observed values (mean absolute error of 9.0 m and average error of -0.7 m) and twenty-nine pre-1950 values (mean absolute error of 7.5 m and average error of -3.5 m, fig. 10). The greatest error occurred above elevations of 1,440 m near the Huachuca Mountains where heads were simulated as 10–40 m lower than observed. Hydraulic heads in this part of the model are sensitive to variations in hydraulic properties because hydraulic gradients are steep and water levels are close to the land surface. Water levels in this area varied as much as 10–30 m with climate variations during 1940–2002 (Dickinson and others, 2004; Pool, 2005).

Vertical and horizontal hydraulic properties in three areas near Lewis Springs, Cottonwood, and Palominas were calibrated by using observed vertical hydraulic gradients near the San Pedro River during 1995–2005 (fig. 5). Simulated steady-state hydraulic gradients were less than gradients that were observed at each site. Observed gradients near Lewis Springs were derived from several piezometers that were screened at depths of 7–10 m and 60 m within the pre-entrenchment alluvium and basin fill, respectively. Observed water-level altitudes in the deep wells during 1995–2005 were 1.5–1.9 m greater than those in shallow wells, and simulated steady-state water-level altitudes in layers 2 and 4 were 0.7 and 1.1 m greater than those in layer 1, respectively. Observed gradients near Cottonwood were derived from piezometers that were screened at depths of 5 m and 60 m within the pre-entrenchment alluvium and basin fill, respectively. Observed deep water-level altitudes near Cottonwood were 6 m greater than those in shallow wells, and simulated steady-state water-level altitudes in layers 2 and 4 were about 4.2 and 6.1 m greater than those in layer 1, respectively. Observed gradients near Palominas were derived from piezometers that were screened at depths of 23 m and 60 m within the basin fill. Observed water-level altitude in the deep well near Palominas was more than 2 m greater than the water-level altitude in the shallow well during 2001–03, and simulated steady-state water-level altitudes in layers 2 and 4 were 0.6 and 1.7 m greater than those in layer 1, respectively.

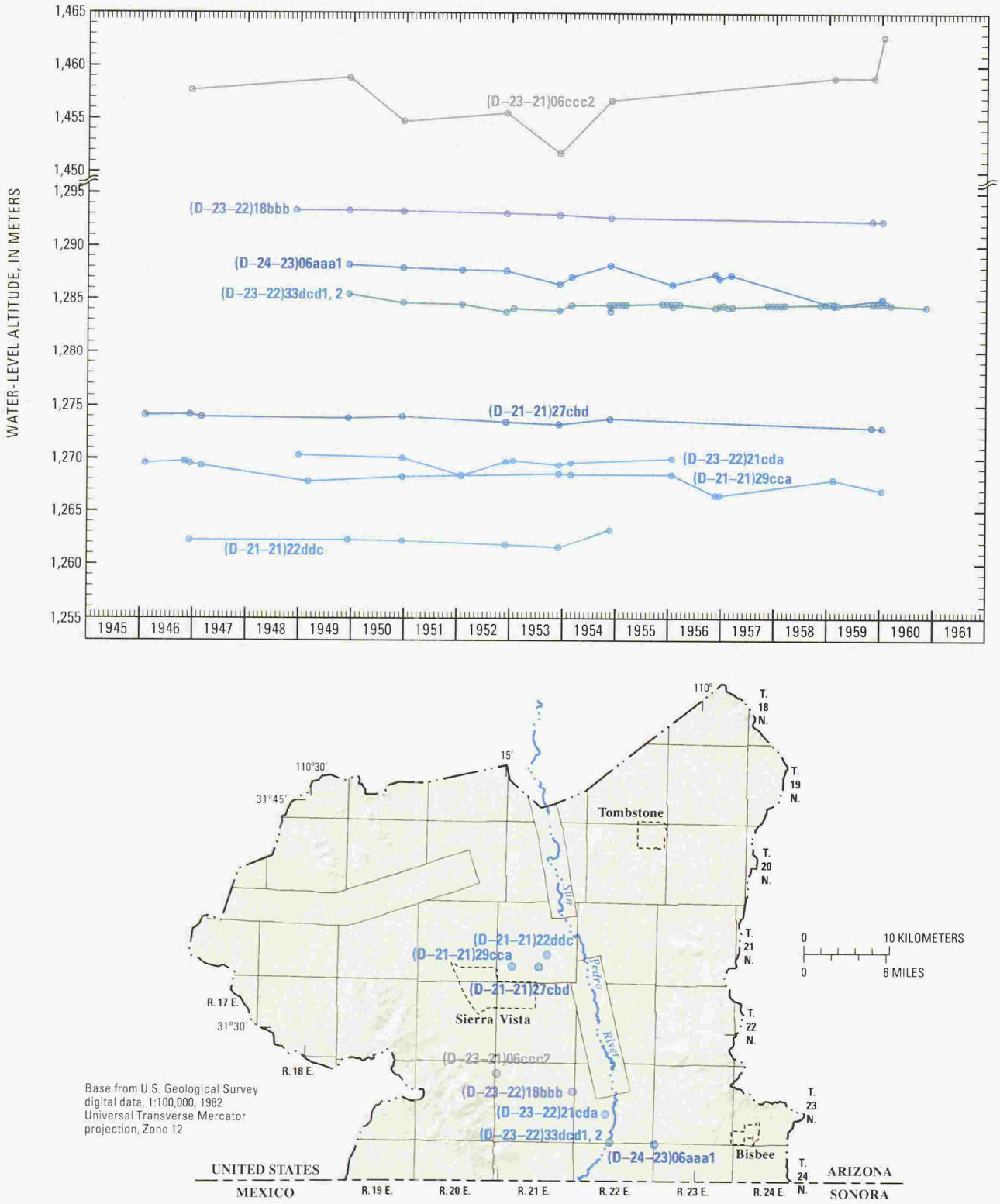

Figure 9. Pre-1961 water-level hydrographs for the Sierra Vista subwatershed of the Upper San Pedro Basin, United States.

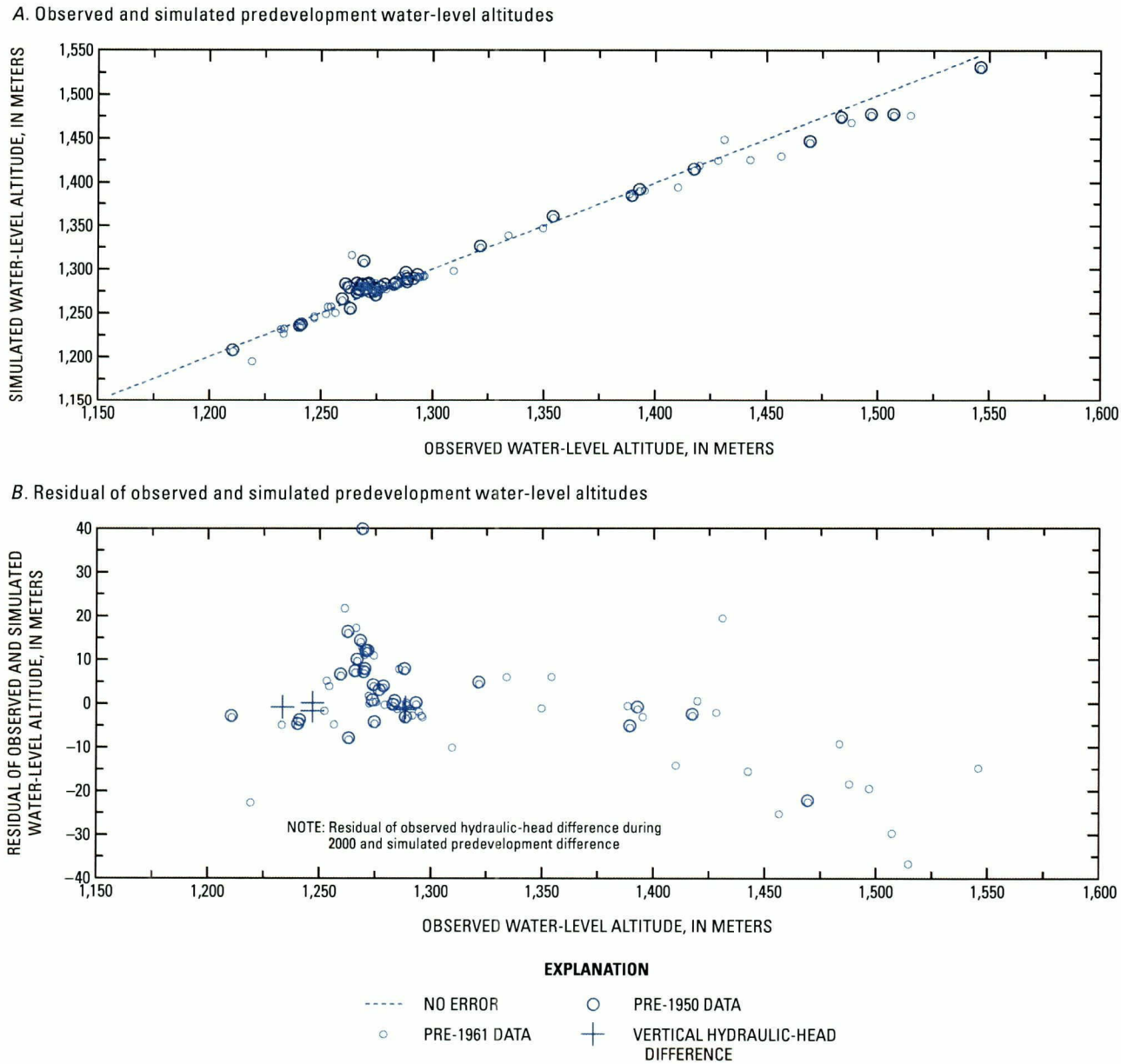

Figure 10. Observed and simulated predevelopment water-level altitude error for selected monitoring wells, Upper San Pedro Basin, United States and Mexico. 10*A*, Observed and simulated predevelopment water-level altitudes; 10*B*, Residual of observed and simulated predevelopment water-level altitudes.

Oscillatory Steady-State Conditions

An oscillatory steady-state simulation was completed to simulate predevelopment seasonal evapotranspiration conditions and to establish initial conditions for transient simulations of seasonal pumping and evapotranspiration. Simulation of average-annual steady-state conditions approximated the oscillatory steady-state conditions, but did not include the effects of seasonal evapotranspiration on streamflow and storage change that would be expected during the initiation of the seasonal transient simulation. Lack of inclusion of these seasonal initial conditions could result in errors in the transient simulation.

The oscillatory steady-state simulation included seasonal evapotranspiration stresses—fall/winter and spring/summer—for a 30-year period by using initial conditions from the steady-state simulation. Water levels near the streams attained oscillatory steady-state conditions after 30 years of simulation, but water levels continued to change at low rates across the regional aquifer.

The oscillatory steady-state simulation resulted in hydraulic head distributions that were similar to those of the average-annual steady-state simulation, but the average-annual water budget was slightly different (table 4).

Recharge rates were identical to the average-annual steady-state rate of 58,100 m^3/d. Seasonal variation in evapotranspiration resulted in seasonal variations in streamflow and storage. Inflow to the ground-water system from streams ranged from 24,000 m^3/d in fall/winter to 29,000 m^3/d in spring/summer and averaged 27,000 m^3/d annually. Inflow from streams represents streamflow that reinfiltrates into the ground-water flow system after previously discharging to the stream in upstream reaches and was not inflow to the ground-water system that was in addition to recharge. Average seasonal outflow to streams ranged from 54,800 m^3/d in spring/summer to 62,400 m^3/d in fall/winter and averaged 57,900 m^3/d annually. Seasonal evapotranspiration rates ranged from an average of 36,500 m^3/d during spring/summer to 0 m^3/d during fall/winter and averaged 21,700 m^3/d annually. Underflow to the adjacent downgradient basin was 2,700 m^3/d during both spring/summer and fall/winter seasons. Discharge to drains was 1,500 m^3/d during spring/summer and fall/winter. Water was removed from storage (inflow to the ground-water flow system) at an average seasonal rate of 10,000 m^3/d during spring/summer and 300 m^3/d during fall/winter. Water flowed into storage (outflow from the ground-water flow system) at average seasonal rates of 16,100 and 1,500 m^3/d during the fall/winter and spring/summer, respectively.

The oscillatory simulation of seasonal predevelopment conditions resulted in seasonal baseflow variation at Charleston and Palominas that can be compared with observed baseflow during the late 1930s. Minimum seasonal baseflows at Charleston were simulated as 26,800 m^3/d (10.9 ft^3/s) and 12,600 m^3/d (5.2 ft^3/s) for fall/winter and spring/summer, respectively. Observed seasonal baseflows at Charleston were 40,300 m^3/d (16.5 ft^3/s) and 9,000 m^3/d (3.7 ft^3/s) in the late winter and early summer (June), respectively. A portion of the greater observed seasonal variation may be related to ground-water withdrawals near Palominas that may have removed 9,000 m^3/d (3.7 ft^3/s) from the ground-water system or directly from the stream during the spring/summer. A portion of observed baseflow also was supplied by near-stream recharge during flood events and was not simulated by the model. Minimum seasonal baseflows at Palominas were simulated as 12,300 m^3/d (5.0 ft^3/s) and 8,300 m^3/d (3.4 ft^3/s) for fall/winter and spring/summer, respectively. Observed seasonal baseflows at Palominas were 11,700 m^3/d (4.8 ft^3/s) and 1,700 m^3/d (0.7 ft^3/s) for late winter and early summer (June), respectively.

Transient-State Conditions

Transient conditions resulting from ground-water withdrawals and variations in evapotranspiration rates were simulated for 1902–2002. Water-level hydrographs representing several hydrogeologic conditions across the basin were used to calibrate transient conditions by adjusting storage and vertical hydraulic properties to approximate observed trends (fig. 11 and 12). Observed seasonal and long-term low flows at Palominas and Charleston and simulated seasonal baseflow (fig. 13) were compared. Long-term water-level hydrograph records are few. Records of two to four decades in length are, however, available for several wells (fig. 11). Primary water-level hydrographs for the Palominas-Hereford agricultural area include a long-term record for well (D-23-22)33dcd1,2 and records of monthly values for 2000–2002 for wells (D-23-22)17acc, PAL-SUM, and PAL-UWD. Other long-term records near the agricultural area include those for wells (D-23-22)18bbb and (D-24-23)06aaa1. Primary hydrographs for the Sierra Vista area include pre-1980 records for well (D-21-21)29cca, post-1980 records for well (D-22-22)06dac, bi-monthly records beginning in 1995 for several observation wells at Fort Huachuca, and continuous records for a well cluster near the San Pedro River at Highway 90 [(D-22-22)06aaa1,2,3,4,5 and (D-22-22)06abd, also known as Lewis Springs MW1–5 and MW6, respectively]. Fort Huachuca water-level data compared with simulated water-level trends include MW1, (D-21-21)10ada; MW3, (D-21-21)19ddc; MW4, (D-21-20)15acd; MW5, (D-21-21)16aaa; MW7, (D-20-21)33ddc; TW4, (D-20-20)35ccb; and TW6, (D-20-20)35ccb. Hydrographs for the Sonoran portion of the model area include data at several wells beginning about 1980 (Consultores en Agua Subterranea S.A. por Mexicana de Cananea, S.A. de C.V., 2000), but the well locations are not known.

Table 4. Simulated predevelopment ground-water budget.

[cubic-meters per day]

Water-budget component	Steady-state simulation		Oscillatory steady-state simulation					
	Average annual		Average spring/summer		Average fall/winter		Average annual	
	Inflow	Outflow	Inflow	Outflow	Inflow	Outflow	Inflow	Outflow
Recharge	58,100	0	58,100	0	58,100	0	58,100	0
Stream baseflow[1]	27,000	58,700	29,000	54,800	24,000	62,400	27,000	57,900
Evapotranspiration	0	22,000	0	36,500	0	0	0	21,700
Ground-water under flow	0	2,700	0	2,700	0	2,700	0	2,700
Drains[2]	0	1,500	0	1,500	0	1,500	0	1,500
Subtotal[3]	85,100	84,900	87,100	95,500	82,100	66,600	85,100	83,800
Storage[4]	0	0	10,000	1,500	300	16,100	6,100	7,400
TOTAL[5]	85,100	84,900	97,100	97,000	82,400	82,700	91,200	91,200

[1]Inflow from stream baseflow represents stream baseflow that reinfiltrated the ground-water system after discharging to the stream and is not additional inflow to the ground-water system.

[2]Drains include discharge to several springs in the Huachuca Mountains.

[3]Subtotal of ground-water flow components.

[4]Storage inflow represents removal from storage and input to the ground-water flow system. Storage outflow represents removal from the ground-water flow system and input to storage.

[5]Total flow is the sum of all flow and storage components.

Observed water-level trends are well simulated for most hydrograph comparison sites (fig. 12). Simulated water-level records include data for the model layer that represents water-table conditions—layer 1, 2, or 4—and the model layer that represents the deeper confined aquifer—usually layer 4. Trends that were similar but showed no significant differences in hydraulic head between the water-table and confined aquifers were simulated for several wells in regions of thick silt and clay, including Fort Huachuca wells MW4, TW6, MW4, MW5, (D-22-22)06dac, (D-23-22)33dcd1,2, and (D-23-22)17acc; piezometers near Lewis Springs (Lewis Springs MW1 through 6); and piezometers near Palominas, PAL-SUM, PAL-UWD, and PAL-UWS. Water-level declines of 2–4 m observed before 1970 in wells (D-21-21)29cca, (D-23-22)18bbb, and (D-24-23)06aaa1 were slightly greater than simulated water levels. Differences in the water-level decline observed before 1970 and simulated water-level decline may be caused by no simulation of low recharge rates during the mid-century drought from 1945 to 1960, not simulating possible changes in evapotranspiration rates and changes in stream elevation, or simulating the spatial distribution of withdrawals inaccurately. Simulated declines in the confined portions of the aquifer near Palominas were greater than the observed water-level decline at well (D-23-22)33dcd1,2. This well was open to both the basin fill and the stream alluvium, and water levels in the well likely are more representative of the higher hydraulic head in the water-table aquifer within the stream alluvium than the lower hydraulic head in the basin fill.

The accuracy of the simulation of post-1990 water-level trends was an important measure of model calibration because distributions of seasonal ground-water withdrawals are well known for the period. Withdrawals are best defined during 2001–03 on the basis of recent surveys that documented withdrawal rates and locations (Arizona Department of Water Resources, 2005). Water levels during the 2001–03 period were monitored at several observation wells in the Sierra Vista and Palominas areas, including deep and shallow piezometers near Lewis Springs (Lewis Springs MW1 through 6) and Palominas (wells PAL-SUM and PAL-UWD; fig. 11).

Simulated water-level trends match observed trends during 1995–2003 at several wells in the Sierra Vista area. At wells that are believed to represent water-table conditions, Fort Huachuca wells TW4, MW1, MW3, MW4, and MW5, simulated water-level altitudes in the shallowest active layer, normally layer 2, are within about 6 m of observed altitudes, and simulated trends are similar to observed trends (fig. 12). Wells that have screened intervals beneath significant thicknesses of silt and clay, Fort Huachuca wells TW6, MW7, and(D-22-22)06dac, are believed to represent confined conditions at wells. Simulated water-level altitudes in layer 4 at these wells are within about 6 m of those observed, and simulated trends are similar to those observed.

Downward ground-water flow was simulated among layers in the region of thick silt and clay between the San Pedro River and Sierra Vista. Significantly lower water-

level altitudes of 5–18 m were simulated in layer 4 with respect to layer 2 for wells TW6, MW4, and MW5. Upward ground-water flow was simulated for well (D-22-22)06DAC and Lewis Springs piezometers MW1–5 with water-level altitudes in layer 4 that were about 2–3 m greater than the water-level altitude in layer 1. Agricultural withdrawals from layer 4 at several nearby wells during 1973–86 resulted in strong seasonal water-level variations of about 1–2.5 m at (D-22-22)06dac and in the deep piezometers at Lewis Springs, Lewis Springs MW5 and MW6. Vertical directions of ground-water flow in the Sierra Vista area did not change during the simulation, but downward gradients increased for TW6, MW4, and MW5 after about 1950, and upward gradients increased for well (D-22-22)06dac and Lewis Springs piezometers MW1–6 following the cessation of nearby agricultural withdrawals after 1986.

Water-level trends and seasonal variations in water levels in the Palominas area during 2001–03 were well simulated for wells (D-23-22)33dcd1,2, (D-23-22)17acc, PAL-SUM, PAL-UWD, and PAL-UWS. The greater seasonal withdrawal during spring/summer simulated in layers 2 and 4 was caused by nearby agricultural withdrawals. Only well (D-23-22)33dcd1,2 had included a long-term water-level record, which began about 1950. A slightly declining simulated water-level trend in the unconfined aquifer before 1980, layer 1 at (D-23-22)33dcd1,2, was similar to the observed trend; but simulated water-level altitudes were about 3–4 m below observed values. Simulation of the declining water-level trend before 1970 in layer 2 resulted in a significant reduction in upward hydraulic gradients toward layer 1 from about 3 m in 1940 to less than 1 m after about 1970. Stronger upward hydraulic gradients were reestablished after 1986 when withdrawals in nearby agricultural areas were reduced. Simulated seasonal water-level variations of about 2.5 m in layer 4 at well (D-23-22)17acc during 2001–03 were slightly greater than observed variations of 1.5–2 m. Well (D-23-22)17acc is more than 400 m deep. No lithologic log exists, but the well likely penetrates a thick sequence of silt and clay, and water levels likely represent confined conditions. Simulated water-level altitude, upward vertical gradients, and seasonal water-level variations in layers 1, 2, and 4 at shallow and deep piezometers PAL-UWS, PAL-UWD, and PAL-SUM, respectively, are similar to observed conditions during 2001–03. Piezometer PAL-SUM is screened across about 3 m about 60 m beneath a thick sequence of silt and clay, and water levels likely represent confined conditions. Piezometer PAL-UWD is screened across about 3 m about 20 m beneath an interbedded sequence of clay, silt, sand, and gravel, and water levels likely represent confined conditions. Piezometer PAL-UWS is screened across about 1.5 m at a depth of about 9 m within sand and gravel, and water levels likely represent water-table conditions.

Observed summer and winter stream baseflow at the Charleston and Palominas streamflow-gaging stations are important calibration constraints. Discharge from the regional ground-water flow system to the stream—baseflow—was approximated by using the seasonal 7-day minimum flow at each station. Seven-day minimum flows, however, normally include a surface-water component, especially following periods of high runoff. Seven-day minimum flows were, therefore, considered as high estimates of ground-water discharge except for periods of extended drought. Simulated stream baseflow at each station was approximated by using rates of streamflow during the time steps of each seasonal stress period. The magnitude of summer baseflow was well simulated for both stations. Simulated winter baseflow at Palominas was similar to that observed; simulated winter baseflow at Charleston was less than that observed (fig. 13).

Simulated rates of summer and winter baseflow at Charleston are similar to estimated rates during 1936–40 (fig. 13*A*). Simulated minimum summer baseflow for the period was about 13,900 m^3/d (5.7 ft^3/s). The observed average 7-day minimum low flow was about 9,000 m^3/d (3.7 ft^3/s). Simulated winter baseflow during 1936–40, 28,500 m^3/d (10.9 ft^3/s), was less than the minimum 7-day low flow, 30,400 m^3/d (12.4 ft^3/s). Simulated and estimated baseflow decline followed the initiation of significant near-stream ground-water withdrawals for agricultural use in the Palominas-Hereford area and growth for riparian woodland vegetation after 1940. Simulated and estimated minimum summer baseflows were similar in magnitude and generally declined throughout the simulation period; both baseflows declined from about 8,800 m^3/d (3.6 ft^3/s) during the early 1940s to about 2,800 m^3/d (1.1 ft^3/s) near the end of the simulated period. Overall declines in rates of the maximum recovery of baseflow during the winter at Charleston were estimated and simulated as about 17,000 m^3/d (7.0 ft^3/s) and 18,500 m^3/d (7.6 ft^3/s), respectively. Much of the simulated decline in winter baseflow, however, occurred during 1940–46. Similar estimated declines occurred during 1940–50, but estimated values were highly variable after 1950. Much of the variability was likely caused by including significant amounts of runoff in the estimated 7-day minimum seasonal flow during and following extended wet periods. Declines in the lowest estimated winter baseflow values that occurred during periods of drought in 1938, 1950, 1952, and 1997 approximately matched the simulated declines.

Simulated rates of winter baseflow at Palominas during 1936–40, 12,100 m^3/d (4.9 ft^3/s), are similar to estimated rates; however, simulated summer rates, 8,100 m^3/d (3.3 ft^3/s), are greater than observed rates of about 1,700 m^3/d (0.7 ft^3/s; fig.13*B*). Simulated and estimated baseflow decline followed the initiation of significant near-stream ground-water withdrawals for agricultural use in the Palominas-Hereford area and growth of riparian woodland vegetation after 1940.

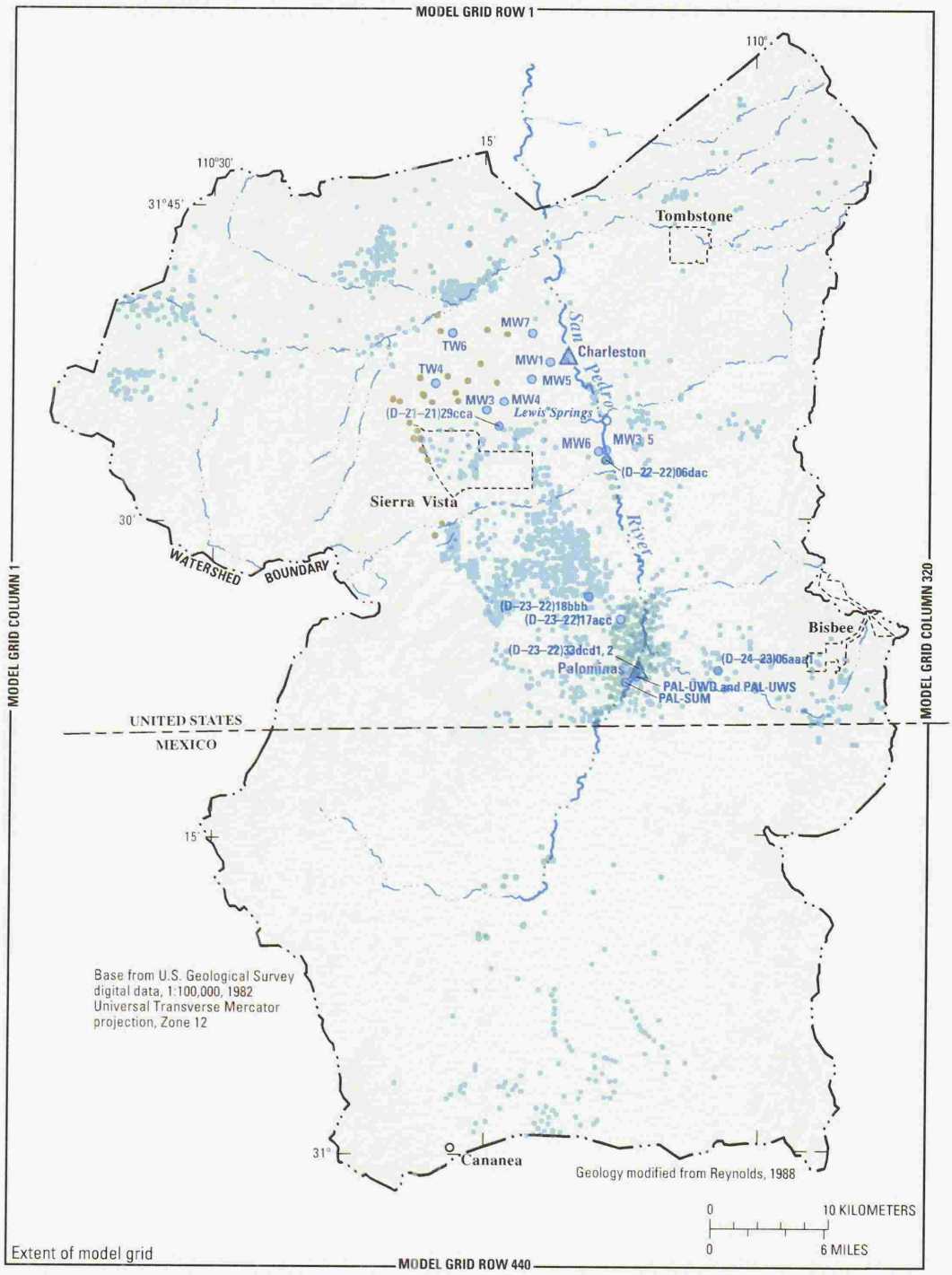

Figure 11. Distributions of simulated withdrawal wells and selected hydrograph comparison sites, Upper San Pedro Basin, United States and Mexico.

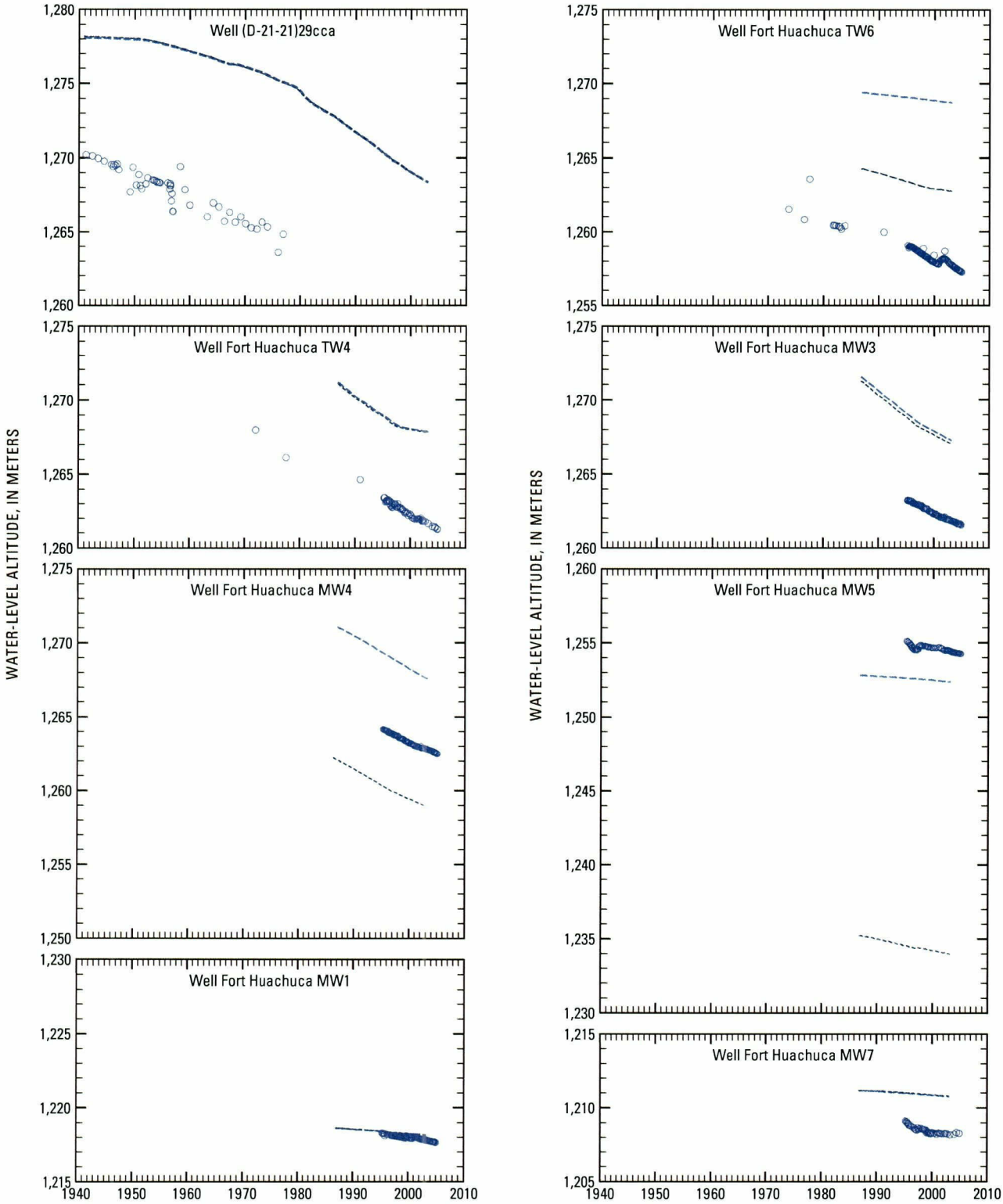

Figure 12. Hydrographs showing observed and simulated water-level altitudes at selected wells, 1940–2003, Upper San Pedro Basin, United States and Mexico.

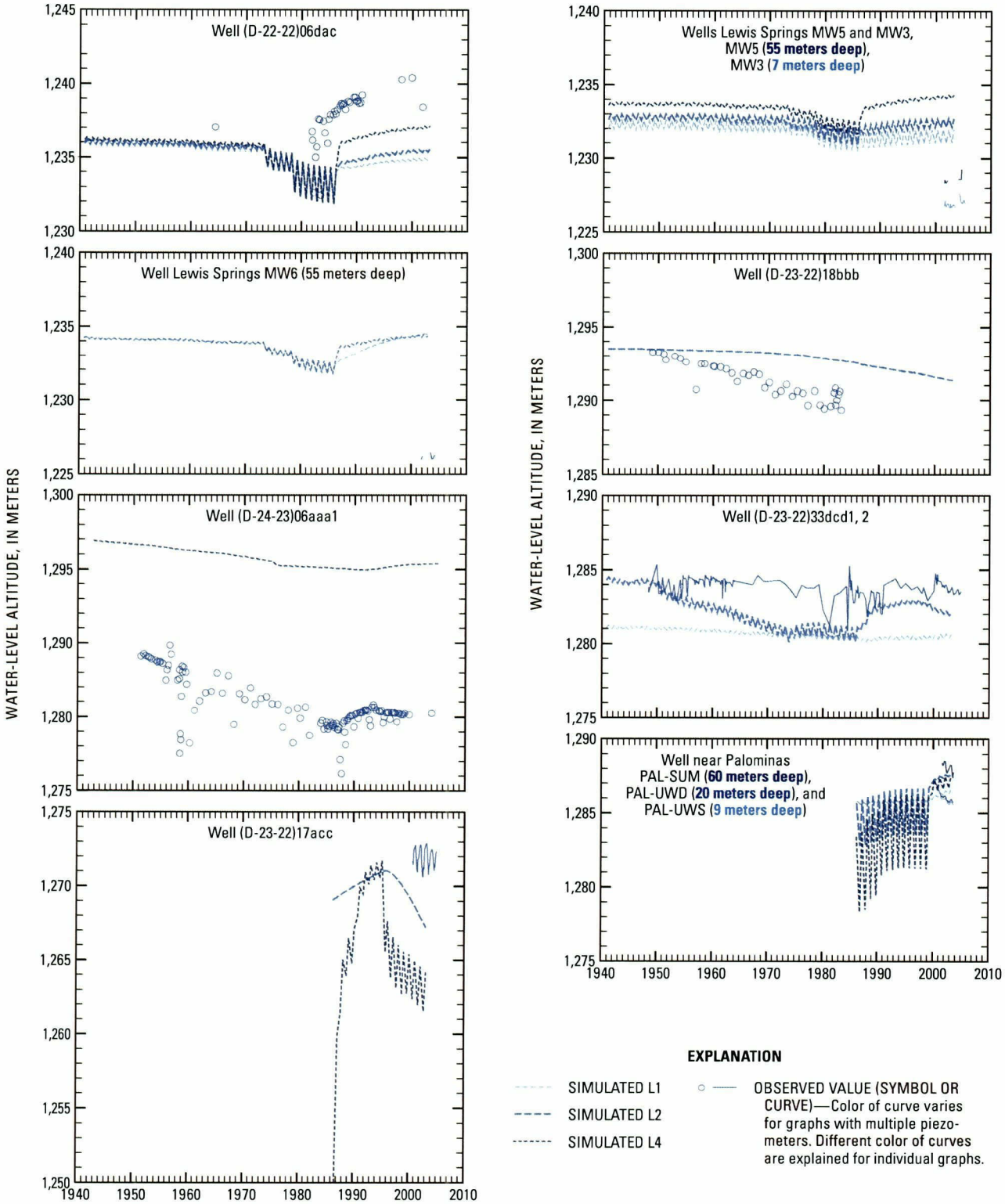

Figure 12. Continued.

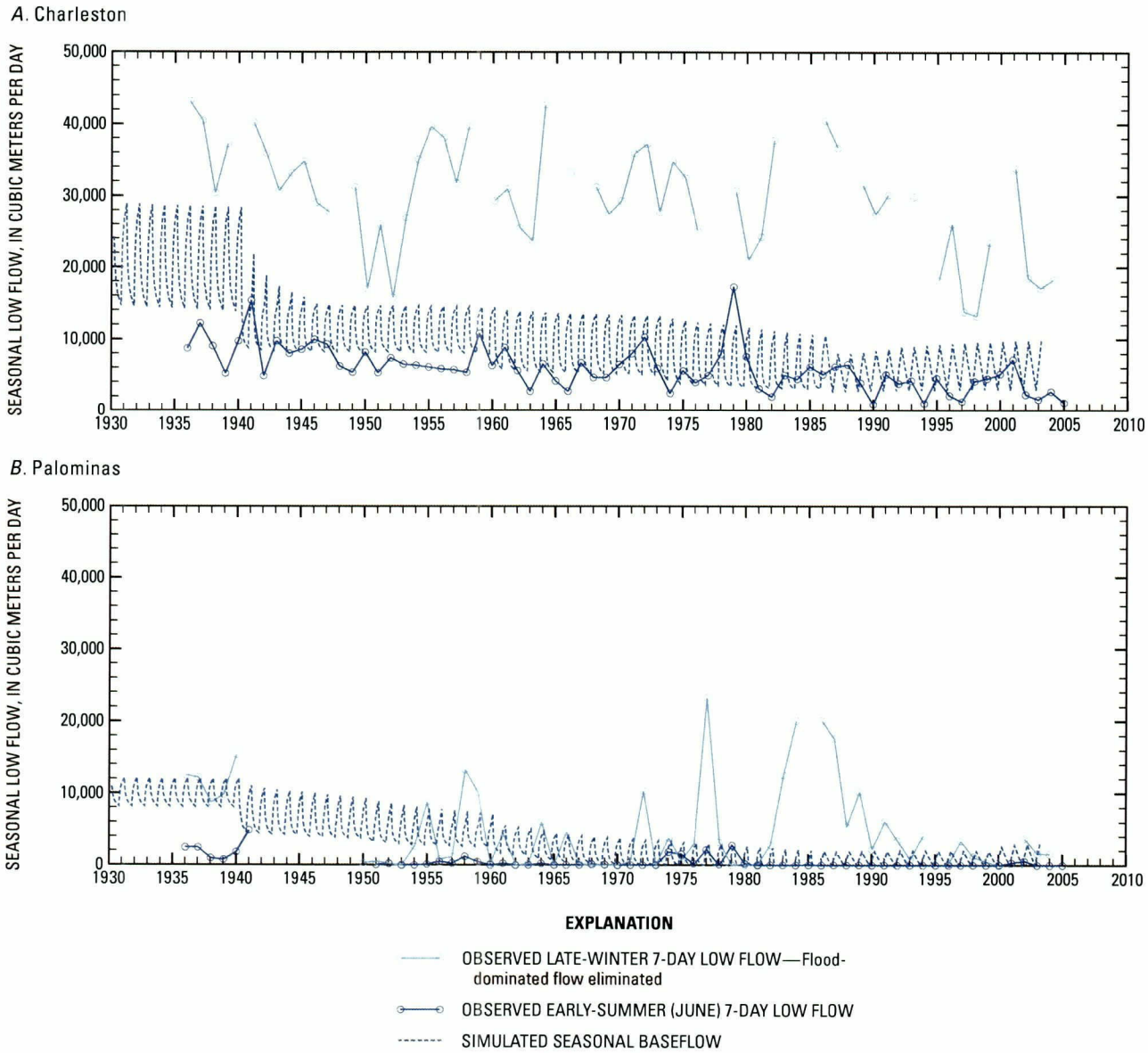

Figure 13. Estimated and simulated seasonal baseflow at streamflow-gaging stations on the San Pedro River, Arizona, 1929–2003. 13*A*, Charleston; 13*B*, Palominas.

The simulated decline in the maximum baseflow recovery during winter of about 9,300 m^3/d (3.8 ft^3/s) occurred more gradually than the estimated decline in the maximum winter 7-day low flow, which mostly occurred during 1940–50 when the streamflow-gaging station was not operating. Estimated summer baseflow declined to near zero during 1940–50. Simulated summer baseflow declined to zero more gradually during 1940 to about 1970. Differences in the simulated and estimated baseflow trends at Palominas may have been caused by inaccurately simulating the poorly known spatial distribution of ground-water withdrawals, or by simulated vertical hydraulic properties that are lower than in the real system.

A large amount of water-level data was available for comparison of observed and simulated water-level altitudes during the winter of 2002 (fig. 14). Observed and simulated water-level altitudes generally are within about 10 m of each other throughout the regional alluvial aquifer. Differences are greater than 10 m in the higher altitudes of Walnut Gulch where simulated values were much less than those observed. Simulated water-level altitude in the Huachuca Mountains also was less than those observed.

Rates of outflow from the ground-water flow system during the final year simulated (March 2002–March 2003) were greater than rates of inflows (table 5, subtotal), and the difference is equivalent to net change in ground-water storage. Inflow from recharge through natural sources was equivalent to the steady-state rate of 58,000 m^3/d (17,200 acre-ft/yr). Additional recharge through artificial sources included 6,500 m^3/d (1,900 acre-ft/yr) at turf and recharge facilities and 7,200 m^3/d (2,100 acre-ft/yr) in agricultural areas and at septic systems that were simulated at recharge wells. Discharge to wells, evapotranspiration, drains, and ground-water underflow to the adjacent basin averaged 171,700 m^3/d (50,800 acre-ft/yr). Annual ground-water withdrawals were 140,000 m^3/d (41,400 acre-ft/yr). A portion of annual withdrawals was returned to the ground-water flow system as artificial recharge at several municipal facilities, irrigated areas, and septic systems. Artificial recharge at municipal facilities was simulated as 6,500 m^3/d (1,900 acre-ft/yr). Artificial recharge in irrigated areas and at septic systems was simulated as 7,200 m^3/d (2,100 acre-ft/yr). Net ground-water withdrawals, after accounting for artificial recharge, were 126,300 m^3/d (37,400 acre-ft/yr), of which 73,800 m^3/d (21,800 acre-ft/yr) were in Mexico and 52,500 m^3/d (15,500 acre-ft/yr) were in the United States. Discharge from the ground-water system to stream baseflow was about 26,600 m^3/d (7,900 acre-ft/yr), and inflow to the ground-water system from stream baseflow was about 17,000 m^3/d (5,000 acre-ft/yr). Discharge through evapotranspiration was simulated as about 27,600 m^3/d (8,200 acre-ft/yr), about 2,200 m^3/d (700 acre-ft/yr) of which occurred in Mexico. The simulated rate of evapotranspiration in the Sierra Vista subwatershed was about 25,400 m^3/d (7,500 acre-ft/yr), which was near the estimated rate of 25,000–30,000 m^3/d (7,300-9,000 acre-ft/yr; Leenhouts and others, 2005). Simulated discharge through ground-water underflow across the northern boundary was 2,600 m^3/d (800 acre-ft/yr), nearly the same as the estimated rate, which indicates that the simulated ground-water flow system near the outflow boundary was minimally affected by transient changes in the system.

The imbalance between ground-water outflows and inflows was offset by a decrease in ground-water storage (table 5). Net removal from ground-water storage (inflow from storage minus outflow from storage) averaged 109,400 m^3/d (32,400 acre-ft/yr) for the final year of the simulation. The storage deficit was distributed among the Sierra Vista subwatershed and Mexico portions of the model area as about 38,300 and 71,100 m^3/d (11,300 and 21,100 acre-ft/yr), respectively.

Model Limitations and Possible Improvements

The numerical ground-water flow model described here simulates an improved conceptualization of the ground-water system in the Upper San Pedro Basin; however, further improvements can be implemented. Additional improvements could be made in the simulation of boundary conditions, streamflow, variations in recharge rates, and evapotranspiration. Improved knowledge of the spatial distribution of ground-water withdrawals is needed for the unincorporated areas of the United States and in Mexico. Improved knowledge of the vertical distribution of ground-water withdrawals also could improve simulations, especially for confined parts of the aquifer system, such as in the Palominas-Hereford area.

All numerical ground-water flow models are limited by boundary conditions. Models will produce invalid results when changes within the system result in significant changes at incorrectly simulated boundaries. All boundaries in this model, except some flow boundaries along the northern extent, were assumed to be no-flow. There were several simulated areas where ground water could flow to adjacent ground-water flow systems; therefore, significant changes would render the no-flow assumption invalid. These conditions may occur where saturated permeable rocks, such as limestone or alluvial deposits, are continuous across the model boundary as in several areas, including the Mule Mountains, the Huachuca Mountains, and areas near Elgin and along the northern and southern model boundaries. These boundaries could be modified by simulating a larger extent, or by simulating the boundary as a general head boundary. Observed changes near boundaries are likely significant in the current simulations only where withdrawals for mine use have occurred near the Copper Queen and Cananea mines. Withdrawals near the Copper Queen mine were not simulated because of a lack of understanding of the ground-water flow system in the area. These withdrawals could only be simulated by using a greater extent in the area. Withdrawals near the Cananea mine were simulated, but induced inflow from the adjacent basin was assumed to be minimal because withdrawals also occur south of the boundary. Errors in the simulation of the regional ground-water flow system that were caused by inaccurate boundaries near both mines likely are small because of the great distance from the nearest areas of natural discharge along streams.

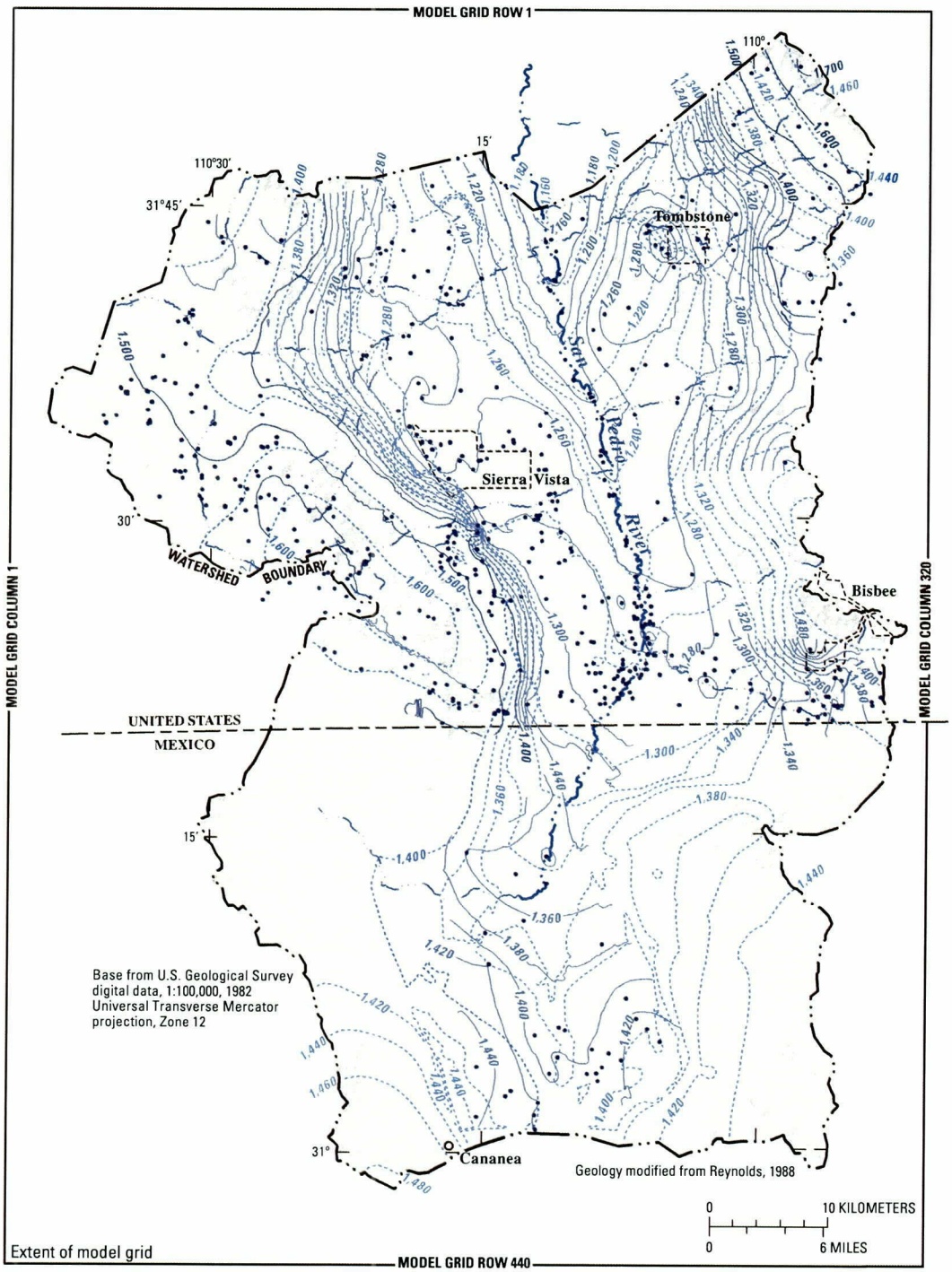

Figure 14. Observed and simulated water-level altitudes, winter 2002, Upper San Pedro Basin, United States and Mexico.

Table 5. Simulated ground-water budget for March 2002 to March 2003.

[cubic-meters per day]

Water-budget component	Simulated transient ground-water budget, March 2002 to March 2003					
	Spring/summer		Fall/winter		Average annual	
	Inflow	Outflow	Inflow	Outflow	Inflow	Outflow
Natural recharge	58,000	0	58,000	0	58,000	0
Artificial recharge	6,500	0	6,400	0	6,500	0
Stream baseflow[1]	17,000	22,400	17,000	32,700	17,000	26,600
Evapotranspiration	0	46,500	0	0	0	27,600
Ground-water underflow	0	2,600	0	2,600	0	2,600
Drains[2]	0	1,500	0	1,500	0	1,500
Wells[3]	7,200	165,400	7,200	102,500	7,200	140,000
Subtotal[4]	88,700	238,400	88,600	139,300	88,700	198,300
Storage[5]	156,100	6,400	111,800	61,400	138,100	28,700
TOTAL	244,800	244,800	200,400	200,700	226,800	227,000

[1]Inflow from stream baseflow represents stream baseflow that reinfiltrated the ground-water system after discharging to the stream and is not additional inflow to the ground-water system.

[2]Drains include discharge to several springs in the Huachuca Mountains.

[3]Well inflow is from recharge wells that simulate deep percolation and recharge of excess irrigation water and at septic systems.

[4]Subtotal of ground-water flow components.

[5]Storage inflow includes removal from ground-water storage and input to the ground-water flow system. Storage outflow includes removal from the ground-water flow system and input to storage.

Boundaries along the northern extent of the model were simulated as no-flow and constant-head boundaries throughout the period of transient stress. The flow system could, however, change near these boundaries. In this case, these boundaries may be simulated as general-head boundaries, or the model domain may be extended to an impermeable boundary. Inaccurate simulation of the flow boundaries may be significant locally, but should have minimal influence on the simulation of the regional ground-water flow system because estimated ground-water flow across the flow boundaries is less than 5 percent of the simulated water budget.

Recent hydrologic investigations and this numerical simulation have shown that near-stream recharge during floods is an important process that maintains streamflow for several months. The streamflow-routing package used in this simulation is inadequate for simulation of flood flows. More complex and appropriate stream-aquifer interaction can be simulated by using a new streamflow-routing package SFR1 (Prudic and others, 2004) that would allow simulation of floods and resulting streamflow infiltration. Climate-based recharge variations also could improve the simulations. Recharge rates in the area have been shown to vary significantly on decadal and seasonal scales with observed climate variations (Dickinson and others, 2004; Pool 2005). Variation in recharge rates likely causes some of the observed multiyear variation in stream baseflow. Recharge variations can now be estimated by using climate data. Simulation of evapotranspiration can be improved. Rates of evapotranspiration were simulated in this model as a single stress period with constant evapotranspiration parameters and a linear depth-to-water versus evapotranspiration relation. Evapotranspiration rates, however, vary throughout the growing season, and the depth versus evapotranspiration relation is nonlinear. Information on seasonal evapotranspiration rates and depth-to-water versus evapotranspiration is now available for several plant types. Improved simulation of streamflow, variations in recharge rates, and evapotranspiration should significantly improve simulation of seasonal and multiyear ground-water flow.

Summary and Conclusions

A numerical ground-water model was constructed to simulate seasonal and long-term variations in ground-water flow in portions of the Upper San Pedro Basin in the Sierra Vista subwatershed, Ariz., United States, and Sonora, Mexico. The simulation used a numerical MODFLOW model for 1902–2003. Several improvements from previous simulations of ground-water flow were incorporated. New concepts of ground-water flow that were developed on the basis of data

collected during 1995–2002 were simulated. Ground-water flow in the entire watershed was simulated, including flow in the sedimentary rocks within the mountains that surround and underlie the alluvial basin deposits. Simulation of flow in the sedimentary rocks allowed for inclusion of ground-water withdrawals for dewatering purposes at the Tombstone mine and discharge to springs in the Huachuca Mountains. The model also was constructed to allow for simulation of significantly different water levels and vertical ground-water flow between deep-confined and shallow-unconfined systems separated by thick silt and clay intervals. Recharge was distributed throughout the model area rather than only along the mountain fronts, which was the paradigm used in previous models, on the basis of recent investigations that estimated ephemeral channel recharge and new streamflow records in upland areas. Variations in discharge from ground-water withdrawals for agricultural, public, domestic, and military uses were simulated by using two seasons, fall/winter and spring/summer, each year.

A 5-layer model was constructed by using water-level data, geologic mapping, and geophysical surveys. Boundary conditions included no-flow boundaries that mostly coincided with the watershed boundaries, which were no-flow at a depth of 1,500 m below land surface throughout the model area, and specified-head conditions where ground water discharges to the north. The upper boundary of the flow system includes water-table conditions, streams, evapotranspiration, and drains at springs. The deepest layer, layer 5, extends throughout the model area and represents the sedimentary, volcanic, and crystalline rocks that outcrop in the mountains and underlie the alluvial basin. Layer 4 represents basin fill throughout the Mexico portion of the basin and sand and gravel in the lower basin fill unit in the Sierra Vista subwatershed. Layers 2 and 3 include the silt and clay facies of upper and lower basin fill, respectively, within the Sierra Vista subwatershed and adjacent areas that include sand and gravel and interbedded facies in the basin fill. Low permeability regions of silt and clay were mapped by using available subsurface electrical surveys and lithologic logs. Layer 1 represents stream alluvium along the San Pedro and Babocomari Rivers in the Sierra Vista subwatershed and saturated sand and gravel facies of basin fill that overlie the silt and clay facies of upper basin fill. Variations in hydraulic properties were distributed throughout each layer with polygons representing different rock types, facies within the basin fill, stream alluvium, and subareas within parts of each rock type.

Steady-state and transient conditions were simulated. No true steady-state initial conditions exist according to available records that indicate the ground-water flow system has changed in response to changes in discharge through well withdrawals and evapotranspiration rates and changes in stream-channel morphology, including channel incision and widening of the floodplain. Initial conditions for both the steady-state and transient simulation were determined by using the earliest streamflow and water-level records, which began in about 1930 and 1940, respectively. Changes in the ground-water flow system, following initial ground-water withdrawals for mining use in 1902 and before early water levels were measured, were assumed to be minimal. Estimated evapotranspiration rates and observed steady-state streamflow and water levels were used as controls to calibrate evapotranspiration rates and aquifer-system hydraulic properties, hydraulic conductivity and streambed conductance. An oscillatory steady-state simulation that included seasonal variations in evapotranspiration was done to establish initial conditions for simulations of transient conditions during 1902–2003. Calibration of vertical hydraulic conductivity and storage properties was accomplished by matching simulated and observed vertical hydraulic gradients and changes in water levels and streamflow.

The ground-water flow model approximates observed trends in water levels throughout most of the model area and streamflow at the Charleston streamflow-gaging station on the San Pedro River. Differences between observed and simulated water-level and streamflow trends occur near Palominas, where observed water-level declines were less than those simulated. Observed rapid streamflow declines during 1940–50 at the streamflow-gaging station at Palominas were simulated as a gradual declining trend during the simulation period. Much of the difference in observed and simulated conditions near Palominas may be related to insufficient information on agricultural withdrawal rates and the vertical distribution of withdrawals among the unconfined and confined parts of the ground-water flow system. Estimated increases in evapotranspiration rates in the Sierra Vista subwatershed could not be approximated because simulated water-level decline was greater than that observed in some areas near the San Pedro River, including the Palominas area. Simulation of near-stream conditions and evapotranspiration rates could be improved by simulating available climate-related variations in recharge rates and recharge from flood flow infiltration by using available improved streamflow-routing methods.

References Cited

Anderson, T.W., Freethey, G.W., and Tucci, Patrick, 1992, Geohydrology and water resources of alluvial basins in southcentral Arizona and adjacent states: U.S. Geological Survey Professional Paper 1406-D, 74 p.

Arizona Department of Water Resources, 1990, Hydrographic survey report (HSR) for the San Pedro River watershed, Volume 1: Arizona Department of Water Resources, 548 p.

Arizona Department of Water Resources, 2005, Upper San Pedro Basin active management area report, March 2005: Phoenix, Arizona Department of Water Resources, 146 p., appendices A-M.

Barnes, R.L, and Putman, F., 2004, Maps showing groundwater conditions in the Upper San Pedro Basin, Cochise, Graham, and Santa Cruz Counties, Arizona: Phoenix, Arizona Department of Water Resources Hydrologic Map Series Report No. 34, 2 sheets.

Brown, S.G., Davidson, E.S., Kister, L.R, and Thomsen, B.W., 1966, Water resources of Fort Huachuca Military Reservation, southeastern Arizona: U.S. Geological Survey Water-Supply Paper 1819–D, p. D1–D57.

Coes, A.L., and Pool, D.R., 2005, Ephemeral-channel and basin-floor infiltration in the Sierra Vista subwatershed, Arizona: U.S. Geological Survey Open-File Report 05–1023, 67 p.

Condor Consulting, Inc., 2003, Inversion of airborne EM data—Fort Huachuca and Sierra Vista areas, Arizona: Consultants Report, 7 p., 1 compact disc.

Consultores en Agua Subterranea S.A. por Mexicana de Cananea, S.A. de C.V., 2000, Actualizacion del estudio geohidrologico de las cuencas del Rio San Pedro y norte del Rio Sonora en Cananea, Son., 136 p., 5 appendices.

Corell, S.W., Putman, F., Lovvik, Daryl, and Corkhill, Frank, 1996, A groundwater flow model of the Upper San Pedro Basin, southeastern Arizona: Phoenix, Arizona Department of Water Resources Modeling Report no. 10, 85 p.

Dickinson, J.E., Hanson, R.T., Ferré, T.P.A., and Leake, S.A., 2004, Inferring time-varying recharge from inverse analysis of long-term water levels: Water Resources Research, v. 40, W07403, doi:10.1029/Water Resources Research.2003.002650, 15 p.

Esparza, Jose Guillermo De Aguinaga Ruiz, 2002, Modelacion geohydrologica del aquifero del Rio San Pedro: Hermosillo, Sonora, Mexico, Universidad De Sonora, professional thesis in Geology.

Fleming, John, and Pool, D.R., 2002, Geophysical surveys for delineation of shallow structure and lithology near the San Pedro River, Southeast Arizona: Proceedings of the Society of Environment and Engineering Geophysical Society, February 2002, accessed March 28, 2007, at http://www.eegs.org/sageep/proceedings.cfm

Freethey, G.W., 1982, Hydrologic analysis of the upper San Pedro Basin from the Mexico–United States international boundary to Fairbank, Arizona: U.S. Geological Survey Open-File Report 82–752, 52 p.

Gettings, M.E., and Houser, B.B., 1995, Preliminary results of modeling the gravity anomaly field in the Upper San Pedro Basin, southeastern Arizona: U.S. Geological Survey Open-File Report 95–76, 12 p.

Goode, Tomas, and Maddock, Thomas III, 2000, Simulation of groundwater conditions in the Upper San Pedro Basin for the evaluation of alternative futures: Tucson, Department of Hydrology and Water Resources and University of Arizona Research Laboratory for Riparian Studies, HWR no. 00-30, 113 p.

Goodrich, D.C., Williams, D.G., Unkrich, K.L., Hogan, J.F., Scott, R.L., Hultine, K.R., Pool, D., Coes, A.L., and Miller, S., 2004, Comparison of methods to estimate ephemeral channel recharge, Walnut Gulch, San Pedro River Basin, Arizona: *in* J.F. Hogan, F.M. Phillips, and B.R. Scanlon, eds., Groundwater recharge in a desert environment, the southwestern United States, Water Science and Applications Series: American Geophysical Union, v. 9, p. 77–99.

Gray, R.S., 1965, Late Cenozoic sediments in the San Pedro Valley near St. David, Arizona: Tucson, University of Arizona, Ph.D. dissertation, 198 p.

Halverson, P.H., 1984, An exploratory gravity survey in the upper San Pedro Valley, southeastern Arizona: Tucson, University of Arizona, masters thesis, 1984, 85 p.

Hanson, R.T, Newhouse, M.W., and Dettinger, M.D., 2004, A methodology to assess relations between climate variability and variations in hydrologic time-series in the southwestern United States: Journal of Hydrology, v. 287, issues 1–4, p. 252–269.

Harbaugh, A.W., Banta, E.R., Hill, M.C., and McDonald, M.G., 2000a, MODFLOW-2000, The U.S. Geological Survey modular ground-water model—User guide to modularization concepts and the ground-water flow process: U.S. Geological Survey Open-File Report 00–92, 121 p.

Harbaugh, A.W., Banta, E.R., Hill, M.C., and Anderman, E.R., 2000b, MODFLOW-2000, The U.S. Geological Survey modular ground-water model—User guide to observation, sensitivity, and parameter-estimation processes and three post-processing programs: U.S. Geological Survey Open-File Report 00–184, 209 p.

Hereford, Richard, 1993, Entrenchment and widening of the upper San Pedro River, Arizona: Geological Society of America Special Paper 282, 46 p.

Hollyday, E.F., 1963, A geohydrologic analysis of mine dewatering and water development, Tombstone, Cochise County, Arizona: Tucson, University of Arizona, master's thesis, 90 p.

Kepner, W.G., and Edmonds, C.M., 2002, Remote sensing and geographic information systems for decision analysis in the public resource administration: A case study of 25 years of landscape change in a southwestern watershed: U.S. Environmental Protection Agency, EPA/600/R-02/039, 31 p.

Leenhouts, J.M., Stromberg, J.C., and Scott, R.L., 2005, Hydrologic requirements of and consumptive ground-water use by riparian vegetation along the San Pedro River, Arizona: U.S. Geological Survey Scientific Investigations Report, 2005–5163, 211 p.

Phelps Dodge Corporation, 1998, Hydrologic assessment for the tailing impoundments-CTSA APP Project Area, Bisbee, Arizona: Golden, Colo., Consultant report, SAVCI Environmental Technologies, LLC, 102 p., 47 figs., 1 appendix.

Pool, D.R., 2005, Variations in climate and natural recharge in southeast Arizona: Water Resources, 41, W11403, doi:10.1029/2004WR003255, 24 p.

Pool, D.R., and Coes, A.L., 1999, Hydrogeologic investigations of the Sierra Vista subwatershed of the Upper San Pedro Basin, Cochise County, southeast Arizona: U.S. Geological Survey Water-Resources Investigations Report 99–4197, 41 p.

Pool, D.R., and Leenhouts, J.M., 2002, A multiparameter approach for measuring flood-induced aquifer- and bank-storage changes along the San Pedro River, Arizona [abs.], *in* Program & Abstracts, AGU fall 2002 meeting, December 6-10, 2002, San Francisco, accessed March 28, 2007, at http://www.agu.org/meetings/fm02/program.shtml

Prudic, D.E., 1989, Documentation of a computer program to simulate stream-aquifer relations using a modular, finite-difference, ground-water flow model: U.S. Geological Survey Open-File Report 88–729, 113 p.

Prudic, D.E., Konikow, L.F., and Banta, E.R., 2004, A new streamflow-routing (SFR1) package to simulate stream-aquifer interaction with MODFLOW-2000: U.S. Geological Survey Open-File Report 2004–1042, 104 p.

Reichardt, K.L., Schladweiler, Brenda, and Stelling, J.L., 1978, An inventory of riparian habitats along the San Pedro River: Tucson, University of Arizona, The Applied Remote Sensing Program, Office of Arid Lands Studies, 22 p.

Reynolds, S.J., 1988, Geologic map of Arizona: Arizona Geological Survey, Map 26, 1 sheet.

Schwartzman, P.N., 1990, A hydrologic assessment of the lower Babocomari watershed, Arizona: University of Arizona, master's thesis, 3 pls., 212 p.

Southwest Ground-Water Consultants, 2004, Water supply potential Phelps Dodge Copper Queen Mine: Phoenix, Ariz., Consultant report, Southwest Ground-water Consultants, Inc., 24 p.

Thomas, Blakemore, and Pool, D.R., 2006, Seasonal precipitation and streamflow trends in southeastern Arizona and southwestern New Mexico: U.S. Geological Survey Professional Paper 2005–1712, 79 p.

University of Arizona Geophysics Field Camp, 2001, Geophysical surveys near Sierra Vista, Arizona: Laboratory for Advanced Subsurface Imaging (LASI) Report LASI-01-01, May 4, 2001, 34 p.

University of Arizona Geophysics Field Camp, 2002, Geophysical surveys near Fort Huachuca, Arizona: Laboratory for Advanced Subsurface Imaging (LASI) Report LASI-02-01, May 4, 2002, 34 p.

University of Arizona Geophysics Field Camp, 2004, Geophysical surveys near Sierra Vista, Arizona: Laboratory for Advanced Subsurface Imaging (LASI) Report LASI-04-01, June 7, 2004, 109 p.

U.S. Army Corps of Engineers (Topographic Engineering Center), 2001, Vegetation map of the San Pedro Riparian National Conservation Area and Babocomari River: Fort Huachuca, Ariz., Final report submitted to U.S. Army Garrison, 63 p.

U.S. Department of Defense, 2002, Fort Huachuca programmatic biological assessment for ongoing and programmed future military operations and activities: Fort Huachuca, Ariz., Environmental and Natural Resources Division, Directorate of Installation Support, U.S. Army Garrison, 468 p.

Vionnet, L.B., and Maddock, T., 1992, Modeling of ground-water flow and surface water/groundwater interactions in the San Pedro River Basin—Part I—Cananea, Mexico to Fairbank, Arizona: Tucson, University of Arizona, Department of Hydrology and Water Resources, HWR No. 92-010, 96 p.

Webb, R.H., and Betancourt, J.L., 1992, Climatic variability and flood frequency of the Santa Cruz River, Pima County, Arizona: U.S. Geological Survey Water-Supply Paper 2379, 40 p.

Manuscript approved for publication, 2007.

Prepared by the U.S. Geological Survey Reports Section,
Tucson, Arizona.

USGS Publishing staff
Tracey L. Suzuki, Technical Editor
John Callahan, Illustrator

For more information concerning the research in this report,
contact the Arizona Water Science Center Director,
U.S. Geological Survey, 520 N. Park Ave., Suite 221,
Tucson, AZ 85719
http://az.water.usgs.gov

This page left blank intentionally.

Inside Back Cover
BLANK

Pool and Dickinson—GROUND-WATER FLOW MODEL OF THE SIERRA VISTA SUBWATERSHED AND SONORA PORTIONS OF THE UPPER SAN PEDRO BASIN, SOUTHEASTERN ARIZONA, UNITED STATES, AND NORTHERN SONORA, MEXICO—U.S. Geological Survey Scientific Investigations Report 2006–5228